

University of Alberta

Post-combustion Carbon Dioxide Capture using Amine Functionalized
Solid Sorbents

by

Nikhil Mittal

A thesis submitted to the Faculty of Graduate Studies and Research
in partial fulfillment of the requirements for the degree of

Master of Science
in
Chemical Engineering

Department of Chemical and Materials Engineering

©Nikhil Mittal
Fall 2013
Edmonton, Alberta

Permission is hereby granted to the University of Alberta Libraries to reproduce single copies of this thesis and to lend or sell such copies for private, scholarly or scientific research purposes only. Where the thesis is converted to, or otherwise made available in digital form, the University of Alberta will advise potential users of the thesis of these terms.

The author reserves all other publication and other rights in association with the copyright in the thesis and, except as herein before provided, neither the thesis nor any substantial portion thereof may be printed or otherwise reproduced in any material form whatsoever without the author's prior written permission.

Abstract

This work is divided into two parts: (1) Synthesis of amine functionalized adsorbents using grafting technique for post-combustion CO₂ capture, (2) Performance evaluation of structured bed configuration with straight gas flow channels using amine impregnated adsorbent for post-combustion CO₂ capture.

Brief description of each part is given below:

- (1) N-(3-trimethoxysilylpropyl)diethylenetriamine (DAEAPTS) grafted SBA-15 adsorbents were synthesized for CO₂ capture. The adsorption of CO₂ on the amine-grafted sorbents was measured by thermogravimetric method over a CO₂ partial pressure range of 8–101.3 kPa and a temperature range of 25–105 °C under atmospheric pressure. The optimal amine loaded SBA-15 adsorbent was examined for multi-cycle stability and adsorption/desorption kinetics.
- (2) The performance of structured bed and packed bed configurations for post-combustion CO₂ capture was evaluated using PEI impregnated SBA-15 adsorbent. The effect of adsorption temperature (25-90 °C), adsorption /desorption kinetics and multi-cycle stability was studied in both structured and packed bed configurations.

Acknowledgements

I would like to extend my thanks and gratitude towards my research supervisor, Dr Rajender Gupta, for his continuous help and support throughout my masters degree. I would like to thank Dr Partha Sarkar for his guidance and extensive support. I am very grateful to them for giving me the privilege of working under their mentorship.

I would also like to express my gratitude and appreciation towards Dr Arunkumar Samanta for his whole-hearted support in every phase of my research work. I am very grateful to Mr Juan Segura and Mr Luis Yamarte for their help and assistance in my work at AITF.

I would also like to thank Dr Moshfiqur Rahman for his help and encouragement for my research. I would like to thank my colleagues, An Zhao, Su Tian, Zhe Bai, Navjot Kaur Sandhu and Zhengyi Liu, for their valuable insight and technical assistance. I would like to thank all the group members for their co-operation and support in building a positive working atmosphere.

I would like to acknowledge the financial support of Carbon Management Canada (CMC), Canadian Centre for Clean Coal/Carbon and Mineral Processing Technology (C5MPT), Alberta Innovates Technology Futures (AITF) and Coal Mining Research Company Graduate Scholarship.

Table of Contents

Abbreviations

Nomenclature

1 Introduction.....	1
1.1 Background	1
1.2 Carbon capture and storage (CCS).....	2
1.2.1 Post-combustion CO ₂ capture	6
1.2.1.1 Absorption process	7
1.2.1.2 Adsorption process	9
References.....	14
2 Literature Review	16
2.1 Overview	17
2.2 Physical adsorbents	19
2.2.1 Carbon-based adsorbents	19
2.2.1.1 Activated Carbon (AC)	21
2.2.1.2 Carbon Nanotubes (CNTs).....	23
2.2.1.3 Carbon Molecular Sieves (CMSs).....	24
2.2.2 Zeolite-based adsorbents.....	25
2.2.3 Metal Organic Frameworks (MOFs).....	28
2.3 Chemical adsorbents	30
2.3.1 Amine functionalized solid adsorbents.....	30
2.3.1.1 Reaction mechanism	33
2.3.1.2 Amine impregnated solid adsorbents	35
2.3.1.3 Amine grafted solid adsorbents.....	39
2.4 Bed configuration for CO ₂ capture.....	45
2.4.1 Monolith bed configuration	46
2.4.2 Parallel passage contactor configuration.....	49
2.4.3 Hollow fiber bed	52
2.4.4 Other structured bed configurations.....	54
2.5 Summary	57

2.6	Motivation	58
2.7	Objectives.....	60
	References.....	62
3	Materials and Methods.....	76
3.1	Materials.....	77
3.2	Synthesis.....	77
3.2.1	Preparation of SBA-15.....	77
3.2.2	Preparation of DAEAPTS amine grafted SBA-15.....	78
3.2.3	Preparation of PEI amine impregnated SBA-15.....	79
3.3	Characterization	80
3.3.1	N ₂ adsorption/desorption	80
3.3.2	SEM and HRTEM.....	81
3.3.3	Amine loading using TGA and Elemental analysis	81
3.3.4	Fourier Transform Infrared Spectroscopy (FTIR)	81
3.4	CO ₂ adsorption and desorption using TGA.....	82
3.5	CO ₂ adsorption/desorption using different bed configurations.....	84
3.5.1	Packed bed	84
3.5.2	Structured bed	88
3.5.3	Capacity calculation.....	93
	References.....	94
4	Results and Discussion.....	95
4.1	Characterization	96
4.1.1	N ₂ adsorption/desorption	97
4.1.2	SEM and HRTEM.....	98
4.1.3	FTIR analysis	99
4.1.4	Amine loading using TGA and Elemental analysis	100
4.2	Adsorption performance.....	104
4.2.1	Effect of amine loading on CO ₂ adsorption performance.....	104
4.2.2	Effect of adsorption temperature and CO ₂ partial pressure	106
4.2.3	Heat of adsorption.....	108

4.2.4	Kinetics	112
4.2.5	Effect of moisture	115
4.2.6	Multi-cycle stability	118
4.3	Bed performance	122
4.3.1	Single-tube structured bed	123
4.3.1.1	Effect of adsorption temperature	123
4.3.1.2	Effect of CO ₂ concentration	124
4.3.2	Three-tube structured bed	126
4.3.2.1	Effect of adsorption temperature	126
4.3.2.2	Kinetics.....	128
4.3.2.3	Multi-cycle stability	129
4.3.3	Packed bed performance	130
4.3.3.1	Effect of adsorption temperature	130
4.3.3.2	Effect of gas flowrate	132
4.3.3.3	Multi-cycle stability	134
4.3.3.4	Kinetics.....	136
4.3.4	Packed and structured bed comparison.....	138
	Notes	141
	References.....	141

5 Conclusions and Future Work..... 143

5.1	Conclusions	143
5.2	Future work	146

List of Tables

Table 1.1. CO ₂ concentrations in common industrial processes.	5
Table 2.1. Comparison of CO ₂ and N ₂ on the basis of kinetic diameter, polarizability and quadrupole moment.	18
Table 2.2. Textural properties of different carbonaceous solid adsorbents.	19
Table 2.3. CO ₂ adsorption capacity with operating conditions of different carbonaceous solid adsorbents used in the literature.	20
Table 2.4. Textural properties of different zeolite-based solid adsorbents.	25
Table 2.5. CO ₂ adsorption capacity with operating conditions of different zeolite-based solid adsorbents used in the literature.	26
Table 2.6. Structure of different amines used for adsorbent functionalization in the literature.	32
Table 2.7. CO ₂ adsorption performance with operating conditions of different amine impregnated solid adsorbents reported in the literature.	38
Table 2.8. CO ₂ adsorption performance with operating conditions of different amine grafted solid adsorbents reported in the literature.	44
Table 2.9. Review of structured sorbent bed applications for adsorption/ desorption processes.	56
Table 4.1. Textural properties of raw and amine grafted SBA-15 samples.	97

Table 4.2. Amine content of DAEAPTS grafted SBA-15/D-x sorbents prepared with different initial amine loadings using TGA and elemental analysis. 103

Table 4.3. Amine loading, nitrogen content, CO₂ adsorption capacity and amine adsorption efficiency of amine grafted sorbents with variable amine loadings. Adsorption capacity and amine adsorption efficiency measured in 8.8% CO₂/91.2% N₂ gas mixture at 75 °C and 1 atm. 105

Table 4.4. Heat of adsorption values of SBA-15/D-4 sample using dry CO₂, humid CO₂ and moisture streams in N₂ at different adsorption temperatures. 111

List of Figures

Figure 1.1. The schematic representation of the three CO ₂ capture approaches.	4
Figure 1.2. Schematic representation of a typical CO ₂ capture absorption process.	8
Figure 2.1. Schematic representation of a typical monolith configuration.	49
Figure 2.2. Schematic of a parallel passage sorbent contactor, (a) side view, (b) front view.	51
Figure 2.3. Schematic of a typical single hollow fiber configuration, (a) front view, (b) side view.	53
Figure 2.4. Schematic representation of multiple hollow fiber bed, (a) front view, (b) top view.	54
Figure 3.1. Schematic representation of DAEAPTS amine grafting over SBA-15 surface.	79
Figure 3.2. TGA experimental set-up for performance evaluation of amine functionalized SBA-15 adsorbent.	84
Figure 3.3. Diagram of U-tube used as packed bed for CO ₂ adsorption/desorption tests.	85
Figure 3.4. Packed bed experimental set-up used for CO ₂ adsorption/desorption tests.	87
Figure 3.5. Proposed structured bed adsorption/desorption system with single tube, (a) lateral view, (b) cross-sectional view.	88

Figure 3.6. Proposed structured bed adsorption/desorption system with three tubes, (a) lateral view, (b) cross-sectional view.	89
Figure 3.7. Structured bed experimental set-up used for CO ₂ adsorption/desorption tests.	92
Figure 4.1. N ₂ adsorption/desorption isotherm and pore size distribution of calcined SBA-15.	98
Figure 4.2. Raw calcined SBA-15 sample: (a) SEM image, (b) and (c) High resolution TEM images.	99
Figure 4.3. FITR analysis of calcined SBA-15 and amine grafted SBA-15 adsorbent sample.	100
Figure 4.4. Thermal behavior of calcined SBA-15 and amine grafted adsorbents SBA-15/D-x with different amine loadings using TGA.	102
Figure 4.5. A typical thermal behavior curve of calcined SBA-15 and DAEAPTS grafted adsorbent SBA-15/D-4 using TGA.	103
Figure 4.6. CO ₂ adsorption capacity variation with amine loading for different SBA-15/D-x adsorbent samples in 88.2% CO ₂ /11.8% N ₂ and 8.8% CO ₂ /91.2% N ₂ gas mixtures at 75 °C and 1 atm.	105
Figure 4.7. Amine grafted sorbent SBA-15/D-4 variation of CO ₂ adsorption capacity with adsorption temperature for 88.2% CO ₂ and 8.8% CO ₂ in N ₂ at 1 atm.	107
Figure 4.8. Amine grafted sorbent SBA-15/D-4 variation of CO ₂ adsorption capacity with CO ₂ partial pressure at 75 °C and 1 atm.	108

Figure 4.9. Heat of adsorption variation with adsorption temperature for SBA-15/D-4 sample in 8.8% CO ₂ /91.2% N ₂ and 88.2% CO ₂ /11.8% N ₂ gas mixtures.	110
Figure 4.10. Heat of adsorption variation with adsorption temperature for SBA-15/D-4 sample in dry and humid 8.8% CO ₂ /91.2% N ₂ gas mixtures.	111
Figure 4.11. CO ₂ adsorption capacities of different SBA-15/D-x adsorbents as a function of time in 88.2% CO ₂ /11.8% N ₂ gas mixture at 75 °C and 1 atm.	113
Figure 4.12. Derivative adsorption capacity variation with time in 88.2% CO ₂ /11.8% N ₂ gas mixture at 75 °C for different SBA-15/D-x adsorbents.	114
Figure 4.13. Comparison of adsorption-desorption kinetics of SBA-15/D-4 sample in dry and humid 88.2% CO ₂ /11.8% N ₂ gas mixtures at 75 °C and 1 atm.	115
Figure 4.14. Comparison of CO ₂ adsorption capacity of SBA-15/D-4 sample in dry and humid CO ₂ streams at different adsorption temperatures. 8.8% CO ₂ /91.2% N ₂ gas mixture was used.	116
Figure 4.15. Comparison of dry CO ₂ , moisture and N ₂ adsorption capacities at different adsorption temperatures for SBA-15/D-4 sample.	117
Figure 4.16. Comparison of dry 88.2% CO ₂ /N ₂ , humid 88.2% CO ₂ /N ₂ , moisture and N ₂ adsorption capacities as a function of time for SBA-15/D-4 sample at 75 °C.	118
Figure 4.17. Multi-cycle stability of SBA-15/D-4 sample in dry and humid 88.2% CO ₂ /11.8% N ₂ gas mixture at 1 atm.	120

Figure 4.18. FTIR analysis of fresh amine grafted SBA-15 sample and amine grafted samples after 100 cycles with dry and humid CO ₂ /N ₂ gas mixtures.	121
Figure 4.19. Variation of adsorption capacity with adsorption temperature in pure CO ₂ . SBA-15/P-50 sample used inside single-tube structured bed.	124
Figure 4.20. Breakthrough curve for SBA-15/P-50 sample inside single-tube structured bed in 10% CO ₂ /90% N ₂ at 75 °C.	125
Figure 4.21. Breakthrough curve for SBA-15/P-50 sample inside single-tube structured bed in pure CO ₂ at 75 °C.	126
Figure 4.22. Comparison of structured bed breakthrough profiles of SBA-15/P-50 sorbent in 10% CO ₂ /90% N ₂ at different adsorption temperatures.	127
Figure 4.23. Variation of adsorption capacity with adsorption temperature for SBA-15/P-50 sample in three-tube structured bed. 10% CO ₂ /90% N ₂ gas mixture used.	128
Figure 4.24. Adsorption/desorption kinetics of SBA-15/P-50 sample in three-tube structured bed.	129
Figure 4.25. Multi-cycle stability of SBA-15/P-50 sample in three-tube structured bed.	130
Figure 4.26. Variation of CO ₂ adsorption capacity with adsorption temperature for SBA-15/P-50 sample in packed bed using 10% CO ₂ /90% N ₂ gas mixture.	131
Figure 4.27. Comparison of packed bed breakthrough curves at different adsorption temperatures in 10% CO ₂ /90% N ₂ gas mixture.	132

Figure 4.28. Variation of CO ₂ adsorption capacity with gas flowrate for SBA-15/P-50 sample inside packed bed at 75 °C.	133
Figure 4.29. Comparison of packed bed breakthrough curves at different gas flowrates comprising 10% CO ₂ /90% N ₂ gas mixture at 75 °C.	134
Figure 4.30. Multi-cycle stability of SBA-15/P-50 sample inside packed bed in dry and humid 10% CO ₂ /N ₂ gas streams at 75 °C.	136
Figure 4.31. Adsorption/ desorption kinetics of SBA-15/P-50 sample inside packed bed in dry 10% CO ₂ /N ₂ gas mixture.	137
Figure 4.32. Adsorption/ desorption kinetics of SBA-15/P-50 sample inside packed bed in humid 10% CO ₂ /N ₂ gas mixture.	138
Figure 4.33. Comparison of adsorption capacity of SBA-15/P-50 sample using structured bed and packed bed at different adsorption temperatures.	140

Abbreviations

AC	Activated carbon
AEAPS	N-(2-aminoethyl)-3-aminopropyltriethoxysilane
AEAPTS	N-[3-(trimethoxysilyl)propyl]-ethylenediamine
APTES	3-aminopropyltriethoxysilane
APTS	3-aminopropyltrimethoxysilane
BET	Brunauer Emmett Teller
BJH	Barrett Joyner Halenda
CCS	Carbon capture and storage
CMS	Carbon molecular sieves
CNT	Carbon nanotube
CPSI	Cells per square inch
DAEAPTS	N-(3-trimethoxysilylpropyl)diethylenetriamine
DEHAPTS	Diethylhydroxyl-aminopropyl-trimethoxysilane
DWSNT	Double-walled silica nanotubes
ESA	Electric swing adsorption
FTIR	Fourier transform infrared spectroscopy
GC	Gas chromatography
HAS	Hyperbranched aminosilica
HMS	Hexagonal mesoporous silica
HRTEM	High-resolution transmission electron microscopy
IPCC	Intergovernmental panel on climate change

LDF	Linear driving force
MFC	Mass flow controller
MOF	Metal organic framework
MS	Mass spectrometry
PC	Pulverized coal
PEI	Polyethylenimine
PSA	Pressure swing adsorption
RH	Relative humidity
SEM	Scanning electron microscopy
SWCNT	Single-walled carbon nanotube
TCD	Thermal conductivity detector
TEM	Transmission electron microscopy
TEOS	Tetraethyl orthosilicate
TEPA	Tetraethylenepentamine
TGA	Thermogravimetric analysis
TPD	Temperature programmed desorption
TSA	Temperature swing adsorption
VSA	Vacuum swing adsorption

Nomenclature

$p(\text{CO}_2)$	CO_2 partial pressure
d_p	Average pore diameter
wt%	Weight percent
mmol/g	(mmol of CO_2) / (g of adsorbent)
mg/g	(mg of CO_2) / (g of adsorbent)
mmol N/g	(mmol of N) / (g of adsorbent)
t_{ad}	Equivalent adsorption time
T	Total adsorption time
C_a	CO_2 concentration at any time t using the adsorbent sample
C_b	CO_2 concentration at any time t using the inert alumina powder
C_0	CO_2 concentration in the feed
F	Feed gas flowrate
m	Weight of adsorbent used during the run
q	Adsorption capacity
ΔH_{dry}	Heat of adsorption in dry 8.8% CO_2 /91.2% N_2
ΔH_{humid}	Heat of adsorption in humid 8.8% CO_2 /91.2% N_2
$\Delta H_{moisture}$	Heat of adsorption in the presence of only moisture

Chapter 1

Introduction

The content of this chapter is arranged as:

- The chapter provides a background on the contribution of CO₂ in global greenhouse gas emissions and explains why it is necessary to reduce CO₂ concentration in the atmosphere.
- The three main approaches used for carbon capture and storage are discussed in brief in this chapter. The challenges faced in post-combustion approach for CO₂ capture from the flue gas of existing power-plants and the different processes that can be used for post-combustion CO₂ capture are presented.
- This chapter gives a comparison between conventional absorption based CO₂ capture process and relatively new adsorption based CO₂ capture process under post-combustion conditions. In the end, important requirements (adsorption capacity, kinetics, long-term stability, regeneration energy, selectivity and cost) for the selection of a solid adsorbent for post-combustion CO₂ capture are described.

1.1 Background

The average temperature of earth is observed to be increasing in the past 50 years due to significant increase in the global emissions of anthropogenic greenhouse

gases.¹ The major source of anthropogenic greenhouse gas emissions is fossil fuels combustion, which is around 86% of the total emissions. The other sources are deforestation, chemical processes, etc. Carbon dioxide (CO₂) constitutes a big part of the anthropogenic greenhouse gases and there is considerable increase in its concentration in the atmosphere in the last 20-30 years.² As per the report of IPCC, the increase in world-wide atmospheric concentration of CO₂ is quite significant, from around 250 ppmv in preindustrial period to 390 ppmv recently.¹ According to IPCC 2007, the contribution of CO₂ concentration in global radiative-forcing is estimated around 1.66 W/m² and it is the largest contributor to global radiative-forcing.³ In future, CO₂ concentration will increase even faster if its release stays the same. The CO₂ emission level in 2050 is estimated to be twice the 2007 CO₂ emission levels if no measures will be taken to halt the CO₂ emissions.⁴ Other environment friendly energy sources are still in their early stages and cannot meet the global energy requirements in the coming few decades. Energy requirements will continue to be provided by combustion of fossil fuels in the near future, hence global greenhouse gas emissions will keep increasing unless proper actions will be taken.

1.2 Carbon capture and storage (CCS)

Since CO₂ emission will keep rising in the coming future, the governmental funding and research activities concerning carbon capture and storage has heavily increased in the past few years due to the growing awareness of the detrimental effects of CO₂ accumulation in the atmosphere. The number of CCS projects is

anticipated to be around 100 by 2020 and 3000 by 2050.⁵ A complete CCS project encompasses CO₂ capture, compression, transport and storage. It has been estimated that CO₂ capture alone costs approximately two-thirds of the entire CCS project, which means an efficient capture process can result in lower energy penalty for the overall process.⁶ As the capital costs to install CCS in any plant will be almost same, so economically it would be more beneficial to remove the CO₂ from larger CO₂ emission sources like thermal power plants, etc. than smaller ones.

Three general approaches are currently studied in CCS for CO₂ capture, which are post-combustion CO₂ capture, pre-combustion CO₂ capture and oxyfuel-combustion CO₂ capture.^{2,7,8} Figure 1.1 shows the schematic representation of the three types of CO₂ capture systems.⁹ Short description of each CO₂ capture approach is given below:

Post-combustion CO₂ capture: CO₂ is captured from the flue gas mixture generated after burning of fuel.

Pre-combustion CO₂ capture: CO₂ is removed from gasified fuel mixture prior to burning the fuel.

Oxyfuel combustion CO₂ capture: It involves the separation of air to produce high purity oxygen (O₂ > 95%). The combustion of fuel takes place in this high purity O₂ stream to produce flue gas mixture containing mainly pure CO₂ with H₂O. CO₂ can then be separated from this flue gas mixture easily.

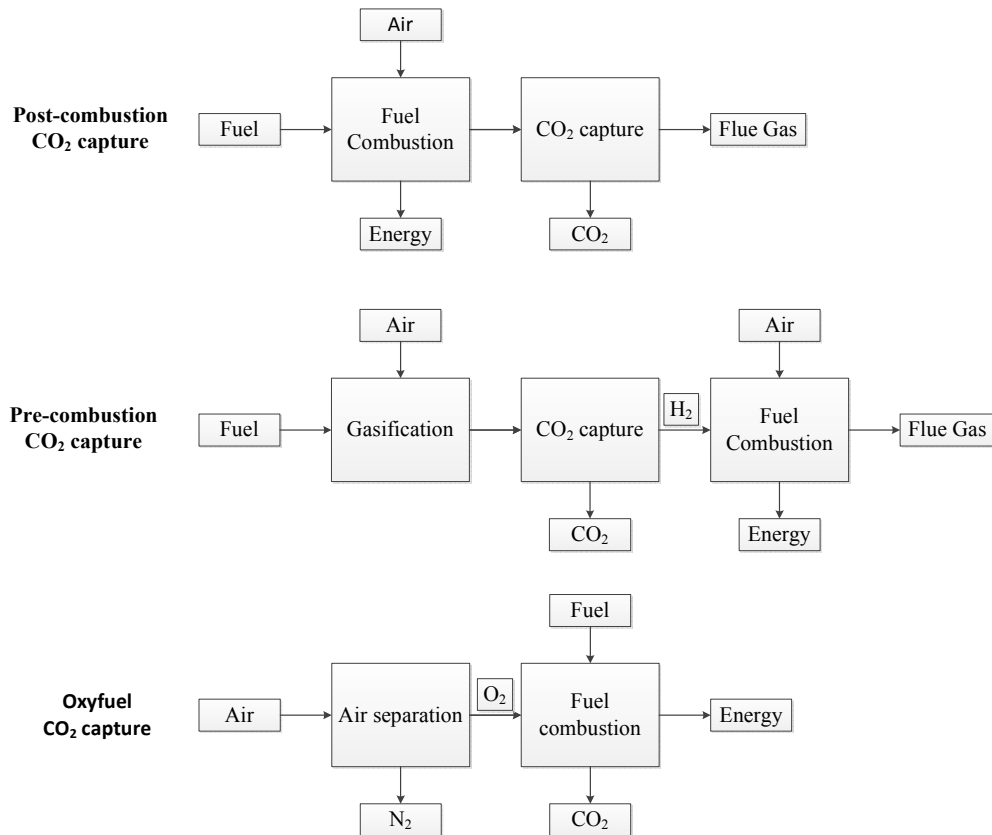


Figure 1.1. The schematic representation of the three CO₂ capture approaches.⁹

The main benefit of pre-combustion CO₂ capture compared to post-combustion capture is high operating pressure and higher CO₂ concentration, which can result in energy penalty reduce down to half of the energy penalty in post-combustion capture.¹⁰ But the initial step in post-combustion CO₂ capture is cheaper as compared to pre-combustion CO₂ capture. The oxyfuel capture is based on zero CO₂ emission but the air separation required in oxyfuel capture is very energy intensive. Out of the three capture systems, post-combustion CO₂ capture system is the easiest to implement in any existing plant and most economical.²

Each of the three CO₂ capture systems discussed above require different CO₂ capture conditions and will be suited for CO₂ capture under that conditions only. The CO₂ capture system to be used for a particular gas stream depends on number of factors like gas composition, CO₂ concentration, pressure and temperature of the stream, type of fuel used, etc. Table 1.1 presents the CO₂ concentration in the gas streams of some standard industrial applications.^{2,11} As can be seen from this Table, CO₂ concentration range is different for different applications so one CO₂ capture system would not be effective for all the applications. The gas streams of all the industrial processes mentioned in this Table contains impurities like SO_x, NO_x, O₂, etc.¹¹ These impurities also play a big factor in deciding the type of CO₂ capture system to be used, as their removal prior or post CO₂ removal will be required to obtain gas stream free of CO₂.

Table 1.1. CO₂ concentrations in common industrial processes.^{2, 11}

Process	Dry CO₂ (vol%)	Gas Pressure [MPa]
Coal fired boiler	12-14	0.1
Gas fired boiler	7-10	0.1
Gas turbine exhaust	3-4	0.1
Blast furnace gas: post-combustion	27	0.1
Cement furnace off-gas	14-33	0.1
Natural gas processing	2-65	0.9-8
IGCC syngas: post-gasification	8-20	2-7

1.2.1 Post-combustion CO₂ capture

As CO₂ is separated at the end of fuel combustion from flue gas mixture in post-combustion capture, so retrofitting any existing process for CO₂ capture can be done very economically.² Post-combustion CO₂ capture from large-point sources like thermal power plants face several challenges in order to keep the energy penalty down.

The following design constraints are identified for post-combustion CO₂ capture from a power plant¹²:

1. A 500 MW power plant normally produces very large flue gas flowrate of more than 2.04×10^6 m³/h.
2. The flue gas pressure is close to atmospheric in a typical power plant, which is quite low for CO₂ capture. According to Tarka et al.¹³, around 3 psi of pressure drop can only be afforded in flue gas mixture for CO₂ capture in order for the capture process to be economical. Additional pressure drop of flue gas mixture will lead to extra cost.
3. CO₂ concentration in the flue gas mixture is very low in post-combustion conditions, ranging from 10-15%.
4. Presence of impurities like H₂O, SO_x, NO_x, etc. in the flue gas mixture in post-combustion conditions present additional challenges for CO₂ separation.

Generally, CO₂ can be removed from flue gas mixture in post-combustion CO₂ capture using these main processes: (i) cryogenic distillation, (ii) membrane

separation, (iii) absorption with liquids, and (iv) adsorption with solid adsorbents.¹⁴ Cryogenic distillation, common for separation of gases, is not usually used for CO₂ capture due to large energy penalty and associated cost. Membranes can only give good separation when the species to be separated is present in large concentration or high pressure¹⁵ whereas for post-combustion capture conditions, CO₂ is present in low concentration, so membrane separation is not suitable for CO₂ capture from flue gas mixture in post-combustion conditions. Absorption using liquid amine solvents and adsorption using solid sorbents are more suited in post-combustion CO₂ capture conditions and will be discussed further in this section.

1.2.1.1 Absorption process

Post-combustion CO₂ capture using aqueous amine based absorption system has been practiced in industry for over 50 years. The technology is mature enough and easy to implement in large-scale industrial processes. The absorption process offers better selectivity and efficiency as compared to other processes in use for post-combustion CO₂ capture.² The schematic representation of a typical post-combustion CO₂ capture system using absorption process is shown in Figure 1.2. Most of the absorption processes are based on 25-30 wt% aqueous amine (generally MEA/ DEA/ MDEA) solvents to separate acid gases like CO₂. In a typical absorption process, flue gas mixture containing CO₂ is fed into the absorption reactor from the bottom and lean amine solvent enters the reactor from the top. The lean amine solvent absorbs the CO₂ from flue gas mixture via

reversible reaction between amine and CO₂. Flue gas mixture free of CO₂ leaves from the absorption reactor top whereas rich amine solvent containing CO₂ exits from the absorption reactor bottom. The CO₂ rich amine solvent is regenerated using steam in a regenerator column. The lean amine solvent produced after regeneration again cycles back to the top of absorption reactor.

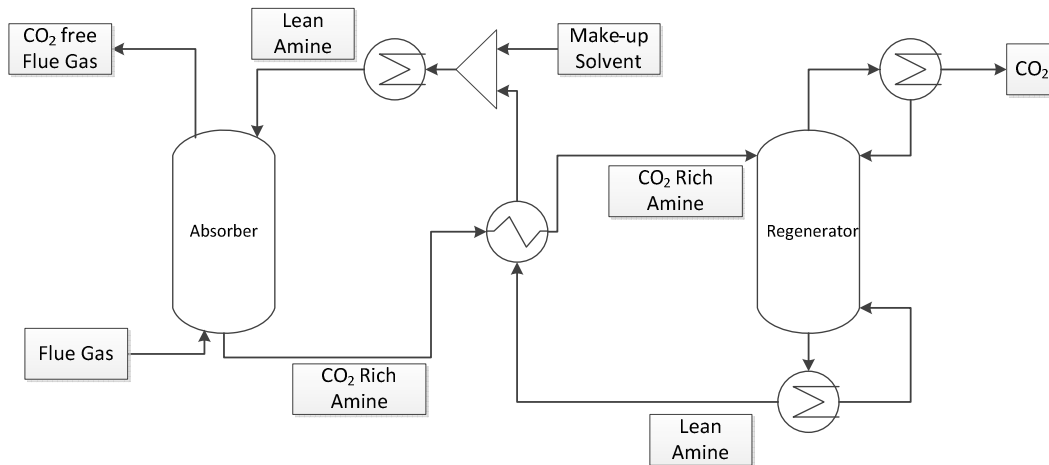


Figure 1.2. Schematic representation of a typical CO₂ capture absorption process.

The main problem in the post-combustion CO₂ capture using absorption process is significantly high regeneration energy. The energy requirement in absorption process for regeneration of solvent and steam use is estimated around 2.7-3.3 GJ/tCO₂, which is regarded very high.² The energy penalty for CO₂ capture using aqueous MEA solvent in a coal-fired power plant is approximately 25-40%.⁶ For CO₂ capture process to be energy efficient, the solvent regeneration has to be improved and needs to be looked into more detail in order to reduce the associated energy penalty.

Moreover, the presence of oxygen in flue gas mixture in absorption process results in oxidative degradation and corrosion. The process also suffers from chemical degradation due to presence of impurities like SO_x , NO_x in the flue gas mixture. The above mentioned problems of high regeneration energy and degradation pose a significant challenge in the economic efficiency of the absorption system for post-combustion CO_2 capture. Improvements in the absorption process are needed to increase the efficiency of the process and reduce the energy penalty.

1.2.1.2 Adsorption process

Adsorption process using solid adsorbents is gaining significant attention as an alternative CO_2 capture technique under post-combustion conditions.¹⁶ The solid adsorbents show great promise as they are easy to use and needs low regeneration energy.¹⁰ Solid adsorbents release less waste and waste management is easier as compared to liquid absorption process.¹⁷ Generally, solid adsorbents are classified into two types based on their interaction with CO_2 : 1) physical adsorbents and 2) chemical adsorbents. The physical adsorbents such as carbon based materials, alumino-silicate materials like zeolites, MOFs, etc. interact with CO_2 via physical adsorption only. On the other hand, chemical adsorbent materials interact with CO_2 via chemical reaction. The chemical adsorbents usually contain some basic functional groups which can react with CO_2 from the flue gas mixture and selectively separates CO_2 from the flue gas. Most of the chemical adsorbents contain amino functional group to separate CO_2 .

CO₂ capture using solid adsorbents comprises two segments. In the first segment, CO₂ is adsorbed over the selected solid adsorbent material and then in the second segment, the solid adsorbents are regenerated by desorption of CO₂ from the solid adsorbents. Adsorption and desorption are combined to form one complete CO₂ capture cycle. Several cyclic processes like Pressure Swing Adsorption (PSA), Vacuum Swing Adsorption (VSA), Electric Swing Adsorption (ESA), Temperature Swing Adsorption (TSA) have been studied for application using solid adsorbents. The cyclic process to be used depends on the type of adsorbent used and the conditions of the operation.

There have been many solid adsorbents available in the literature but each one lags in some way. There are many factors which describe the quality of a CO₂ adsorbent. The key criteria for the selection of a solid adsorbent for CO₂ capture are described below:^{11,18}

1. Adsorption capacity: Equilibrium adsorption capacity, by definition, is the maximum possible amount of CO₂ adsorbed by the adsorbent at given capture conditions. Adsorption capacity needs to be sufficiently high in order for the adsorbent to be effective in post-combustion capture conditions of low pressure and low CO₂ partial pressure. Generally, any adsorbent takes very long time to reach equilibrium adsorption capacity, so in order to be more practical the adsorbent should have high working adsorption capacity (adsorption capacity in some specified time period) rather than equilibrium adsorption capacity so that the adsorbent can work in the industrial scale

- where cycle time has to be short. The CO₂ working adsorption capacity is suggested to be around 3-4 mmol/g for the adsorption process to be comparable with amine based absorption process.¹¹
2. Kinetics: The adsorbent should be able to adsorb and desorb CO₂ fast enough to allow short cycle time. The number of adsorption/desorption cycles increase as the cycle time reduces, which in turn means more CO₂ capture. Fast adsorption kinetics is indicated by sharp increase in the sorption capacity of the adsorbent at the start of adsorption. Similarly, fast desorption kinetics is indicated by sharp decrease in the sorption capacity of the adsorbent at the start of desorption.
 3. Long-term stability: The adsorbent can only be useful for practical purposes if it can last long enough to justify its cost. The adsorbent should be able to regenerate completely over large number of cycles and maintain its adsorption capacity. Other important qualities for any adsorbent to have long-term usability are mechanical and hydrothermal stability.
 4. Regeneration Energy: The main problem of aqueous amine based absorption system is high regeneration energy of the process. In order for adsorption process to be cost effective than absorption process, the adsorbent should be able to regenerate in mild conditions with low energy input. Regeneration energy is indicated by heat of adsorption of the adsorbent. Normally, physical adsorbents have heat of adsorption around -25 to -50 kJ/mol CO₂ whereas chemical adsorbents' heat of adsorption vary from -60 to -90 kJ/mol CO₂.¹¹

Chemical adsorbents normally require higher regeneration energy than physical adsorbents, making the latter more cost-effective.

5. Selectivity: The adsorbent should be highly selective towards CO₂ in presence of other components of flue gas mixture. Generally, chemical adsorbents are more selective than physical adsorbents. Some adsorbents lose CO₂ adsorption capacity in the presence of moisture. As post-combustion flue gas mixture contains appreciable quantity of moisture, so the adsorbent should retain its CO₂ adsorption capacity in the presence of moisture in humid flue gas stream. Flue gas impurities like SO_x, NO_x are also known to hinder the CO₂ selectivity of some adsorbents, especially by irreversibly adsorbing on the adsorbent and deactivating it permanently.
6. Cost: The cost of the adsorbent should be reasonable enough to make the CO₂ capture process economical. Tarka et al.¹³ estimated the effect of adsorbent cost on the total finances of the capture process. It was observed that \$15 per kg adsorbent leads to unfavourable economics while \$5 per kg adsorbent is economical for the process. For the capture process to be economical, it can be concluded that the cost of adsorbent is inversely proportional to its adsorption performance, eg. adsorbent with moderate performance should be available at very low cost and adsorbent with very good performance can be expensive. Hence economics of the capture process will make more sense in terms of \$ per kg of CO₂ captured.

The on-going experimental and theoretical research activities till now on the adsorption process using solid adsorbents have shown that it has good potential for post-combustion CO₂ capture in comparison to conventional amine based absorption process due to the lower regeneration energy requirement and reduced corrosion issues using adsorption process. The next chapter will provide discussion on various different solid adsorbents used for post-combustion CO₂ capture in the literature.

References

1. Climate Change 2007: Synthesis Report. Core Writing Team, Pachauri, R. K.; Reisinger, A., Eds.; IPCC, Geneva, Switzerland.
2. Metz, B.; Davidson, O.; de Coninck, H.; Loos, M.; Meyer, L. Intergovernmental Panel on Climate Change. Special Report on Carbon Dioxide Capture and Storage, Cambridge University Press, Cambridge, 2005, <http://www.ipcc.ch/>.
3. IPCC, 2007: Summary for Policymakers. In: Climate Change 2007: The Physical Science Basis, Cambridge University Press, Cambridge, UK 2007.
4. IEA, Energy Technology Perspectives 2010- Scenarios & Strategies to 2050. 2010; p 650.
5. IEA Technology Roadmap: Carbon Capture and Storage, 2009.
6. Electric Power Research Institute, Program on Technology Innovation: Post-combustion CO₂ Capture Technology Development, Electric Power Research Institute, Palo Alto, 2008.
7. Herzog, H. J. What future for carbon capture and sequestration? *Environ. Sci. Technol.* **2001**, 35, 148A–153A.
8. Yang, H.; Xu, Z.; Fan, M.; Gupta, R.; Slimane, R. B.; Bland, A. E. Progress in carbon dioxide separation and capture: A review. *J. Environ. Sci.* **2008**, 20, 14–27.
9. D'Alessandro, D. M.; Smit, B.; Long, J. R. Carbon dioxide capture: Prospects for new materials. *Angew. Chem. Int. Ed.* **2010**, 49 (35), 6058-6082.
10. Eide, L. I.; Bailey, D. W. Precombustion decarbonisation processes. *Oil Gas Sci. Technol.* **2005**, 60, 475.
11. Samanta, A.; Zhao, A.; Shimizu, G. K. H.; Sarkar, P.; Gupta, R. Post-combustion CO₂ capture using solid sorbents—A review. *Ind. Eng. Chem. Res.* **2012**, 51, 1438-1463.
12. Yang, W. C.; Hoffman, J. Exploratory design study on reactor configurations for carbon dioxide capture from conventional power plants employing regenerable solid sorbents. *Ind. Eng. Chem. Res.* **2009**, 48, 341-351.

13. Tarka, T. J.; Ciferno, J. P.; Gray, M. L.; Fauth, D. CO₂ capture systems using amine enhanced solid sorbents. *5th annual conference on carbon capture & sequestration* **2006**, paper 152.
14. Aaron, D.; Tsouris, C. Separation of CO₂ from flue gas: A review. *Sep. Sci. Technol.* **2005**, 40, 321-348.
15. Pennline, H. W.; Luebke, D. R.; Jones, K. L.; Myers, C. R.; Morsi, B. I.; Heintz, Y. J.; Ilconich, J. B. Progress in carbon dioxide capture and separation research for gasification-based power generation point sources. *Fuel Process. Technol.* **2008**, 89, 897-907.
16. Sjostrom, S.; Krutka, H. Evaluation of solid sorbents as a retrofit technology for CO₂ capture. *Fuel* **2010**, 89 (6), 1298-1306.
17. Harrison, D. P. The role of solids in CO₂ capture: A mini review. *Greenhouse Gas Control Technologies 7* **2005**, 2, 1101-1106.
18. Sayari, A.; Belmabkhout, Y.; Serna-Guerrero, R. Flue gas treatment via CO₂ adsorption. *Chem. Eng. J.* **2011**, 171, 760-774.

Chapter 2

Literature Review

The content of this chapter is arranged as:

- Overview of adsorption process discussing the three factors (kinetic effect, thermodynamic equilibrium effect, molecular sieving effect) on which it works. The molecular properties of CO₂ and N₂ are compared for adsorption based separation process.
- Literature review of the adsorption performance of physical adsorbents for post-combustion CO₂ capture is summarized. Three different carbon-based adsorbents: activated carbons, carbon nanotubes and carbon molecular sieves are discussed. Zeolite-based adsorbents and metal organic frameworks are the other physical adsorbents that are reviewed in this chapter.
- Amine functionalized solid adsorbents are the chemical adsorbents which are discussed in this chapter. Reaction mechanism of the adsorption of CO₂ over amine functionalized adsorbents is explained in brief. Review is done for two different types of amine functionalized sorbents: amine impregnated adsorbents and amine grafted adsorbents.
- The problems associated with conventional fixed and fluidized beds are described for gas separation applications like post-combustion CO₂ capture. Commonly studied structured bed configurations in the literature, mainly

monolith, parallel passage contactor, hollow fiber bed configurations, are discussed as possible replacements.

- Motivation for studying the performance of DAEAPTS amine grafted SBA-15 adsorbent for post-combustion CO₂ capture is explained. Also, justification is given for choosing structured bed configuration with straight gas flow channels for post-combustion CO₂ capture. In the end of this chapter, the major objectives of the present study are listed.

2.1 Overview

Adsorption process has received considerable attention in the past few years as a viable alternative process for post-combustion CO₂ capture. Several adsorbents have been tried and identified in the literature as good potential for CO₂ capture. The adsorption process for gas separation normally works based on three factors:¹

- 1) Kinetic Effect: Different diffusion rates of gas components allows gas separation by kinetic effect.
- 2) Thermodynamic Equilibrium Effect: The difference in interactions of the different gas components with the adsorbent surface allows gas separation by thermodynamic equilibrium effect.
- 3) Molecular Sieving Effect: Molecular sieving effect makes use of the difference in size and shape of various gas components for gas separation.

The difference in two main components, CO₂ and N₂, of flue gas mixture in post-combustion CO₂ capture is very small. The kinetic diameter, quadrupole moment

and polarizability of CO₂ and N₂ is tabulated in Table 2.1.¹ It can be observed from this Table that CO₂ and N₂ have very close kinetic diameters which makes their separation very difficult whereas N₂ has lower polarizability and quadrupole moment as compared to CO₂.

Table 2.1. Comparison of CO₂ and N₂ on the basis of kinetic diameter, polarizability and quadrupole moment.¹

Property	CO₂	N₂
Kinetic diameter [Å]	3.30	3.64
Polarizability [$\times 10^{-25}$ cm ³]	26.3	17.6
Quadrupole moment [$\times 10^{-40}$ Cm ²]	13.4	4.7

This chapter discusses the different types of physical and chemical adsorbents used for post-combustion CO₂ capture in the literature. Physical adsorbents that are covered in this chapter are: carbon-based adsorbents, zeolite-based adsorbents and MOFs. Amine functionalized porous materials are the chemical adsorbents that are discussed in detail in this chapter.

The success of each of these adsorbent materials is also dependent on the contactor type which can utilize their potential and minimize related energy costs. Several bed configurations have been used for post-combustion CO₂ capture to make maximum use of the adsorbent potential. This chapter also provides a review on the different bed configurations used in the literature for CO₂ capture.

2.2 Physical adsorbents

Many physical adsorbents have been tested for post-combustion CO₂ capture. This section provides a discussion on some of the important physical adsorbents used in the literature: 1) carbon-based adsorbents, 2) zeolite-based adsorbents, and 3) MOFs. The discussion includes a brief overview of the adsorption performance of the adsorbents and their usefulness for post-combustion CO₂ capture.

2.2.1 Carbon-based adsorbents

Three main carbon-based adsorbents will be discussed here: 1) Activated carbon, 2) Carbon nanotubes, and 3) Carbon molecular sieves. Structural properties of different carbonaceous solid adsorbents are given in Table 2.2.² Table 2.3 presents the CO₂ adsorption capacity of different carbonaceous solid adsorbents used in the literature.²

Table 2.2. Textural properties of different carbonaceous solid adsorbents.²

Adsorbent	BET Surface Area [m ² /g]	Pore Size [nm]	Pore Volume [cm ³ /g]	Reference
AC	1300	1.5-2.2	0.6-0.8	3
AC-h ^a	2829	2.19	1.55	4
Granular AC	954	2	0.48	5
BPL carbon	1100		0.7	6
CNT	394	8.9	0.91	5
SWNT	1587		1.55	7

a: High surface area activated carbon

Table 2.3. CO₂ adsorption capacity with operating conditions of different carbonaceous solid adsorbents used in the literature.²

Adsorbent	p (CO ₂) ^a [atm]	Temperature [°C]	Process	Capacity [mmol/g]	Reference
AC	1	298	PSA	2.07	8
AC	1	288	PSA	2.45	9
AC	0.2	298		0.75	10
AC	1	298		3.23	3
AC	1	298	PSA	2.61	11
AC	0.1	298	GC-TCD	0.57	5
AC A35/4	1	293	Flow desorption	2	12
AC F30/470	1	288	Volumetric analysis	2.86	13
AC F30/470	0.16	297.3		0.65	14
AC RB	1	303		1.22	6
AC Norit RB1	1	294.2	Gravimetric analysis	2.46	15
AC Norit RB1	0.15	313.1	TPD	0.5	16
AC Norit R1 Extra	0.15	298		0.54	17
Bamboo based AC	2	275	Volumetric analysis	3	18
Anthracite based AC	1	303	TGA	1.38	19
SWCNT	1	308		2.07	7
Grapheme	1	195		0.8	20
CMS	1	303		2.43	21

a: p (CO₂) = CO₂ partial pressure

2.2.1.1 Activated Carbon (AC)

Activated carbon is the most common carbonaceous solid adsorbent used in the literature. The main advantage of activated carbon is they are easy to prepare and inexpensive on industrial-scale production because of wide availability of cheap raw materials.²² Synthesis of activated carbon is a two-step process: 1) carbonization, and 2) activation. The carbonization step involves the pyrolysis of the raw material at a high temperature in inert environment to produce char. Char is carbon rich material with very low porosity and surface area. In the activation step, char is activated to produce adsorbent with high porosity and large surface area.²³ The activation process can be either physical or chemical. In physical activation process, char is partially gasified and heated at high temperature.²⁴ Chemical activation process involves treatment with chemicals like KOH, H₃PO₄, etc.²⁵ AC can be synthesized by either physical/chemical activation of carbonaceous solid materials like coal (bituminous, lignite), fly ash, biomass sources (saw dust, coffee pulp, corn stark, etc.), etc.²³ The type of activation process and the activation conditions produce large variation in the structural properties of the synthesized activated carbon adsorbents. Maroto-Valer et al.¹⁹ performed experiments on anthracite based carbon adsorbents prepared with different activation time and temperature and found that adsorbents prepared at different conditions have different structural properties. It was observed that after 2 h of activation at 890 °C, the maximum pore volume and surface area attained was around 0.6 ml/g and 1071 m²/g respectively. In this work, the highest adsorption capacity reported was around 1.49 mmol/g, which is for carbon

activated at 800 °C with 540 m²/g specific surface area. Here, the highest adsorption capacity was not obtained for activated carbon having maximum pore volume and surface area but for AC with much lower surface area. So, it can be observed that all the pores were not able to adsorb CO₂ and only some pores with certain minimum size were good enough for CO₂ adsorption.

Do and Wang¹⁰ examined the impact of sorption temperature on the adsorption performance of Ajax activated carbon and reported that CO₂ adsorption capacity decreased from 0.75 mmol/g to 0.1 mmol/g as adsorption temperature varied from 25 to 100 °C. Na et al.³ also observed reduction in activated carbon sorption capacity from 3.2 mmol/g at 15 °C to 1.5 mmol/g at 55 °C. It was found that the sorption capacity of AC adsorbents reduce with increase in adsorption temperature.

Sircar et al.²² observed the effect of equilibrium pressure on the adsorption capacity of AC adsorbents and found capacity of 10 mmol/g at 30 °C and 10 bar pressure whereas the adsorption capacity dropped significantly at lower pressures around 1 bar. Sayari et al.²⁶ summed up that the CO₂ over N₂ selectivity of AC lies within 1.2-2 at the adsorption temperature of 25 °C, which is quite low. It was found that the sorption capacity of AC adsorbents reduces considerably in the presence of water due to water adsorption. Water adsorbs competitively with CO₂ on activated carbon which limits the amount of CO₂ adsorption in the presence of moisture.

Although activated carbon have many advantages like fast kinetics, low regeneration energy and low cost but their adsorption capacity and selectivity is only good at low adsorption temperature and high pressure conditions. Post-combustion capture demands low pressure adsorption where activated carbons have very low capacity and selectivity. AC sorbents are also negatively influenced by presence of moisture which is present in post-combustion flue gas mixture. Overall, as of now, activated carbons do not look like good prospect for CO₂ capture in post-combustion conditions.

2.2.1.2 Carbon Nanotubes (CNTs)

Carbon nanotube based solid adsorbents has received a lot of attention in the last few years for their application in CO₂ capture. The controllable structural properties of CNTs have highlighted them for usage in CO₂ capture. Cinke et al.⁷ studied the performance of SWCNT (Single-Walled Carbon NanoTube) in 0-200 °C temperature interval. SWCNT adsorbents showed very good structural properties with pore volume and surface area around 1.55 cm³/g and 1587 m²/g respectively. The adsorbent was reported to give 2 times more adsorption capacity than with activated carbon. Huang et al.²⁷ found that the adsorption capacity of CNTs lies in the range of 4 to 9 mmol/g and observed higher selectivity than ACs, zeolite 13X and MOFs. The adsorption capacity was found to be increasing with the diameter of CNTs. Razavi et al.²⁸ reported that carbon nanotube based solid adsorbents have better CO₂ selectivity than other carbonaceous adsorbents.

Although the adsorption performance of CNTs seems to be better than ACs but they are much more expensive than ACs. The unit cost of CNT is estimated around US \$5/g whereas granular AC costs only around US \$1/g.²⁹ CNT looks promising but more research work is required to understand their adsorption behaviour and their application for CO₂ capture. The cost factor also needs to be put into equation to determine their true potential.

2.2.1.3 Carbon Molecular Sieves (CMSs)

CMSs are microporous carbon materials which can separate gas mixtures on the basis of their kinetic properties and molecular sieving effect like zeolites.³⁰ The textural properties of CMSs allow the separation of gas mixtures because of different diffusion rates of various gas components. Burchell et al.²¹ prepared monolithic CMS material and evaluated its adsorption capacity to be more than 2.27 mmol at 30 °C and 1 atm but the capacity reduced at higher temperatures. Rutherford and Do³¹ performed the equilibrium and kinetics study on Takeda 5A CMS material and observed that the diffusion is slow and the rate-limiting step is micropore diffusion. No molecular sieving effect was observed for this CMS material. Hence, the micropore size and volume of CMS adsorbents have to be sufficiently large to ensure fast diffusion of CO₂ molecules for CO₂ separation from flue gas. Alcañiz-Monge et al.³² used nitrated coal tar for the synthesis of carbon monoliths and studied kinetics of this material for CO₂ capture. They observed that carbon monoliths have faster kinetics than the commercially available CMS material Takeda 3A.

Overall, the structural properties like pore size and pore volume must be high enough for CMS materials to find any practical use for CO₂ capture. Not much work has been done on CMS materials for their application in CO₂ capture. The worth of these materials for CO₂ capture will be known only after some comprehensive study testing all the important criteria for adsorbent selection such as adsorption capacity, selectivity, stability, energy penalty, kinetics, etc.

2.2.2 Zeolite-based adsorbents

Table 2.4. Textural properties of different zeolite-based solid adsorbents.²

Adsorbent	BET Surface Area [m ² /g]	Pore Size [nm]	Pore Volume [cm ³ /g]	Reference
NaX	508	1	0.201	33
NaY	811	1.54	0.46	34
CsX	404		0.14	35
CsY	473	1.58	0.21	34
Zeolite 13X	515	1.1	0.454	36
Chabozite	485	0.43	4.2	37
Clintopile ^a	13.3	0.44	4.5	37
Erionite	426		0.22	38
Mordenite	266		0.19	38
clinoptilolite	23		0.066	38

a: Potassium calcium sodium aluminosilicate.

Table 2.5. CO₂ adsorption capacity with operating conditions of different zeolite-based solid adsorbents used in the literature.²

Adsorbent	p (CO ₂) ^a [atm]	Temperature [°C]	Process	Capacity [mmol/g]	Reference
Zeolite 13X	0.15	293		2.6	39
Zeolite 13X	1	295		4.6	40
Zeolite 13X	1	298		4.7	41
NaX	1	305	Gravimetric analysis	5.7	42
NaY	1	305	Gravimetric analysis	5.5	42
NaY	1	295		4.1	40
NaM	1	298	Gravimetric analysis	2.9	42
Silicalite	0.15	303	Calorimeter- volumetric apparatus	0.5	43
Na-ZSM-5	1	303	GC	0.7	44
MS 13X ^b	1	298	PSA	2.8-3.6	11
MS 4A ^b	1	298	PSA	2.3-3.1	11
MS 13X ^b	0.15	293		2.2	45
MS 4A ^b	0.15	293		1.6	45
MS 13X ^b	0.1		Fluidized bed	2.3	46
MS 5A ^b	0.1		Fluidized bed	2.3	46
Erionite – ZAPS	1	290		2.8	38
HZSM-5-30	1	295		1.9	40

a: p (CO₂) = CO₂ partial pressure

b: MS = Molecular Sieve

Zeolites are crystalline materials which have been used extensively for gas separation. Zeolites are made up of silicate frameworks with some of the Si substituted with Al or some other metal. Each Al causes one negative charge in the framework which is balanced by cations. The framework is made up of interconnected voids occupied by cations and the pore size can be tuned by

exchanging the cations. The size, charge distribution and charge density of these cations is mainly responsible for gas separation in zeolites. Zeolites generally have uniform pore size ranging within 0.5 - 1.2 nm.⁴⁷ Zeolites can separate gas species on the basis of difference in their sizes due to their narrow and uniform pore size distribution. The electric field generated by the free cations in zeolites enable them to separate gas components from a gas mixture on the basis of difference in their quadrupole moments. Table 2.4 provides the structural properties of different types of zeolites used in the literature for CO₂ adsorption.² The performance of various different kinds of natural and synthetic zeolites for CO₂ capture has been investigated in the literature. Adsorption capacities of various zeolites reported in the literature with respective conditions are tabulated in Table 2.5.²

Harlick and Tezel⁴⁰ compared the CO₂ sorption performance of 13 synthetic zeolites. CO₂ sorption capacities of these zeolites were observed as shown below:



Zeolites with lower Si/Al ratio showed higher adsorption capacities due to presence of more cations in lower Si/Al ratio zeolites which can interact with CO₂. Zukal et al.⁴⁸ compared 6 high silica zeolites ($\text{SiO}_2/\text{Al}_2\text{O}_3 > 60$) for CO₂ capture performance. At 1 bar, IM-5 and TNU-9 zeolites showed highest sorption capacities of 2.42 and 2.61 mmol/g respectively.

Brandani and Ruthven⁴⁹ observed that the adsorption capacity of zeolites (like LiLSX, NaLSX, CaX) drops sharply in the presence of H₂O due to preferential adsorption of water over zeolites. The preferential adsorption of water heavily reduces the CO₂ sorption in the presence of even small amount of moisture. It was reported that as the moisture content varied from 0.8 wt% to 16.1 wt%, the adsorption capacity of zeolite CaX decreased from 2.5 mmol/g to 0.1 mmol/g at 50 °C and 6 kPa CO₂ partial pressure.

In short, zeolites exhibits good CO₂ adsorption capacity with fast kinetics of the order of minutes and low regeneration energy but their performance is heavily affected by operating temperature and pressure. The adsorption capacity is high only near room temperature and starts dropping down as the temperature go high or as the pressure decreases. The adsorption capacity is also negatively influenced by presence of moisture in the flue gas mixture, which is the case in post-combustion conditions. So, further tuning of parameters like pore size, cation types, etc. is required in order for the zeolites to overcome above mentioned problems so that they can be effective for post-combustion carbon capture applications.

2.2.3 Metal Organic Frameworks (MOFs)

MOFs are relatively new crystalline adsorbents with high porosity and surface area.⁵⁰ MOFs are made up of metal ions bridged with organic ligands. The controllable pore size, shape and chemical functionality of MOFs has attracted

large interest for application in CO₂ capture. MOFs are classified into three types based on the stability of their crystal structure:⁵¹

- 1) Type I: Non-porous and damage irreversibly.
- 2) Type II: Keep their structure stable and adsorb gas reversibly.
- 3) Type III: Adsorb gas reversibly by changing their structures.

Type II MOFs behave like zeolites and find wide application in gas separation. Type III MOFs have led to different adsorption mechanisms like “breathing-type” or “gate effect” and can be great potential for CO₂ capture.⁵²⁻⁵⁴

Furukawa et al.⁵⁵ prepared MOF-210 with pore volume and surface area of 3.60 cm³/g and 6240 m²/g respectively. These values reported in this work are the highest values for any crystalline adsorbent material. The adsorption capacity observed for this material was 2400 mg/g at 50 atm and room temperature. Liu et al.⁵⁶ tested the performance of their adsorbent Ni-MOF74 in post-combustion capture conditions and reported sorption capacity of 3.28 mmol/g at 25 °C and 0.1 atm CO₂ partial pressure. The capacity reported for Ni-MOF74 was higher than that of zeolite 5A and NaX in the same conditions. The effect of H₂O on the sorption performance of Ni-MOF74 was also studied in this work. It was observed that drop in capacity due to presence of water was lower than that in zeolite 5A and NaX. The adsorbent was also shown to be stable over 10 cycles. This work provided the first complete analysis of CO₂ capture performance of MOFs in the presence of H₂O. The Ni-MOF74 material reported in this work has shown great potential for utility in post-combustion CO₂ capture.

Most of the work on MOFs has shown high capacity and selectivity at very high pressures and very few studies have been performed for low CO₂ pressure. But for application in post-combustion conditions their performance at low CO₂ partial pressure needs thorough investigation. MOFs are still new and hold great promise for CO₂ capture but more research work is required focussing on the real industrial post-combustion flue gas conditions.

2.3 Chemical adsorbents

The problem with physical adsorbents (carbon based adsorbents, zeolite based adsorbents, MOFs, etc.) is their low adsorption capacity and selectivity at post-combustion conditions of low CO₂ pressure. There is growing interest in the research field for the use of chemical adsorbents to improve adsorption capacity and selectivity of solid adsorbents by chemical modification of the high surface area materials. One common technique of chemical modification is by employing basic amino groups on the high surface area porous supports (mainly silica based) to chemically adsorb acidic CO₂ with higher selectivity and capacity. This section provides an overview on the use of amine functionalized solid adsorbents for CO₂ capture.

2.3.1 Amine functionalized solid adsorbents

Amine functionalized adsorbents have been widely used for application in post-combustion CO₂ capture. In comparison to aqueous amine based absorption process, amine functionalized solid adsorbents offer several advantages. In the

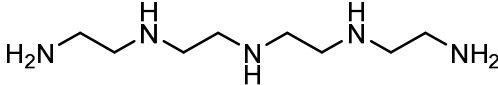
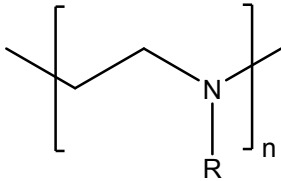
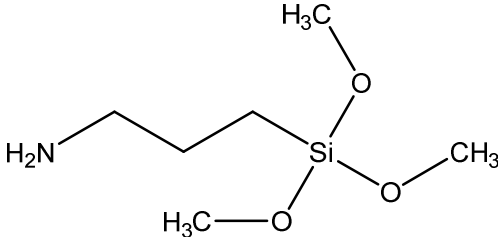
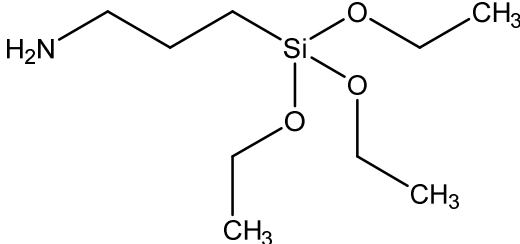
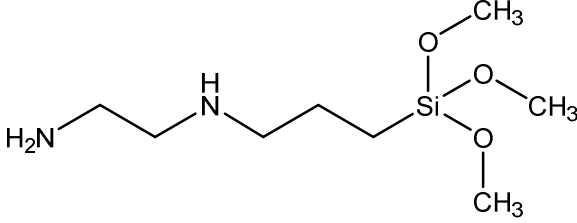
CO₂ stripping step, water in the aqueous amine based system needs considerably large quantity of energy to heat up. This heat energy can be reduced heavily by using solid silica based adsorbents having lower heat capacity instead of aqueous amine solvents. Mesoporous silica support SBA-15 has heat capacity of around 0.8 kJ/(kg.K)⁵⁷ whereas heat capacity for H₂O is 4.2 kJ/(kg.K). Amine functionalized solid adsorbents are also less prone to degradation as in aqueous amine based systems due to vaporization of water. However, amine functionalized solid adsorbents face challenges in the form of lower adsorption capacity and more expensive adsorbent material than aqueous amine based system.

Table 2.6 presents structures of various amines commonly used in the literature for functionalization of porous solid supports. Based on the interaction of amine with porous support, amine functionalized solid adsorbents have been categorized into three groups:²

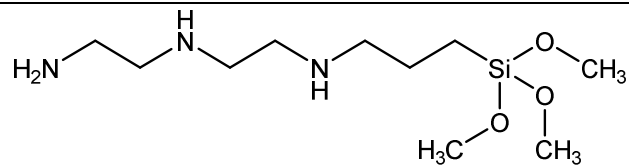
1. Class 1: Amine impregnated porous solid supports, in which amine is physically loaded over porous solid support. No chemical reaction takes place between amine group and support material.
2. Class 2: Amine grafted porous solid supports, in which silane group amines are covalently bonded over the porous support. In this class, amine groups are tethered to the porous support by covalent bonds. Since the connection between amine group and support is much stronger than amine impregnated solid adsorbents, this class of material show great promise for long-term application.

3. Class 3: Mixture of above two classes. This class of materials are prepared by in-situ polymerization of amino-polymers with porous solid supports.⁵⁸

Table 2.6. Structure of different amines used for adsorbent functionalization in the literature.

Tetraethylenepentamine (TEPA)	
Polyethylenimine (PEI)	 <p data-bbox="719 846 1255 877">(R = H for linear, R = H or CH_x for branched)</p>
3-aminopropyltrimethoxysilane (APTS)	
3-aminopropyltriethoxysilane (APTES)	
N-[3-(trimethoxysilyl)propyl]-ethylenediamine (AEAPTS)	

N-(3-trimethoxysilylpropyl)-
diethylenetriamine
(DAEAPTS)



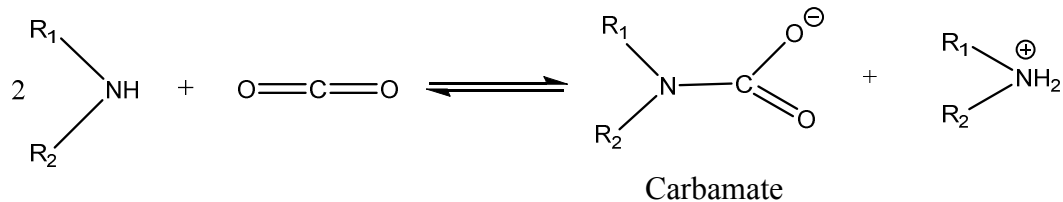
Aziridine



2.3.1.1 Reaction mechanism

Amine functionalized adsorbents adsorb CO₂ by chemical adsorption where reaction takes place between amine group and CO₂. Therefore, it is important to explain the mechanism of that reaction in order to understand its effect on kinetics and amine efficiency of the adsorbent. Amine efficiency is defined as the molecules of N (Nitrogen) required to adsorb each molecule of CO₂. Primary/secondary amino groups react with CO₂ directly and produce carbamates via zwitterion intermediates. This mechanism was first reported by Caplow.⁵⁹ This mechanism is explained in two steps: 1) carbon from CO₂ reacts with lone electron pair of primary/secondary amine to form zwitterion, 2) deprotonation of zwitterion with free base to produce carbamate.⁶⁰ In the absence of water, amine acts as base in the second step whereas in the presence of water, hydroxide ion from water molecule can act as the base. The reaction mechanism in the absence of H₂O for primary/secondary amines is shown as:

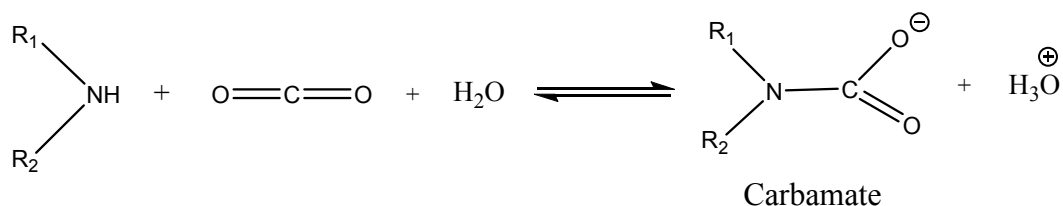
Reaction (1):



where $R_1 = \text{H}$ for primary amine

Amine efficiency for primary/secondary amines in the absence of water from Reaction (1) comes out as 0.5 mol CO_2 / mol N. Reaction mechanism in the presence of water for primary/secondary amines to produce carbamate is given as:

Reaction (2):

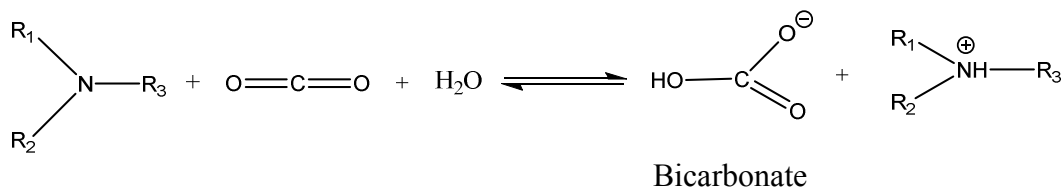


where $R_1 = \text{H}$ for primary amine

From Reaction (2), amine efficiency for primary/secondary amines in the presence of water is 1 mol CO_2 / mol N. Tertiary or sterically hindered primary/secondary amines⁶¹ cannot react with CO_2 directly and requires base like water for reaction with CO_2 . These amines use different reaction mechanism than shown above although this mechanism can be used by primary/secondary amines also. This reaction mechanism involves three steps: 1) amine reacts with water to produce hydroxide ion and quaternary ion, 2) CO_2 reacts with hydroxide ion to give bicarbonate ion, 3) bicarbonate ion associates with quaternary cation to

capture CO₂.⁶⁰ This mechanism was first proposed by Donaldson and Nguyen⁶² and later summarized by Vaidya and Kenig⁶³. The reaction mechanism for CO₂ capture in the presence of water to form bicarbonate is given as:

Reaction (3):



where, R₁ = H for secondary amine

R₁ = R₂ = H for primary amine

Amine efficiency using Reaction (3) for tertiary or sterically hindered primary/secondary amines in the presence of water is 1 mol CO₂/ mol N.

2.3.1.2 Amine impregnated solid adsorbents

Xu et al.⁶⁴ was the first work to use the amine impregnated over porous silica support for CO₂ capture and named the adsorbent “molecular basket”. This group impregnated high surface area mesoporous silica support MCM-41 with PEI using wet impregnation technique.⁶⁴⁻⁶⁸ Xu et al.⁶⁶ impregnated MCM-41 with PEI using one-step wet impregnation method. The reported adsorption capacity for impregnated adsorbent containing 75 wt% PEI was 3.02 mmol/g under pure CO₂ at 75 °C. Higher adsorption capacities were found for higher loadings of PEI. Xu et al.⁶⁶ observed that working adsorption capacity increases with adsorption temperature as opposed to physical adsorbents like carbon, zeolites. The lower working sorption capacity at lower adsorption temperatures around 25 °C was due

to the result of diffusion limitation in limited adsorption time. Equilibrium adsorption capacity at lower temperatures was found to be higher than that at elevated temperatures. This group⁶⁴⁻⁶⁸ thoroughly investigated the adsorption performance of PEI impregnated MCM-41. Under flue gas comprising 14.9% CO₂/80.85% N₂/4.25% O₂, CO₂/N₂ selectivity > 1000 and CO₂/O₂ selectivity around 180 was reported in 25-100 °C temperature range.⁶⁷ The adsorbent showed stability after 10 adsorption-desorption cycles at 75 °C. The presence of moisture in small amount positively influenced the adsorption performance of adsorbent by increasing adsorption capacity. Whereas the presence of NO_x negatively impacted the performance of adsorbent as NO_x competitively adsorbed with CO₂.^{65,68} Ma et al.⁶⁹ impregnated PEI over SBA-15 and obtained 3.18 mmol/g sorption capacity for amine loading of 50 wt% at 75 °C and 15 kPa CO₂ partial pressure. Under same conditions, this capacity was 50% higher than the sorption capacity found for PEI loaded MCM-41. The increase may be because SBA-15 has higher pore volume, surface area and pore size.

Ahn's group⁷⁰ impregnated 50 wt% PEI over variety of mesoporous silica supports (KIT-6, SBA-15, MCM-41, SBA-16, MCM-48) and compared their performance. All the adsorbents displayed high adsorption capacities, fast kinetics and stability. The CO₂ adsorption capacities of these adsorbents were found to be in the order of their average pore diameters. The order of adsorption capacities observed as MCM-41 ($d_p = 2.1$ nm) < MCM-48 ($d_p = 3.1$ nm) < SBA-16 ($d_p = 4.1$

nm) < SBA-15 ($d_p = 5.5$ nm) < KIT-6 ($d_p = 6.5$ nm), where d_p represents the average pore diameter (pore size).

Zhao et al.⁷¹ impregnated SBA-15 with TEPA and studied its multi-cycle stability for 10 cycles. The results showed CO₂ adsorption capacities of 3.48 mmol/g and 3.67 mmol/g after first cycle in dry and humid 10% CO₂/ 90% N₂ gas mixture at 75 °C respectively. For both dry and humid streams, it was found that the capacities decreased by around 10% after 10 adsorption/desorption cycles using N₂ as regeneration gas at 105 °C. After 10 cycles, TEPA leaching was observed around 8.2 wt% of fresh adsorbent in dry gas stream and 5.8 wt% of fresh adsorbent in humid gas stream. Hicks et al.⁷² loaded SBA-15 with TEPA and PEI. They observed that TEPA impregnated SBA-15 starts to drop capacity from 2nd cycle and capacity keeps on dropping further in subsequent cycles due to leaching of TEPA physically impregnated onto SBA-15 surface. For PEI impregnated SBA-15, it was found that the adsorbent material was sticky in nature and the adsorbent started clogging the adsorption column creating large pressure drop and reduction in volumetric flow rate. Drage et al.⁷³ impregnated their proprietary silica support material with PEI and observed consecutive loss in adsorption capacity after large number of adsorption-desorption cycles. CO₂ adsorption capacities with respective experimental conditions of various amine impregnated adsorbents reported in the literature are tabulated in Table 2.7.²

Table 2.7. CO₂ adsorption performance with operating conditions of different amine impregnated solid adsorbents reported in the literature.²

Support	Amine	Amine content [wt%]	p (CO ₂) ^a [atm]	Temp ^b [°C]	Adsorption capacity dry (humid) [mmol/g]	No. of cycles	Ref ^c
KIT-6	PEI	50	0.05	75	1.95		70
SBA-15	PEI	50	0.15	75	3.18		69
MCM-41	TEPA	50	0.05	75	4.54	6	74
SBA-15	PEI	50	0.01	75	1.52	20	75
SBA-15	PEI	60	0.15	75	3.50		76
Precipitated silica	PEI	67	1.00	100	4.55		77
PMMA	TEPA	41	0.15	70	(14.03)		78
SBA-15	TEPA	50	0.05	75	3.23	6	79
SBA-15	DEA+	50	0.05	75	3.61	6	80
	TEPA						
MCM-41	PEI	50	0.10	75	2.05		64
MCM-41	PEI	50	0.13	75	(3.08)	10	65
SBA-15	PEI	50	0.12	75	1.36		81
Mesoporous carbon	PEI	65	0.15	75	4.82	10	82
Silica-microsphere	TEPA	34	1	75	4.27	10	83
ACF ^d /CNT	PEI	11.6	1	60	2.75	5	84
PMMA	DBU	29	0.10	25	(3)	1	85
PMMA	DBU	29	0.10	65	(2.34)	6	85
PE-MCM-41	DEA	73	0.05	25	2.81 (2.89)		86

a: p (CO₂) = CO₂ partial pressure

b: Temp = Temperature

c: Ref = Reference

d: ACF = Activated carbon fiber

Overall, amine impregnated silica adsorbents display high sorption capacity and selectivity for CO₂ capture at low CO₂ partial pressure conditions. The adsorbents

show fast adsorption kinetics in the order of minutes. Their performance is not deteriorated in the presence of moisture and in some cases adsorption capacity enhanced by presence of moisture. But amine leaching and their regenerability over large number of cycles is still not satisfactorily answered. More research efforts are needed to completely overcome these challenges and justify their selection for post-combustion CO₂ capture.

2.3.1.3 Amine grafted solid adsorbents

The grafting technique provides stronger connection between amine and porous support and hence generated a lot of interest to develop amine functionalized adsorbents with potential of long term stability. First use of amine grafting on mesoporous ordered silica support was given in Leal et al.⁸⁷. This work used APTES amine for grafting on silica gel surface. The adsorbent exhibited CO₂ adsorption capacity of 0.41 mmol/g in dry and 0.89 mmol/g in humid pure CO₂ stream at 27 °C, which is very low as compared to other conventional solid adsorbents. This work observed that in the absence of H₂O two amine groups react with one CO₂ molecule as shown in Reaction (1) and in the presence of H₂O only one amine group is sufficient for each CO₂ molecule as shown in Reaction (2) and (3).

Khatri et al.⁸⁸ and Zheng et al.^{89,90} prepared several amine grafted SBA-15 adsorbents and found that the thermal degradation of grafted amino groups in the solid sorbents did not happen upto 250 °C. It was also observed that CO₂ sorption

capacity becomes negligible in the presence of SO₂ because of preferential adsorption, so there is a need to remove SO₂ from flue gas mixture before CO₂ capture using these adsorbents.⁸⁸ Delaney et al.⁹¹ grafted several silane group amines like APTS, AEAPTS, DAEAPTS, DEHAPTS on hexagonal mesoporous silica (HMS). These amine functionalized HMS materials were reported to give better adsorption capacity than that observed by Leal et al.⁸⁷ for functionalized silica gel. It was because of much higher surface area of HMS material (~1425 m²/g)⁹¹ as compared to silica gel (~340 m²/g)⁸⁷. Delaney et al.⁹¹ observed that around 2 N atoms are required for 1 CO₂ molecule for APTS, AEAPTS, DAEAPTS grafted HMS material whereas only around 1 N atom is required for 1 CO₂ molecule for DEHAPTS grafted HMS material. The reason being APTS, AEAPTS, DAEAPTS contain primary/secondary amino groups which capture CO₂ by carbamate formation (as shown in Reaction 1) but DEHAPTS contain tertiary amino group which cannot form stable carbamate via zwitterion and need hydroxyl group for CO₂ capture (as shown in Reaction 3).

As each silane group amine used for grafting has different structure and nitrogen content, so type of amine used for grafting also has significant influence in determining the performance of an adsorbent for CO₂ capture. Chaffee's group⁹²⁻⁹⁴ prepared APTS, AEAPTS and DAEAPTS grafted HMS adsorbents and examined their performance. It was seen that DAEAPTS grafted adsorbent has generally higher capacities than the analogous APTS, AEAPTS grafted adsorbents in dry conditions. But the DAEAPTS grafted adsorbents were found to have lower

amine efficiencies than the APTS, AEAPTS grafted ones.⁹⁴ The reason being reduced accessibility of amino group by the CO₂ molecules in DAEAPTS grafted materials due to more proximity of amino groups and entanglements provided by larger DAEAPTS molecules than smaller APTS, AEAPTS molecular structures. It was reported that, in both pure N₂ atmosphere and lightly oxygenated (2% O₂) N₂ atmosphere, all APTS, AEAPTS, DAEAPTS grafted adsorbents were stable till 170 °C and the adsorbents did not adsorb any N₂ or O₂. At 150 °C, the degradation of DAEAPTS grafted adsorbents were observed in more oxygen rich atmosphere (room atmosphere).⁹⁴ Hiyoshi et al.^{95,96} grafted APTES, AEAPTS, DAEAPTS on SBA-15 surface and determined the order of CO₂ adsorption capacity as DAEAPTS > AEAPTS > APTES in both dry and humid gas. The amine efficiency order for same amine loading was found as APTES > AEAPTS > DAEAPTS. It can be suggested from this result that the reason for this order of CO₂ sorption capacity most likely seems to be the presence of 3 amino groups in DAEAPTS, 2 amino groups in AEAPTS and 1 amino group in APTES. Although each amino group of DAEAPTS is not as effective as each amino group of AEAPTS/ APTES but overall good enough to give higher CO₂ adsorption capacity than the other two amines. Among the different amines used in the literature for grafting over silica support, DAEAPTS is very promising for synthesizing adsorbents using grafting technique because of its higher nitrogen content (around 15.8 wt%) and higher CO₂ adsorption capacity compared to other amines like APTS, AEAPTS, etc.

Sayari's group⁹⁷⁻¹⁰⁸ prepared pore expanded MCM-41 (PE-MCM-41) after pore expansion of MCM-41. This group grafted these PE-MCM-41 silica supports with silane group amine. The pore size of regular MCM-41 was increased from 3-4 nm to maximum of 20 nm whereas pore volume was increased from 0.7-1 cm³/g to maximum of 3.5 cm³/g on pore expansion to form PE-MCM-41. Surface area remained almost same on pore expansion.^{107,108} On comparison of DAEAPTS amine grafted MCM-41 and PE-MCM-41, it was observed that amine grafted PE-MCM-41 gives higher CO₂ adsorption capacity (50% higher) and faster kinetics (30% faster) than amine grafted MCM-41 using 5% CO₂/95% N₂ gas mixture at 25 °C.⁹⁷ Harlick and Sayari⁹⁸ optimized the grafting conditions to further improve the CO₂ adsorption performance. The optimum conditions reported for grafting DAEAPTS on PE-MCM-41 were: amount of DAEAPTS = 3 ml/g of silica support, amount of H₂O = 0.3 ml/g of silica support at 85 °C synthesis temperature. After using the optimized grafting process, CO₂ adsorption capacity of adsorbent prepared using conventional dry grafting increased from 1.55 to 2.65 mmol/g in 5% CO₂/95% N₂ gas mixture at 25 °C. Amine loading of DAEAPTS grafted PE-MCM-41 raised by around 30 wt% after following these optimum grafting conditions. This group compared the performance of zeolite 13X and DAEAPTS grafted PE-MCM-41. Under moist gas stream containing 27% RH in 5% CO₂/95% N₂ gas mixture, it was reported that the sorption capacity of DAEAPTS grafted PE-MCM-41 adsorbent (2.94 mmol/g) was significantly higher than that of zeolite 13X (0.09 mmol/g). The adsorption kinetics of amine grafted PE-MCM-41 was also much faster than that of zeolite 13X. Sayari and

Belmabkhout¹⁰⁶ studied the cyclic performance of amine grafted adsorbent. It was noticed that the adsorption capacity drops down gradually in dry conditions even at mild regeneration temperature of 70 °C (loses 15% capacity in around 750 cycles) but the adsorbent remains stable for over more than 700 cycles in humid conditions (7% RH at 70 °C). The adsorbent degradation in dry conditions was explained due to urea groups formation which do not regenerate under dry desorption conditions but these urea groups can be hydrolyzed in presence of moisture, thus the adsorbent maintained its capacity in humid conditions.

Jones research group^{72,109} proposed hyperbranched aminosilica (HAS) adsorbent to remove CO₂ from flue gas mixture. The synthesis process of the adsorbent involved one-step surface polymerization of the aziridine over SBA-15 surface which leads to aziridine ring opening inside SBA-15 to produce amine grafted HAS adsorbent. The HAS adsorbent showed stability over 12 cycles (130 °C desorption temperature) in humid conditions. The adsorption capacity reported in 10% CO₂/90% Ar humid gas mixture at 25 °C was 3.11 mmol/g.⁷² Drese et al.¹⁰⁹ tuned the synthesis process of HAS adsorbent in order to further improve the CO₂ sorption performance. After these modifications, the highest CO₂ adsorption capacity and corresponding amine loading reported were 5.55 mmol/g and 9.78 mmol N/g respectively in 10% CO₂/Ar humid gas mixture at 25 °C.

Table 2.8 presents the CO₂ adsorption performance of various amine grafted solid adsorbents reported in the literature.² Overall, amine grafted adsorbents have

shown high adsorption capacity, selectivity and fast kinetics under post-combustion flue gas conditions. Even their performance in the presence of moisture is good. Amine grafted adsorbents because of their covalent linkage have also displayed thermal stability and multi-cycle regenerability over large number of cyclic runs. The effect of impurities in flue gas mixture like SO_x, NO_x on the performance of amine grafted adsorbents is yet to be established. More investigations in the future are required to completely understand the performance of amine grafted adsorbents for post-combustion CO₂ capture.

Table 2.8. CO₂ adsorption performance with operating conditions of different amine grafted solid adsorbents reported in the literature.²

Support	Amine	Amine content	p (CO ₂) ^a	Temp ^b	Adsorption capacity	Reference
		[mmol/g]	[atm]	[°C]	dry (humid)	
					[mmol/g]	
SBA-15	APTES	2.7	0.15	60	0.52 (0.5)	95
SBA-15	AEAPS ^c	4.2	0.15	60	0.87 (0.9)	95
SBA-15	DAEAPTS	5.1	0.15	60	1.1 (1.21)	95
SBA-15	APTES	2.6	0.15	60	0.66 (0.65)	96
SBA-15	AEAPS ^c	4.6	0.15	60	1.36 (1.51)	96
SBA-15	DAEAPTS	5.8	0.15	60	1.58 (1.80)	96
HMS ^d	APTS	2.3	0.90	20	1.59	93
HMS ^d	DAEAPTS	4.6	0.90	20	1.34	94
SBA-15	AEAPTS		0.15	25	0.45	90
SBA-15	DAEAPTS	1.6	0.10	25	1.19	110
SBA-15	APTES	2.7	0.10	25	1.53	111
SBA-12	APTES	2.8	0.10	25	1.04	111
PE-MCM-41	DAEAPTS	7.8	0.05	70	2.28	101
SBA-15	Aziridine	9.8	0.10	75	(4)	109
SBA-15	Aziridine	7	0.10	25	(3.11)	72
SBA-16	AEAPTS	0.8	1	27	1.4	112

MCM-48	APTES	2.3	1	25	2.05	113
MCM-48	APTES	2.3	0.05	25	1.14	113
DWSNT ^e	DAEAPTS	1.6	1	25	2.23	114
Silica gel	APTES	1.3	1	50	0.89	87
CNTs	APTES		0.15	20	1.32	115
CNTs	AEAPTS		0.50	20	2.59	29

a: $p(\text{CO}_2) = \text{CO}_2$ partial pressure

b: Temp = Temperature

c: AEAPS = N-(2-aminoethyl)-3-aminopropyltriethoxysilane

d: HMS = Hexagonal mesoporous silica

e: DWSNT = Double-walled silica nanotubes

2.4 Bed configuration for CO₂ capture

The most-common bed configuration for contacting flue gas stream containing CO₂ with solid adsorbents is packed bed configuration. Bed is usually filled with sorbent particles packed into beads/extrudes. The flue gas mixture enters from one side of the packed bed, CO₂ preferentially gets adsorbed by the adsorbent and the remaining non-adsorbing flue gas components then exit from the other end of the packed bed. The sorbent gradually becomes saturated with CO₂ along the length of the bed. When the saturation reaches the end of the bed, CO₂ starts to appear from the outlet and its concentration quickly reaches the feed concentration. The effluent CO₂ concentration when plotted against time gives breakthrough curve which indicates the mass transfer characteristics of the bed.

Conventional packed bed performance is often compromised by excessive pressure drop and mass transfer resistances due to very high flue gas stream volumetric flowrate and small adsorbent particle size, which decreases the system efficiency and increases overall energy consumption. In order to overcome the

pressure drop problem, packed bed designs with large bed diameter and shorter bed lengths were used, which in turn led to problems like channelling, flow maldistribution and loss of adsorbent particles.¹¹⁶

Another bed configuration which is quite often used in industrial applications for gas separation is fluidized bed. Fluidized bed offers reduced diffusion limitations, better solid-gas mixing, faster kinetics, and better temperature uniformity as compared to fixed bed configuration. However, in comparison to fixed bed, fluidized bed arrangement also suffers from several problems like adsorbent attrition and entrainment in the discharge stream, erosion of adsorption reactor, operation complexity, etc.¹¹⁷ Therefore there is a need to explore some novel structured adsorbent bed designs which can overcome the limitations associated with the conventional adsorbent beds and improve their overall performance. These structured beds should fulfill certain conditions, namely give fast adsorption/desorption kinetics, low pressure drop and efficient heat transfer to/from the adsorbent bed. This section reviews briefly various structured bed designs used for gas separation processes and examine the performance of different bed configurations in adsorption based processes.

2.4.1 Monolith bed configuration

An alternative approach to packed bed is adsorbent material placed in a structured monolith. In comparison to conventional bed configurations, honeycomb-type monolithic adsorbent offers improved mass transfer characteristics with lower

pressure drop. The tunable structural parameters like wall thickness, cell size, density, shape, etc. of monolithic structured bed configurations allow them to find application in separation processes. Various research groups have used monolith configuration for adsorption based gas separation processes.¹¹⁸⁻¹²² Figure 2.1 shows a typical monolith configuration.¹²¹

CO₂ capture in a structured carbon monolith is widely reported in the literature.^{123,124} An et al.¹²⁵ investigated the effect of various structural parameters of carbon honeycomb monolithic structure on the sorption behavior of CO₂. This work reported that the CO₂ adsorption performance can be improved by using high cell density and the adsorption performance is very slightly affected by adsorbent sample diameter provided that porosity of the bed remains same. It was also noticed that decrease in channel wall thickness or increase in void fraction results in improved sorption performance.

Patton et al.¹²⁶ discussed the design considerations of monolithic adsorbents. It was observed that the separation performance of adsorbent structure can be improved by optimizing the design variables like channel shape, channel width, wall thickness, etc. In this work, the assumption of parabolic concentration gradient was taken along with Linear Driving Force (LDF) approximation for design of various monolithic channel shapes such as rectangular, triangular and hexagonal. It was reported that the regular hexagon channel with reduced wall

thickness provides the best mass transfer performance and this channel geometry can be approximated with circular geometry with least error.

Ribeiro et al.¹²⁷ examined the sorption performance of CO₂, CH₄ and N₂ in carbon honeycomb monoliths. The authors studied the diffusion of single gases like CO₂, CH₄ and N₂ in the monolith's microporous structure. The adsorption capacity was found to be highest for CO₂ and lowest for N₂. Mosca et al.¹²⁸ studied CO₂ adsorption potential of supported thin zeolite NaX film structured sorbents grown on cordierite monolith supports with cell density of 400 cpsi. The structured adsorbent showed 67 times lower sorption capacity per unit volume of adsorber column as compared to packed bed. The lower adsorption capacity was because of lower adsorbent loading in the structured adsorbent bed as compared to fixed bed. However, the pressure drop for traditional NaX fixed bed was found to be 100 times higher than that for structured sorbent configuration. It was suggested that the adsorption capacity can be raised without adding any significant pressure drop by increasing the thickness of NaX films or by increasing the cell density of substrate monoliths.

The monolith geometric parameters like wall thickness, porosity, channel width, thickness of zeolite X sorbent films were studied by Rezaei et al.¹²⁹ to investigate their influence on the CO₂ adsorption performance. It was observed that the cordierite monolith pores gives rise to dispersion instead of adsorption as the pore gets filled with carbon dioxide. Zeolite X film thickness of 2.5 μm gave

adsorption capacity of 0.13 mmol/cm^3 adsorbent as compared to 2.3 mmol/cm^3 adsorbent by zeolite X beads. It was shown that increase in zeolite film thickness led to increase in adsorption capacity. Using the model, it was estimated that $10 \text{ }\mu\text{m}$ is the maximum zeolite film thickness in order for the dispersion to not exceed and adsorption capacity to reach near the bead capacity.

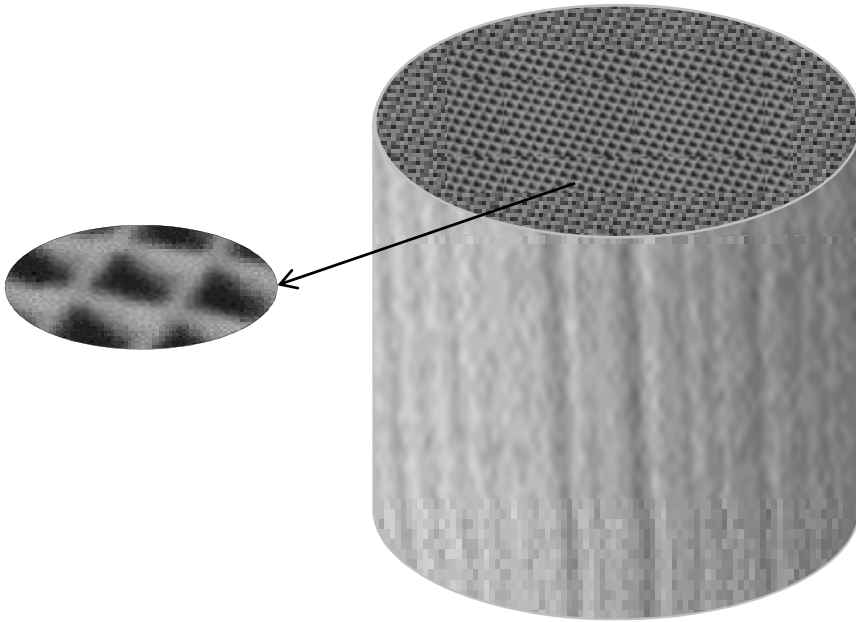
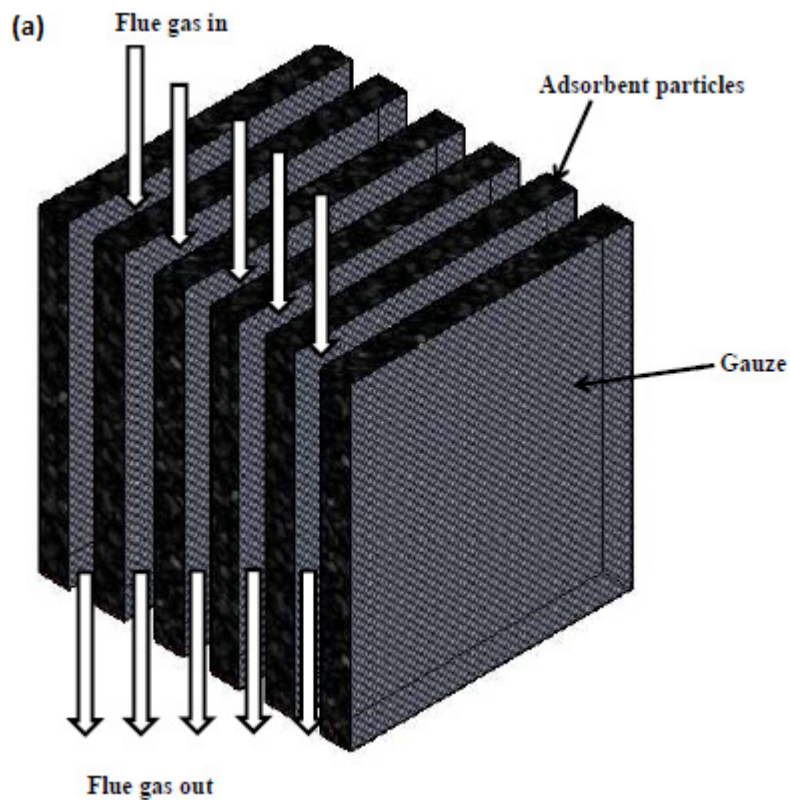


Figure 2.1. Schematic representation of a typical monolith configuration.¹²¹

2.4.2 Parallel passage contactor configuration

The parallel passage adsorbent contactor, another possible configuration is also suggested for CO_2 capture from flue gas mixture.¹³⁰ In this configuration, parallel layers of sorbent particle beds are contained between wire meshes. Flue gas mixture flows into the channel spacings provided between the alternate adsorbent layers. Gas mixture diffuses via the wire meshes into the sorbent layers. The

sorbent selectively adsorbs some components of the gas stream and the remaining comes out from other end of the gas channel. The schematic of parallel passage contactor is shown in Figure 2.2.¹³¹ The straight gas flow channels in this configuration provide very little resistance, hence leads to much lower pressure drop as compared to conventional fixed bed. In this respect, the parallel passage sorbent contactor should be compared to the monolithic contactor or honeycomb contactor. An important advantage of the parallel passage sorbent contactor is that the regular adsorbents can be filled in the parallel passage sorbent contactor whereas monolithic contactor sorbent manufacturing process is quite complex.



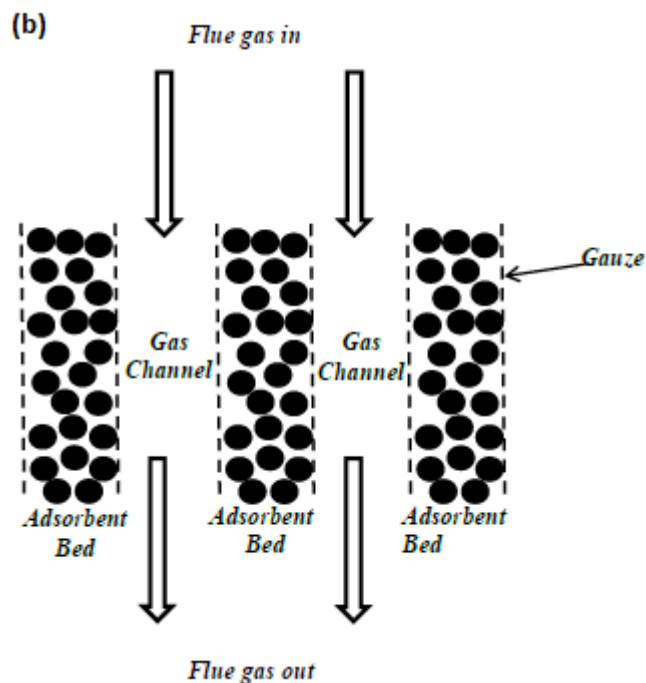


Figure 2.2. Schematic of a parallel passage sorbent contactor, (a) side view, (b) front view.¹³¹

Ruthven and Thaeon¹³⁰ compared the adsorption performance of parallel passage sorbent contactor and conventional packed bed. It was observed that the major advantage of parallel passage contactor compared to packed bed is lower pressure drop which can save considerable energy costs. It was suggested that parallel passage contactors with ACF (activated carbon fiber) coating would provide good results for low cost and large flowrate applications like CO₂ capture from flue gas mixture.

The use of upgraded parallel passage adsorbent contactors for PSA and TSA systems was described in Rode et al.¹³² It was reported that these configurations can be used in kinetic-controlled processes as well as in adsorptive separation

systems. This group demonstrated the performance of the improved sheet based parallel passage structures for air, CH₄/CO₂ and CH₄/N₂ separation processes. It was reported that the sheet thickness and sheet spacing must be kept minimum (as permitted to contain the pressure drop) for the efficient working of the laminate structure. It was claimed that this structure will provide significant increase in kinetic selectivity of chosen adsorption processes in comparison to conventional extrude/bead bed.

2.4.3 Hollow fiber bed

Another structured sorbent bed configuration that is also widely studied in literature is hollow-fiber bed. Figure 2.3 shows a typical single hollow fiber configuration.¹³³ Figure 2.4 shows the schematic representation of multiple hollow fiber bed.¹³⁴ Gilleskie et al.¹³³ studied gas separation measurements in single and multiple hollow-fiber beds. It was observed that although hollow-fiber structure offers lower pressure drop as compared to the packed bed but the advantages of lower pressure drop were negated by flow resistance due to availability of lower void fraction in hollow fiber structure. Therefore, the overall productivity of fiber bed was found to be no more than that of conventional packed bed. The authors also commented that the performance of hollow fiber structured sorbent is not always better than conventional packed bed.

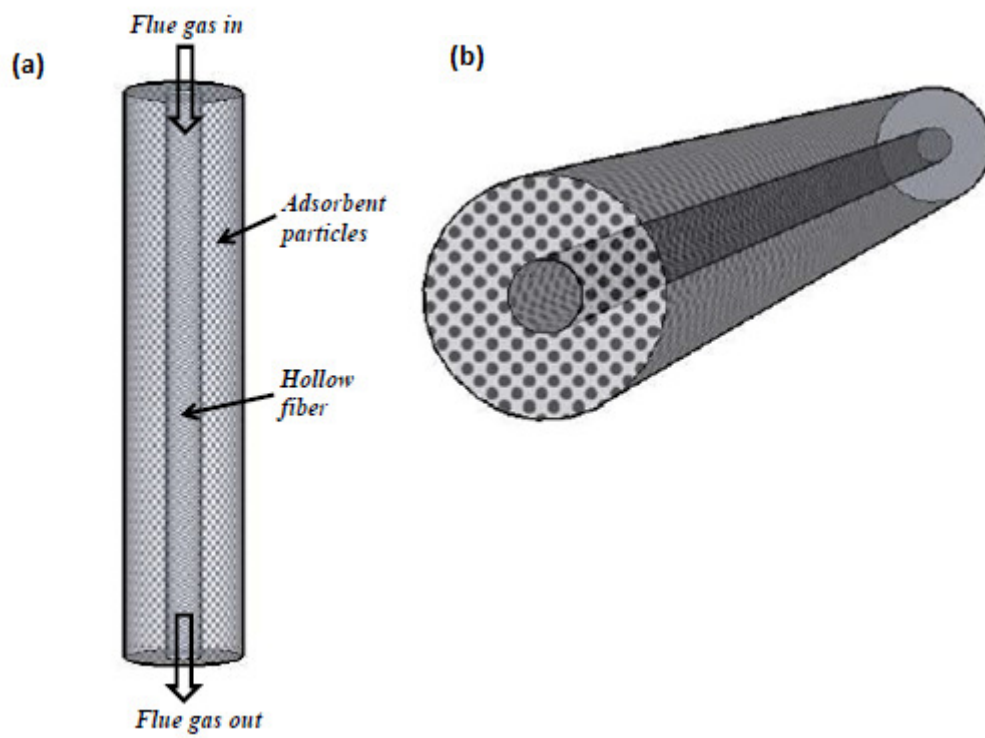


Figure 2.3. Schematic of a typical single hollow fiber configuration, (a) front view, (b) side view.¹³³

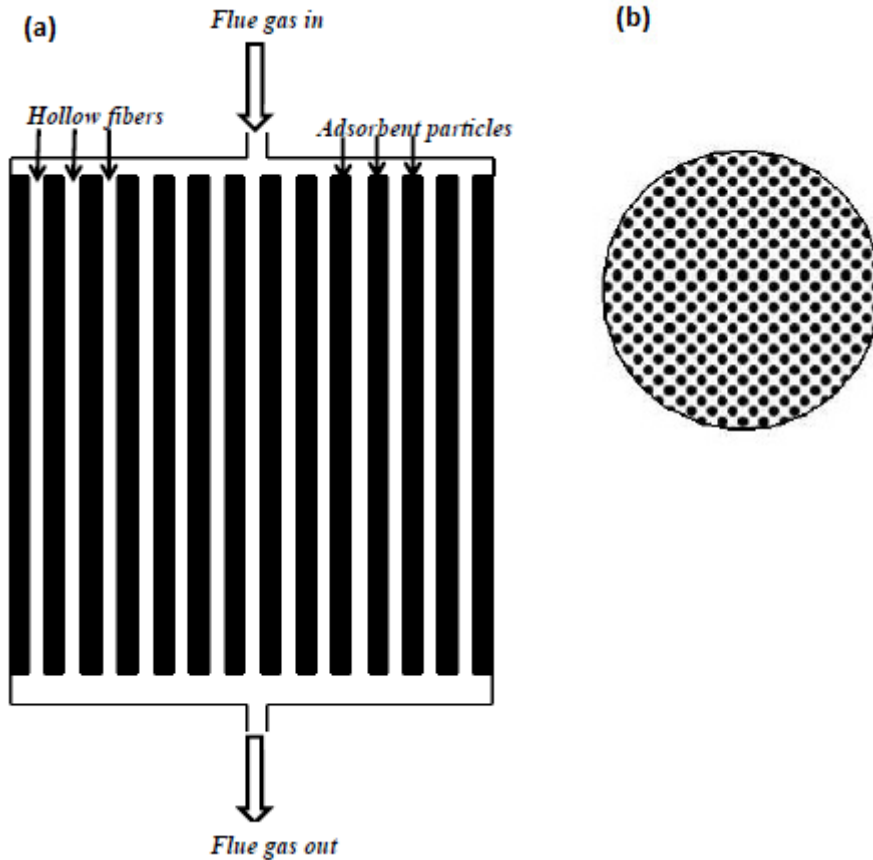


Figure 2.4. Schematic representation of multiple hollow fiber bed, (a) front view, (b) top view.¹³⁴

2.4.4 Other structured bed configurations

Fixed bed, fluidized bed, and radial-flow fixed bed were studied by Tarka et al.¹³⁵ for CO₂ capture performance. It was observed that fixed bed operated with large pressure drop and could not satisfy the required design limitations whereas fluidized bed provided low pressure drop but suffered from sorbent attrition. Radial-flow fixed bed however offered low pressure drop without any additional problems. In comparison to MEA based absorption process, 8-9% decrease in electricity cost was observed with both fluidized and novel radial-flow beds.

Yang and Hoffman¹³⁶ reported preliminary design analysis of a fluidized bed and moving bed working as a CO₂ adsorber and stripper respectively. Due to unavailability of sufficient design information, reverse engineering method for a 500 MWe supercritical PC plant with its boundary constraints was used. They estimated that moving bed contactor is not promising as regenerator due to excessive pressure drop and insufficient heat transfer in case adsorbent particles are small and it required significantly high bed height for slow desorption kinetics, which mean high regenerator cost. It was suggested to use an assisted self-fluidization bed with nested heat transfer area in place of moving bed system.

Rezaei and Webley¹³⁷ compared the sorption performance of various structured sorbent bed configurations, particularly monolith, laminate and foam structured configurations, with packed bed of adsorbent pellets for CO₂/N₂ separation system using mathematical and analytical models. It was shown that throughput for structured sorbents can be larger than that of fixed bed as long as the structured adsorbents perform at their optimal velocity. For instance, laminate structures were observed to be advantageous than packed bed only when they can be synthesized with spacing smaller than 0.2 mm and sheet widths of 0.2 mm. Similar geometrical parameter results were also developed for other structured adsorbent configurations.

Rezaei and Webley¹¹⁶ reviewed the performance of various structured sorbent beds for gas separation processes. The structured sorbent system performance was

discussed corresponding to certain structures like monolith, laminate, fabric and foam structures and compared to the performance of conventional packed bed. The effect of geometric/structural parameters on the performance of structured configurations was evaluated in terms of adsorbent loading, mass transfer behavior, pressure drop, working sorption capacity, channelling and dispersion characteristics, thermal behavior, etc. Table 2.9 presents various structured sorbent bed configurations used in the literature with enhanced adsorption characteristics which have received significant attention as possible replacements for conventional sorbent bed configurations.¹¹⁶

Table 2.9. Review of structured sorbent bed applications for adsorption/desorption processes.¹¹⁶

Structure	Packing details	System	Experimental conditions	Results	Ref
Monolith	Carbon monolith	CO ₂ -N ₂ and CO ₂ -He	P: 23 Torr, T: 23 °C	Diffusivity for CO ₂ /He is around 2 times the pore diffusivity for CO ₂ /N ₂	138
Monolith, 50 cpsi	Honeycomb monolith	Effluent gas purification	P: 1 atm, T: RT	Regeneration temperature can be upto 300 °C	122
Monolith, 300 cpsi	Activated carbon honeycomb monolith	CO ₂ , CH ₄ , and N ₂ adsorption	P: 1 atm, T: 30–150 °C	Sorption capacity: N ₂ < CH ₄ < CO ₂	127
Monolith, 190 cpsi	Activated carbon honeycomb monolithic structure	CO ₂ removal using ESA	P: 101 kPa, T: 24 °C	CO ₂ recovery: >89%, CO ₂ purity: 16%	139
Laminate	Parallel passage sorbent contactor	CO ₂ removal	P: 1 atm, T: RT	High selectivity ratio (CO ₂ /N ₂) for sorption of CO ₂ /N ₂	130

Fabric structure	Activated carbon cloth	Air purification	Electrothermal regeneration	Capture efficiency: 99.9%	140
Paper honeycomb	Rotary bed	CO ₂ recovery	Adsorber: 460mm diameter, 480mm height	CO ₂ recovery: > 80%	141, 142
Monolith, 400 cpsi	Cordierite monolith	CO ₂ capture	P: 1 atm, T: RT	Pressure drop: 100 times lower	128

Ref: Reference

P: Pressure

T: Temperature

RT: Room Temperature

cpsi: cells per square inch

ESA: Electric Swing Adsorption

2.5 Summary

Different types of physical and chemical adsorbents were discussed for CO₂ capture in this chapter. Carbon based adsorbents and zeolites displayed fast kinetics, low regeneration energy and high sorption capacity and selectivity at high pressures but their capacity and selectivity needed improvement at post-combustion conditions of low pressures. These adsorbents also suffered severely in the presence of moisture. The new class of solid sorbents, MOFs also showed high sorption capacity and selectivity at high pressures but barring few not much results are available for their application at post-combustion conditions. Amine functionalized adsorbents exhibited fast kinetics, high adsorption capacity and selectivity at low pressures and no negative effect was observed in the presence of moisture. But amine leaching and multi-cycle stability are still an issue for amine impregnated adsorbents and needs further investigation. Whereas amine grafted adsorbents might show long-term stability due to their stronger connection with

the support. So, overall there is need for improvement in all these adsorbents and more studies will indicate which adsorbent is most suited for post-combustion CO₂ capture.

In this chapter, the performance parameters like pressure drop, mass transfer kinetics, adsorption capacity, heat transfer efficiency, etc. for different types of structured bed configurations were discussed for CO₂ capture from flue gas mixture. Each structure presented some advantages and disadvantages over conventional packed bed configuration. The optimal choice of parameters for each structured bed configuration is yet not known and needs to be determined in future research efforts in order to successfully implement these structured beds for real industrial applications.

2.6 Motivation

Out of all the solid adsorbents discussed in this chapter, amine grafted mesoporous adsorbents look most promising for application in post-combustion CO₂ capture. Although a lot of research work has already been carried out in the field of CO₂ capture using grafting technique over ordered mesoporous silica supports but very few studies are concerned with grafted SBA-15 adsorbent. The systematic study of SBA-15 grafted with DAEPTS amine dealing carbon dioxide capture is still lacking. The CO₂ adsorption performance results reported in literature so far for DAEPTS grafted SBA-15 adsorbent is quite inconsistent and low. There is no work available in the literature which has looked into

adsorption and desorption kinetics of DAEAPTS grafted SBA-15 adsorbent for CO₂ capture. Very few studies have looked into the multi-cycle performance of grafting technique for more than 10 cycles and no research has been done on DAEAPTS grafted SBA-15 adsorbent's multi-cycle stability performance. Keeping the above mentioned points in mind, the present work aims to fill up the gaps in the evaluation of DAEAPTS grafted SBA-15 adsorbent for post-combustion CO₂ capture.

The main hindrance to post-combustion CO₂ capture is cost-effectiveness of the capture processes. The need to find practically feasible solutions for CO₂ capture has led to the development of solid sorbents with very high potential. However, the success of these adsorbent materials will be determined by the contactor type which can utilize their potential and minimize related energy costs. Packed bed and fluidized bed are two most common contactor types used for post-combustion CO₂ capture. However, the conventional packed bed for post-combustion CO₂ capture suffers from significantly high pressure drop whereas the fluidized bed finds problems in adsorbent attrition and loss. So, there is a need of more reliable and efficient bed configuration, which can eliminate these problems of pressure drop and sorbent attrition. An alternative novel configuration of structured bed with straight gas flow channels which can offer lower pressure drop and avoid adsorbent attrition is presented in this work. This kind of structured configuration with straight gas flow channels is not reported anywhere in the literature for CO₂ capture. The present work aims to study the CO₂ adsorption/desorption behaviour

of this structured bed loaded with amine functionalized SBA-15 adsorbent in order to eliminate some of the problems associated with the conventional beds.

2.7 Objectives

The work in this study is divided into two parts: (1) Synthesis of amine functionalized adsorbents using grafting technique for post-combustion CO₂ capture, (2) Performance evaluation of novel structured bed configuration using amine impregnated adsorbent for post-combustion CO₂ capture. The major objectives of each part are listed in this section.

The goal of part (1) of this work is to examine the DAEAPTS grafted SBA-15 adsorbent's application for post-combustion CO₂ capture. The main objectives in the study of DAEAPTS grafted SBA-15 adsorbent are as follows:

1. To synthesize, characterize and evaluate the DAEAPTS grafted SBA-15 adsorbent for the separation of CO₂ from simulated flue gas.
2. To optimize the amine loading of grafted SBA-15 adsorbent for CO₂ adsorption. The optimal amine loaded grafted adsorbent is tested at different adsorption temperatures and CO₂ partial pressures.
3. The main objective of this study is to establish the multi-cycle stability of grafted SBA-15 solid sorbent.
4. Another very important goal of this work is to investigate the adsorption/desorption kinetics of grafted SBA-15 adsorbent to determine its usability from practical standpoint.

5. As the flue gas mixture contains moisture in the post-combustion capture conditions, therefore it is vital that the selected adsorbent should maintain its effectiveness in the presence of moisture. The amine grafted SBA-15 adsorbent is also checked for CO₂ adsorption/desorption performance in the presence of moisture.

The aim of part (2) of this work is to study the performance of CO₂ capture from simulated flue gas using structured bed and packed bed. The main objectives of this study are as follows:

1. Study the multi-cycle stability of amine functionalized sorbent in the structured bed and packed bed set-ups.
2. Study of adsorption and desorption kinetics of amine functionalized sorbent in the structured bed and packed bed set-ups.
3. Evaluate the CO₂ adsorption performance at different adsorption temperatures.
4. Investigation of the CO₂ adsorption performance in the structured bed containing single and multiple tubes. Comparison of the structured bed performance with packed bed.

References

1. D'Alessandro, D. M.; Smit, B.; Long, J. R. Carbon dioxide capture: Prospects for new materials. *Angew. Chem. Int. Ed.* **2010**, 49 (35), 6058-6082.
2. Samanta, A.; Zhao, A.; Shimizu, G. K. H.; Sarkar, P.; Gupta, R. Post-combustion CO₂ capture using solid sorbents—A review. *Ind. Eng. Chem. Res.* **2012**, 51, 1438-1463.
3. Na, B. K.; Koo, K. K.; Eum, H. M.; Lee, H.; Song, H. K. CO₂ recovery from flue gas by PSA process using activated carbon. *Korean J. Chem. Eng.* **2001**, 18, 220–227.
4. Zhang, Z.; Zhang, W.; Chen, X.; Xia, Q.; Li, Z. Adsorption of CO₂ on zeolite 13X and activated carbon with high surface area. *Sep. Sci. Technol.* **2010**, 45, 710–719.
5. Lu, C.; Bai, H.; Wu, B.; Su, F.; Hwang, J. F. Comparative study of CO₂ capture by carbon nanotubes, activated carbons, and zeolites. *Energy Fuels* **2008**, 22, 3050–3056.
6. Sircar, S.; Golden, T. C. Isothermal and isobaric desorption of carbon dioxide by purge. *Ind. Eng. Chem. Res.* **1995**, 34, 2881–2888.
7. Cinke, M.; Li, J.; Bauschlicher Jr., C. W.; Ricca, A.; Meyyappan, M. CO₂ adsorption in single-walled carbon nanotubes. *Chemical Physics Letters* **2003**, 376 (5–6), 761-766.
8. Kikkinides, E. S.; Yang, R. T. Concentration and recovery of CO₂ from flue gas by pressure swing adsorption. *Ind. Eng. Chem. Res.* **1993**, 32, 2714–2720.
9. Chue, K. T.; Kim, J. N.; Yoo, Y. J.; Cho, S. H.; Yang, R. T. Comparison of activated carbon and zeolite 13X for CO₂ recovery from flue gas by pressure swing adsorption. *Ind. Eng. Chem. Res.* **1995**, 34, 591–598.
10. Do, D. D.; Wang, K. A new model for the description of adsorption kinetics in heterogeneous activated carbon. *Carbon* **1998**, 36, 1539–1554.
11. Siriwardane, R. V.; Shen, M.-S.; Fisher, E. P.; Poston, J. A. Adsorption of CO₂ on molecular sieves and activated carbon. *Energy Fuels* **2001**, 15, 279–284.

12. Heuchel, M.; Davies, G. M.; Buss, E.; Seaton, N. A. Adsorption of carbon dioxide and methane and their mixtures on an activated carbon: simulation and experiment. *Langmuir* **1999**, *15*, 8695–8705.
13. Berlier, K.; Frère, M. Adsorption of CO₂ on microporous materials. 1. On activated carbon and silica gel. *J. Chem. Eng. Data* **1997**, *42*, 533–537.
14. Berlier, K.; Frère, M. Adsorption of CO₂ on activated carbon: Simultaneous determination of integral heat and isotherm of adsorption. *J. Chem. Eng. Data* **1996**, *41*, 1144–1148.
15. Vaart, R. V. D.; Huiskes, C.; Bosch, H.; Reith, T. Single and mixed gas adsorption equilibria of carbon dioxide/methane on activated carbon. *Adsorption* **2000**, *6*, 311–323.
16. Foeth, F.; Andersson, M.; Bosch, H.; Aly, G.; Reith, T. Separation of dilute CO₂-CH₄ mixtures by adsorption on activated carbon. *Sep. Sci. Technol.* **1994**, *29*, 93–118.
17. Dreisbach, F.; Staudt, R.; Keller, J. U. High pressure adsorption data of methane, nitrogen, carbon dioxide and their binary and ternary mixtures on activated carbon. *Adsorption* **1999**, *5*, 215–227.
18. Wang, Y.; Zhou, Y.; Liu, C.; Zhou, L. Comparative studies of CO₂ and CH₄ sorption on activated carbon in presence of water. *Colloids Surf., A* **2008**, *322*, 14–18.
19. Maroto-Valer, M. M.; Tang, Z.; Zhang, Y. CO₂ capture by activated and impregnated anthracites. *Fuel Process. Technol.* **2005**, *86*, 1487–1502.
20. Ghosh, A.; Subrahmanyam, K. S.; Krishna, K. S.; Datta, S.; Govindaraj, A.; Pati, S. K.; Rao, C. N. R. Uptake of H₂ and CO₂ by graphene. *J. Phys. Chem. C* **2008**, *112*, 15704–15707.
21. Burchell, T. D.; Judkins, R. R.; Rogers, M. M.; Williams, A. M. A novel process and material for the separation of carbon dioxide and hydrogen sulfide gas mixtures. *Carbon* **1997**, *35*, 1279–1294.
22. Sircar, S.; Golden, T. C.; Rao, M. B. Activated carbon for gas separation and storage. *Carbon* **1996**, *34*, 1-12.

23. Davini, P. Flue gas treatment by activated carbon obtained from oil-fired fly ash. *Carbon* **2002**, 40 (11), 1973-1979.
24. Rodríguez-Reinoso, F.; Molina-Sabio, M. Activated carbons from lignocellulosic materials by chemical and/or physical activation: An overview. *Carbon* **1992**, 30, 1111-1118.
25. Ahmadpour, A.; Do, D. D. The preparation of active carbons from coal by chemical and physical activation. *Carbon* **1996**, 34, 471-479.
26. Sayari, A.; Belmabkhout, Y.; Serna-Guerrero, R. Flue gas treatment via CO₂ adsorption. *Chem. Eng. J.* **2011**, 171 (3), 760-774.
27. Huang, L.; Zhang, L.; Shao, Q.; Lu, L.; Lu, X.; Jiang, S.; Shen, W. Simulations of binary mixture adsorption of carbon dioxide and methane in carbon nanotubes: Temperature, pressure, and pore size effects. *J. Phys. Chem. C* **2007**, 111, 11912–11920.
28. Razavi, S. S.; Hashemianzadeh, S. M.; Karimi, H. Modeling the adsorptive selectivity of carbon nanotubes for effective separation of CO₂/N₂ mixtures. *J. Mol. Model.* **2011**, 17, 1163–1172.
29. Su, F.; Lu, C.; Cnen, W.; Bai, H.; Hwang, J. F. Capture of CO₂ from flue gas via multiwalled carbon nanotubes. *Sci. Total Environ.* **2009**, 407, 3017–3023.
30. Foley, H. C. Carbogenic molecular sieves: synthesis, properties and applications. *Microporous Mater.* **1995**, 4 (6), 407-433.
31. Rutherford, S. W.; Do, D. D. Adsorption dynamics of carbon dioxide on a carbon molecular sieve 5A. *Carbon* **2000**, 38 (9), 1339-1350.
32. Alcañiz-Monge, J.; Marco-Lozar, J. P.; Lillo-Ródenas, M. Á. CO₂ separation by carbon molecular sieve monoliths prepared from nitrated coal tar pitch. *Fuel Process. Technol.* **2011**, 92 (5), 915-919.
33. Zhang, J.; Webley, P. A.; Xiao, P. Effect of process parameters on power requirements of vacuum swing adsorption technology for CO₂ capture from flue gas. *Energy Convers. Manage.* **2008**, 49, 346–356.
34. Díaz, E.; Muñoz, E.; Vega, A.; Ordóñez, S. Enhancement of the CO₂ retention capacity of Y zeolites by Na and Cs treatments: Effect of adsorption temperature and water treatment. *Ind. Eng. Chem. Res.* **2008**, 47, 412–418.

35. Díaz, E.; Muñoz, E.; Vega, A.; Ordóñez, S. Enhancement of the CO₂ retention capacity of X zeolites by Na- and Cs- treatments. *Chemosphere* **2008**, *70*, 1375–1382.
36. Bezerra, D. P.; Oliveira, R. S.; Vieira, R. S.; Cavalcante, C. L.; Azevedo, D. C. S. Adsorption of CO₂ on nitrogen-enriched activated carbon and zeolite 13X. *Adsorption* **2011**, *17*, 235–246.
37. Siriwardane, R. V.; Shen, M.-S.; Fisher, E. P. Adsorption of CO₂, N₂, and O₂ on natural zeolites. *Energy Fuels* **2003**, *17*, 571–576.
38. Hernández-Huesca, R.; Díaz, L.; Aguilar-Armenta, G. Adsorption equilibria and kinetics of CO₂, CH₄ and N₂ in natural zeolites. *Sep. Purif. Technol.* **1999**, *15*, 163–173.
39. Calleja, G.; Jimenez, A.; Pau, J.; Domínguez, L.; Pérez, P. Multicomponent adsorption equilibrium of ethylene, propane, propylene and CO₂ on 13X zeolite. *Gas. Sep. Purif.* **1994**, *8*, 247–256.
40. Harlick, P. J. E.; Tezel, F. H. An experimental adsorbent screening study for CO₂ removal from N₂. *Microporous Mesoporous Mater.* **2004**, *76*, 71–79.
41. Cavenati, S.; Grande, C. A.; Rodrigues, A. E. Adsorption equilibrium of methane, carbon dioxide, and nitrogen on zeolite 13X at high pressures. *J. Chem. Eng. Data* **2004**, *49*, 1095–1101.
42. Choudhary, V. R.; Mayadevi, S.; Singh, A. P. Sorption isotherms of methane, ethane, ethene and carbon dioxide on NaX, NaY and Na-mordenite zeolites. *J. Chem. Soc., Faraday Trans.* **1995**, *91*, 2935–2944.
43. Dunne, J. A.; Mariwala, R.; Rao, M.; Sircar, S.; Gorte, R. J.; Myers, A. L. Calorimetric heats of adsorption and adsorption isotherms. 1. O₂, N₂, Ar, CO₂, CH₄, C₂H₆, and SF₆ on silicalite. *Langmuir* **1996**, *12*, 5888–5895.
44. Katoh, M.; Yoshikawa, T.; Tomonari, T.; Katayama, K.; Tomida, T. Adsorption characteristics of ion-exchanged ZSM-5 zeolites for CO₂/N₂ mixtures. *J. Colloid Interface Sci.* **2000**, *226*, 145–150.
45. Kamiuto, K.; Abe, S.; Ermalina. Effect of desorption temperature on CO₂ adsorption equilibria of the honeycomb zeolite beds. *Appl. Energy* **2002**, *72*, 555–564.

46. Lee, S.-S.; Yoo, J.-S.; Moon, G.-H.; Park, S.-W.; Park, D.-W.; Oh, K.-J. CO₂ adsorption with attrition of dry sorbents in a fluidized bed. *Div. Fuel Chem., Am. Chem. Soc. Prepr. Symp.* **2004**, 49, 314-315.
47. Chester, A. W.; Derouane, E. G. Eds. Zeolite Characterization and Catalysis: A Tutorial; Springer: New York, 2009.
48. Zukal, A.; Mayerová, J.; Kubů, M. Adsorption of carbon dioxide on high-silica zeolites with different framework topology. *Top. Catal.* **2010**, 53, 1361–1366.
49. Brandani, F.; Ruthven, D. M. The effect of water on the adsorption of CO₂ and C₃H₈ on type X zeolites. *Ind. Eng. Chem. Res.* **2004**, 43, 8339-8344.
50. Li, J.-R.; Kuppler, R. J.; Zhou, H.-C., Selective gas adsorption and separation in metal-organic frameworks. *Chem. Soc. Rev.* **2009**, 38 (5), 1477-1504.
51. Kitagawa, S.; Kitaura, R.; Noro, S. Functional porous coordination polymers. *Angew. Chem., Int. Ed.* **2004**, 43, 2334–2375.
52. Bourrelly, S.; Llewellyn, P. L.; Serre, C.; Millange, F.; Loiseau, T.; Férey, G. Different adsorption behaviors of methane and carbon dioxide in the isotopic nanoporous metal terephthalates MIL-53 and MIL-47. *J. Am. Chem. Soc.* **2005**, 127, 13519-13521.
53. Li, D.; Kaneko, K. Hydrogen bond-regulated microporous nature of copper complex-assembled microcrystals. *Chem. Phys. Lett.* **2001**, 335, 50-56.
54. Walton, K. S.; Millward, A. R.; Dubbeldam, D.; Frost, H.; Low, J. J.; Yaghi, O. M.; Snurr, R. Q. Understanding inflections and steps in carbon dioxide adsorption isotherms in metal-organic frameworks. *J. Am. Chem. Soc.* **2008**, 130, 406-407.
55. Furukawa, H.; Ko, N.; Go, Y. B.; Aratani, N.; Choi, S. B.; Choi, E.; Yazaydin, A. O.; Snurr, R. Q.; O’Keeffe, M.; Kim, J.; Yaghi, O. M. Ultrahigh porosity in metal-organic frameworks. *Science* **2010**, 329, 424–428.
56. Liu, J.; Wang, Y.; Benin, A. I.; Jakubczak, P.; Willis, R. R.; LeVan, M. D. CO₂/H₂O adsorption equilibrium and rates on metal-organic frameworks: HKUST-1 and Ni/DOBDC. *Langmuir* **2010**, 26, 14301–14307.

57. Khatri, R. A.; Chuang, S. S. C.; Soong, Y.; Gray, M. Carbon dioxide capture by diamine-grafted SBA-15: A combined Fourier transform infrared and mass spectrometry study. *Ind. Eng. Chem. Res.* **2005**, *44*, 3702–3708.
58. Li, W.; Choi, S.; Drese, J. H.; Hornbostel, M.; Krishnan, G.; Eisenberger, P. M.; Jones, C. W. Steam-stripping for regeneration of supported amine-based CO₂ adsorbents. *ChemSusChem* **2010**, *3* (8), 899-903.
59. Caplow, M. Kinetics of carbamate formation and breakdown. *J. Am. Chem. Soc.* **1968**, *90*, 6795–6803.
60. Choi, S.; Drese, J. H.; Jones, C. W. Adsorbent materials for carbon dioxide capture from large anthropogenic point sources. *ChemSusChem* **2009**, *2*, 796–854.
61. Sartori, G.; Savage, D. W. Sterically hindered amines for carbon dioxide removal from gases. *Ind. Eng. Chem. Fundamen.* **1983**, *22*, 239–249.
62. Donaldson, T. L.; Nguyen, Y. N. Carbon dioxide reaction kinetics and transport in aqueous amine membranes. *Ind. Eng. Chem. Fundamen.* **1980**, *19*, 260–266.
63. Vaidya, P. D.; Kenig, E. Y. CO₂-alkanolamine reaction kinetics: A review of recent studies. *Chem. Eng. Technol.* **2007**, *30*, 1467–1474.
64. Xu, X.; Song, C.; Andresen, J. M.; Miller, B. G.; Scaroni, A. W. Novel polyethylenimine-modified mesoporous molecular sieve of MCM-41 type as high-capacity adsorbent for CO₂ capture. *Energy Fuels* **2002**, *16*, 1463–1469.
65. Xu, X.; Song, C.; Miller, B. G.; Scaroni, A. W. Influence of moisture on CO₂ separation from gas mixture by a nanoporous adsorbent based on polyethylenimine-modified molecular sieve MCM-41. *Ind. Eng. Chem. Res.* **2005**, *44*, 8113–8119.
66. Xu, X.; Song, C.; Andresen, J. M.; Miller, B. G.; Scaroni, A. W. Preparation and characterization of novel CO₂ “molecular basket” adsorbents based on polymer-modified mesoporous molecular sieve MCM-41. *Microporous Mesoporous Mater.* **2003**, *62*, 29–45.

67. Xu, X.; Song, C.; Andresen, J. M.; Miller, B. G.; Scaroni, A. W. Adsorption separation of CO₂ from simulated flue gas mixtures by novel CO₂ ‘molecular basket’ adsorbents. *Int. J. Environ. Technol. Manage.* **2004**, 4, 32–52.
68. Xu, X.; Song, C.; Miller, B. G.; Scaroni, A. W. Adsorption separation of carbon dioxide from flue gas of natural gas-fired boiler by a novel nanoporous “molecular basket” adsorbent. *Fuel Process. Technol.* **2005**, 86, 1457–1472.
69. Ma, X.; Wang, X.; Song, C. “Molecular basket” sorbents for separation of CO₂ and H₂S from various gas streams. *J. Am. Chem. Soc.* **2009**, 131, 5777–5783.
70. Son, W.-J.; Choi, J.-S.; Ahn, W.-S. Adsorptive removal of carbon dioxide using polyethyleneimine-loaded mesoporous silica materials. *Microporous Mesoporous Mater.* **2008**, 113, 31–40.
71. Zhao, A.; Samanta, A.; Sarkar, P.; Gupta, R. Carbon dioxide adsorption on amine impregnated mesoporous SBA-15 sorbents: experimental and kinetics study. *Ind. Eng. Chem. Res.* **2013**, 52 (19), 6480–6491.
72. Hicks, J. C.; Drese, J. H.; Fauth, D. J.; Gray, M. L.; Qi, G.; Jones, C. W. Designing adsorbents for CO₂ capture from flue gas-Hyperbranched aminosilicas capable of capturing CO₂ reversibly. *J. Am. Chem. Soc.* **2008**, 130, 2902–2903.
73. Drage, T. C.; Arenillas, A.; Smith, K. M.; Snape, C. E. Thermal stability of polyethyleneimine based carbon dioxide adsorbents and its influence on selection of regeneration strategies. *Microporous Mesoporous Mater.* **2008**, 116, 504–512.
74. Yue, M. B.; Sun, L. B.; Cao, Y.; Wang, Y.; Wang, Z. J.; Zhu, J. H. Efficient CO₂ capturer derived from as-synthesized MCM-41 modified with amine. *Chem.—Eur. J.* **2008**, 14, 3442–3451.
75. Wang, X.; Ma, X.; Schwartz, V.; Clark, J. C.; Overbury, S. H.; Zhao, S.; Xu, X.; Song, C. A solid molecular basket sorbent for CO₂ capture from gas streams with low CO₂ concentration under ambient conditions. *Phys. Chem. Chem. Phys.* **2012**, 14, 1485–1492.

76. Wang, X.; Ma, X.; Song, C.; Locke, D. R.; Siefert, S.; Winans, R. E.; Möllmer, J.; Lange, M.; Möller, A.; Gläser, R. Molecular basket sorbents polyethylenimine–SBA-15 for CO₂ capture from flue gas: Characterization and sorption properties. *Microporous Mesoporous Mater.* **2013**, 169, 103-111.
77. Goepfert, A.; Meth, S.; Prakash, G. K. S.; Olah, G. A. Nanostructured silica as a support for regenerable high-capacity organoamine-based CO₂ sorbents. *Energy Environ. Sci.* **2010**, 3, 1949–1960.
78. Lee, S.; Filburn, T.; Gray, M.; Park, J. W.; Song, H. J. Screening test of solid amine sorbents for CO₂ capture. *Ind. Eng. Chem. Res.* **2008**, 47, 7419–7423.
79. Yue, M. B.; Chun, Y.; Cao, Y.; Dong, X.; Zhu, J. H. CO₂ capture by as-prepared SBA-15 with an occluded organic template. *Adv. Funct. Mater.* **2006**, 16, 1717–1722.
80. Yue, M. B.; Sun, L. B.; Cao, Y.; Wang, Z. J.; Wang, Y.; Yu, Q.; Zhu, J. H. Promoting the CO₂ adsorption in the amine-containing SBA-15 by hydroxyl group. *Microporous Mesoporous Mater.* **2008**, 114, 74–81.
81. Dasgupta, S.; Nanoti, A.; Gupta, P.; Jena, D.; Goswami, A. N.; Garg, M. O. Carbon dioxide removal with mesoporous adsorbents in a single column pressure swing adsorber. *Sep. Sci. Technol.* **2009**, 44, 3973–3983.
82. Wang, J.; Chen, H.; Zhou, H.; Liu, X.; Qiao, W.; Long, D.; Ling, L. Carbon dioxide capture using polyethylenimine-loaded mesoporous carbons. *J. Environ. Sci.* **2013**, 25, 124-132.
83. Le, Y.; Guo, D.; Cheng, B.; Yu, J. Amine-functionalized monodispersed porous silica microspheres with enhanced CO₂ adsorption performance and good cyclic stability. *J. Colloid Interface Sci.* **2013**, 408, 173-180.
84. Kong, Y.; Jin, L.; Qiu, J. Synthesis, characterization, and CO₂ capture study of micro-nano carbonaceous composites. *Sci. Total Environ.* **2013**, 463-464, 192-198.
85. Gray, M. L.; Champagne, K. J.; Fauth, D.; Baltrus, J. P.; Pennline, H. Performance of immobilized tertiary amine solid sorbents for the capture of carbon dioxide. *Int. J. Greenhouse Gas Control* **2008**, 2, 3–8.

86. Franchi, R. S.; Harlick, P. J. E.; Sayari, A. Applications of pore-expanded mesoporous silica. 2. Development of a high-capacity, water-tolerant adsorbent for CO₂. *Ind. Eng. Chem. Res.* **2005**, *44*, 8007–8013.
87. Leal, O.; Bolívar, C.; Ovalles, C.; García, J. J.; Espidel, Y. Reversible adsorption of carbon dioxide on amine surface-bonded silica gel. *Inorg. Chim. Acta* **1995**, *240*, 183–189.
88. Khatri, R. A.; Chuang, S. S. C.; Soong, Y.; Gray, M. Thermal and chemical stability of regenerable solid amine sorbent for CO₂ capture. *Energy Fuels* **2006**, *20*, 1514–1520.
89. Zheng, F.; Tran, D. N.; Busche, B.; Fryxell, G. E.; Addleman, R. S.; Zemanian, T. S.; Aardahl, C. L. Ethylenediamine-modified SBA-15 as regenerable CO₂ sorbents. *Div. Fuel Chem., Am. Chem. Soc. Prepr. Symp.* **2004**, *49*, 261-262.
90. Zheng, F.; Tran, D. N.; Busche, B.; Fryxell, G. E.; Addleman, R. S.; Zemanian, T. S.; Aardahl, C. L. Ethylenediamine-modified SBA-15 as regenerable CO₂ sorbents. *Ind. Eng. Chem. Res.* **2005**, *44*, 3099–3105.
91. Delaney, S. W.; Knowles, G. P.; Chaffee, A. L. Hybrid mesoporous materials for carbon dioxide separation. *Div. Fuel Chem., Am. Chem. Soc. Prepr. Symp.* **2002**, *47*, 65-66.
92. Knowles, G. P.; Delaney, S. W.; Chaffee, A. L. Amine-functionalized mesoporous silicas as CO₂ adsorbents. *Stud. Surf. Sci. Catal.* **2005**, *156*, 887–896.
93. Knowles, G. P.; Graham, J. V.; Delaney, S. W.; Chaffee, A. L. Aminopropyl-functionalized mesoporous silicas as CO₂ adsorbents. *Fuel Process. Technol.* **2005**, *86*, 1435–1448.
94. Knowles, G. P.; Delaney, S. W.; Chaffee, A. L. Diethylenetriamine[propyl(silyl)]- functionalized (DT) mesoporous silicas as CO₂ adsorbents. *Ind. Eng. Chem. Res.* **2006**, *45*, 2626–2633.
95. Hiyoshi, N.; Yogo, K.; Yashima, T. Adsorption of carbon dioxide on amine modified SBA-15 in the presence of water vapor. *Chem. Lett.* **2004**, *33*, 510–511.

96. Hiyoshi, N.; Yogo, K.; Yashima, T. Adsorption characteristics of carbon dioxide on organically functionalized SBA-15. *Microporous Mesoporous Mater.* **2005**, 84, 357–365.
97. Harlick, P. J. E.; Sayari, A. Applications of pore-expanded mesoporous silicas. 3. Triamine silane grafting for enhanced CO₂ adsorption. *Ind. Eng. Chem. Res.* **2006**, 45, 3248–3255.
98. Harlick, P. J. E.; Sayari, A. Applications of pore-expanded mesoporous silica. 5. Triamine grafted material with exceptional CO₂ dynamic and equilibrium adsorption performance. *Ind. Eng. Chem. Res.* **2007**, 46, 446–458.
99. Sayari, A.; Belmabkhout, Y.; Da'Na, E. CO₂ deactivation of supported amines: Does the nature of amine matter? *Langmuir* **2012**, 28, 4241–4247.
100. Ahmadalinezhad, A.; Tailor, R.; Sayari, A. Molecular-level insights into the oxidative degradation of grafted amines. *Chem. Eur. J.* **2013**, 19, 10543–10550.
101. Serna-Guerrero, R.; Belmabkhout, Y.; Sayari, A. Influence of regeneration conditions on the cyclic performance of amine-grafted mesoporous silica for CO₂ capture: An experimental and statistical study. *Chem. Eng. Sci.* **2010**, 65, 4166–4172.
102. Sayari, A.; Heydari-Gorji, A.; Yang, Y. CO₂-induced degradation of amine-containing adsorbents: Reaction products and pathways. *J. Am. Chem. Soc.* **2012**, 134, 13834–13842.
103. Serna-Guerrero, R.; Belmabkhout, Y.; Sayari, A. Triamine-grafted pore-expanded mesoporous silica for CO₂ capture: Effect of moisture and adsorbent regeneration strategies. *Adsorption* **2010**, 16, 567–575.
104. Belmabkhout, Y.; Serna-Guerrero, R.; Sayari, A. Adsorption of CO₂-containing gas mixtures over amine-bearing pore-expanded MCM-41 silica: Application for gas purification. *Ind. Eng. Chem. Res.* **2010**, 49, 359–365.
105. Belmabkhout, Y.; Sayari, A. Isothermal versus non-isothermal adsorption-desorption cycling of triamine-grafted pore-expanded MCM-41 mesoporous silica for CO₂ capture from flue gas. *Energy Fuels* **2010**, 24, 5273–5280.

106. Sayari, A.; Belmabkhout, Y. Stabilization of amine-containing CO₂ adsorbents: Dramatic effect of water vapor. *J. Am. Chem. Soc.* **2010**, *132*, 6312–6314.
107. Sayari, A.; Kruk, M.; Jaroniec, M.; Moudrakovski, I. L. New approaches to pore size engineering of mesoporous silicates. *Adv. Mater.* **1998**, *10*, 1376–1379.
108. Sayari, A. Unprecedented expansion of the pore size and volume of periodic mesoporous silica. *Angew. Chem. Int. Ed.* **2000**, *112*, 3042–3044.
109. Drese, J. H.; Choi, S.; Lively, R. P.; Koros, W. J.; Fauth, D. J.; Gray, M. L.; Jones, C. W. Synthesis-structure-property relationships for hyperbranched aminosilica CO₂ adsorbents. *Adv. Funct. Mater.* **2009**, *19*, 3821–3832.
110. Li, Y.; Sun, N.; Li, L.; Zhao, N.; Xiao, F.; Wei, W.; Sun, Y.; Huang, W. Grafting of amines on ethanol-extracted SBA-15 for CO₂ adsorption. *Materials* **2013**, *6*, 981–999.
111. Zeleňák, V.; Badaničová, M.; Halamová, D.; Čejka, J.; Zukal, A.; Murafa, N.; Goerigk, G. Amine-modified ordered mesoporous silica: Effect of pore size on carbon dioxide capture. *Chem. Eng. J.* **2008**, *144*, 336–342.
112. Knöfel, C.; Descarpentries, J.; Benzaouia, A.; Zeleňák, V.; Mornet, S.; Llewellyn, P. L.; Hornebecq, V. Functionalised micro-/mesoporous silica for the adsorption of carbon dioxide. *Microporous Mesoporous Mater.* **2007**, *99*, 79–85.
113. Huang, H. Y.; Yang, R. T.; Chinn, D.; Munson, C. L. Amine-grafted MCM-48 and silica xerogel as superior sorbents for acidic gas removal from natural gas. *Ind. Eng. Chem. Res.* **2003**, *42*, 2427–2433.
114. Ko, Y. G.; Lee, H. J.; Oh, H. C.; Choi, U. S. Amines immobilized double-walled silica nanotubes for CO₂ capture. *J. Hazard. Mater.* **2013**, 250–251, 53–60.
115. Hsu, S.-C.; Lu, C.; Su, F.; Zeng, W.; Chen, W. Thermodynamics and regeneration studies of CO₂ adsorption on multiwalled carbon nanotubes. *Chem. Eng. Sci.* **2010**, *65*, 1354–1361.

116. Rezaei, F.; Webley, P. Structured adsorbents in gas separation processes. *Sep. Purif. Technol.* **2010**, *70*, 243-256.
117. Veneman, R.; Li, Z. S.; Hogendoorn, J. A.; Kersten, S. R. A.; Brilman, D. W. F. Continuous CO₂ capture in a circulating fluidized bed using supported amine sorbents. *Chem. Eng. J.* **2012**, 207-208, 18-26.
118. Hasan, F. A.; Xiao, P.; Singh, R. K.; Webley, P. A. Zeolite monoliths with hierarchical designed pore network structure: Synthesis and performance. *Chem. Eng. J.* **2013**, *223*, 48-58.
119. Li, Y. Y.; Perera, S. P.; Crittenden, B. D. Zeolite monoliths for air separation: Part 2: Oxygen enrichment, pressure drop and pressurization. *Chem. Eng. Res. Des.* **1998**, *76*, 931-941.
120. Lee, L. Y.; Perera, S. P.; Crittenden, B. D.; Kolaczowski, S. T. Manufacture and characterisation of silicalite monoliths. *Adsorpt. Sci. Technol.* **2000**, *18*, 147-170.
121. Yu, F. D.; Luo, L. A.; Grevillot, G. Adsorption isotherms of VOCs onto an activated carbon monolith: Experimental measurement and correlation with different models. *J. Chem. Eng. Data* **2002**, *47*, 467-473.
122. Yates, M.; Blanco, J.; Avila, P.; Martin, M. P. Honeycomb monoliths of activated carbons for effluent gas purification. *Microporous Mesoporous Mater.* **2000**, *37*, 201-208.
123. Thiruvengkatachari, R.; Su, S.; Yu, X. X.; Bae, J.-S. Application of carbon fibre composites to CO₂ capture from flue gas. *Int. J. Greenhouse Gas Control* **2013**, *13*, 191-200.
124. Ahn, H.; Brandani, S. Dynamics of carbon dioxide breakthrough in a carbon monolith over a wide concentration range. *Adsorption* **2005**, *11*, 473-477.
125. An, H.; Feng, B.; Su, S. Effect of monolithic structure on CO₂ adsorption performance of activated carbon fiber-phenolic resin composite: A simulation study. *Fuel* **2013**, *103*, 80-86.
126. Patton, A.; Crittenden, B. D.; Perera, S. P. Use of the linear driving force approximation to guide the design of monolithic adsorbents. *Chem. Eng. Res. Des.* **2004**, *82*, 999-1009.

127. Ribeiro, R. P.; Sauer, T. P.; Lopes, F. V.; Moreira, R. F.; Grande, C. A.; Rodrigues, A. E. Adsorption of CO₂, CH₄, and N₂ in activated carbon honeycomb monolith. *J. Chem. Eng. Data* **2008**, 53, 2311–2317.
128. Mosca, A.; Hedlund, J.; Ridha, F. N.; Webley, P. Optimization of synthesis procedures for structured PSA adsorbents. *Adsorption* **2008**, 14, 687-693.
129. Rezaei, F.; Mosca, A.; Hedlund, J.; Webley, P. A.; Grahn, M.; Mouzon, J. The effect of wall porosity and zeolite film thickness on the dynamic behavior of adsorbents in the form of coated monoliths. *Sep. Purif. Technol.* **2011**, 81, 191–199.
130. Ruthven, D. M.; Thaeron, C. Performance of a parallel passage adsorbent contactor. *Sep. Purif. Technol.* **1997**, 12, 43-60.
131. Calis, H. P.; Everwijn, T. S.; Gerritsen, A. W.; Van Den Bleek, C. M.; Goudriaan, F.; Van Dongen, F. G. Mass transfer characteristics of parallel passage reactors. *Chem. Eng. Sci.* **1994**, 49, 4289-4297.
132. Rode, E. J.; Boulet, A. J. J.; Pelman, A. M.; Babicki, M. L.; Keefer, B. G.; Sawada, J. A.; Alizadeh-Khiavi, S.; Roy, S.; Gibbs, A. C.; Kuznicki, S. M. Engineered adsorbent structures for kinetic separation. *US 7645324 B2* **2010**.
133. Gilleskie, G. L.; Parker, J. L.; Cussler, E. L. Gas separations in hollow-fiber adsorbents. *AIChE J.* **1995**, 41, 1413-1425.
134. Feng, X.; Pan, C. Y.; McMinis, C. W.; Ivory, J.; Ghosh, D. Hollow-fiber-based adsorbents for gas separation by pressure-swing adsorption. *AIChE J.* **1998**, 44, 1555–1562.
135. Tarka, T. J.; Ciferno, J. P.; Gray, M. L.; Fauth, D. CO₂ capture systems using amine enhanced solid sorbents. *5th annual conference on carbon capture & sequestration* **2006**, paper 152.
136. Yang, W.-C.; Hoffman, J. Exploratory design study on reactor configurations for carbon dioxide capture from conventional power plants employing regenerable solid sorbents. *Ind. Eng. Chem. Res.* **2009**, 48, 341-351.
137. Rezaei, F.; Webley, P. Optimum structured adsorbents for gas separation processes. *Chem. Eng. Sci.* **2009**, 64, 5182-5191.

138. Brandani, F.; Rouse, A.; Brandani, S.; Ruthven, D. M. Adsorption kinetics and dynamic behavior of a carbon monolith. *Adsorption* **2004**, 10, 99–109.
139. Grande, C. A.; Rodrigues, A. E. Electric swing adsorption for CO₂ removal from flue gases. *Int. J. Greenhouse Gas Control* **2008**, 2, 194–202.
140. Sullivan, P. D.; Rood, M. J.; Hay, K. J.; Qi, S. Adsorption and electrothermal desorption of hazardous organic vapors. *J. Environ. Eng.* **2001**, 127, 217–223.
141. Matsukuma, Y.; Matsushita, Y.; Kakigami, H.; Inoue, G.; Minemoto, M.; Yasutake, A.; Oka, N. Study on CO₂ recovery system from flue gas by honeycomb type adsorbent I - (Results of tests and simulation). *Kagaku Kogaku Ronbunshu* **2006**, 32, 138–145.
142. Matsukuma, Y.; Sadagata, K.; Kakigami, H.; Inoue, G.; Minemoto, M.; Yasutake, A.; Oka, N. Simulation of CO₂ recovery system from flue gas by honeycomb type adsorbent II - (Optimization of CO₂ recovery system and proposal of actual plant). *Kagaku Kogaku Ronbunshu* **2006**, 32, 146-152.

Chapter 3

Materials and Methods

The content of this chapter is arranged as:

- Specification of all the chemicals and gases used in this work is given in materials section.
- The synthesis section provides the procedure for SBA-15 preparation, DAEAPTS grafting over SBA-15 support and PEI impregnation over SBA-15 support.
- The characterization methods used for DAEAPTS amine grafted SBA-15 adsorbent samples are described in brief in characterization section. The characterization methods include N₂ adsorption/desorption, SEM, HRTEM, TGA, Elemental analysis and FTIR analysis.
- This chapter presents the TGA experimental set-up and operating conditions used during performance evaluation of amine grafted adsorbent samples.
- This chapter describes the packed bed and structured bed experimental set-ups and operating conditions for performance evaluation of amine impregnated adsorbent with the two beds. Finally, equations are given for capacity calculation with packed and structured beds.

3.1 Materials

Triblock copolymer Pluronic P-123 surfactant (poly(ethylene glycol)-block-poly(propylene glycol)-block-poly(ethylene glycol), average MW~5800) and tetraethyl orthosilicate (TEOS, 98%) obtained from Sigma Aldrich and were used without further purification for the synthesis of SBA-15. HCl (36.5-38%) used as a pH controlling agent and obtained from J. T. Baker. N-(3-trimethoxysilylpropyl)-diethylenetriamine (DAEPTS, 91.5%), hexane (99%) and anhydrous toluene (99.9%) used for grafting of amine on SBA-15 were also purchased from Sigma Aldrich and used as received. Methanol (Fisher Chemical, 99.9%) and PEI (Sigma Aldrich, average MW~800) were used as received for the preparation of amine impregnated SBA-15 adsorbent. Deionized water was obtained from a Milli-Q integral pure and ultrapure water purification system. Pure carbon dioxide (99.99%) and ultra high pure nitrogen (99.999%) gases were obtained from Praxair for the CO₂ adsorption/desorption measurements.

3.2 Synthesis

3.2.1 Preparation of SBA-15

The mesoporous SBA-15 material used as a porous support for hosting the amino functional groups was synthesized in this work according to the method reported elsewhere.¹ In a typical synthesis procedure, 4 g of Pluronic P-123 was dissolved in 30 ml of deionized water and 120 ml of 2 M HCl solution while stirring for 2 h at 25 °C. The resultant solution was transferred into a teflon autoclave and solution temperature was raised to about 40 °C. 8.5 g of TEOS was added

dropwise to the homogenous solution under vigorous stirring for 30 min and a precipitated product appeared as a result. The resulting gel was stirred at 40 °C for about 20 h at low stirring rate and then aged at 100 °C for 48 h without stirring. The white precipitated solid obtained was then filtered, washed with deionized water, and dried in air at room temperature for 12 h and in an air oven at 100 °C for another 12 h. The organic template was removed from the product by calcination in flowing air at 550 °C for 5 h.

3.2.2 Preparation of DAEAPTS amine grafted SBA-15

The DAEAPTS-grafted sorbents were prepared via wet grafting technique.² Figure 3.1 provides the schematic representation of the reaction between the DAEAPTS amine and hydroxyl groups on SBA-15 support. As shown in Figure 3.1, one DAEAPTS molecule can form one, two or three linkages with the SBA-15 surface. In a typical preparation, about 0.5 g of calcined SBA-15 was dissolved in about 150 ml of anhydrous toluene and allowed to mix for about 0.5 h at room temperature with low stirring. Then 0.2 ml of water was added to the above mixture and continuously mixed at room temperature for about 2 h with low stirring. The temperature of the mixture was then increased and maintained at 100 °C and desired quantity of DAEAPTS amine was added to it. The system was held under vigorous stirring and reflux for about 24 h. The resultant slurry was washed first with toluene and then hexane and finally dried at 70 °C for 12 h under vacuum. The thus formed amine grafted SBA-15 sorbent is denoted as SBA-15/D-x where D indicates the DAEAPTS amine and x represents the

quantity of DAEAPTS amine used in ml per g of SBA-15 used during the synthesis process.

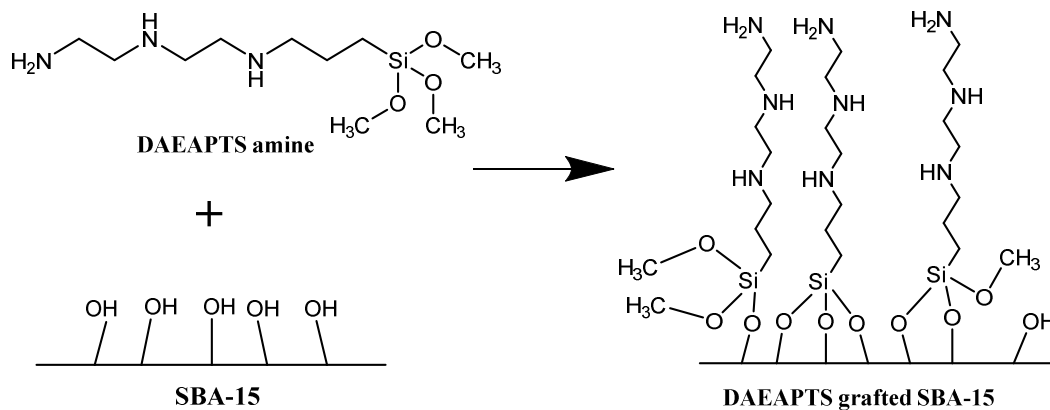


Figure 3.1. Schematic representation of DAEAPTS amine grafting over SBA-15 support.

3.2.3 Preparation of PEI amine impregnated SBA-15

CO_2 capture performance in structured and packed beds was evaluated using PEI impregnated SBA-15 adsorbent. Impregnation of PEI amine over SBA-15 mesoporous support was done using wet impregnation technique.³ First, the desired quantity of PEI amine was mixed for 15 min in 8 g of methanol. 2 g of raw calcined SBA-15 powder was then mixed with the above solution. The slurry formed was mixed for 0.5 h with stirring at room temperature. The resultant mixture was finally dried at 80 °C for 2 h under vacuum. The amine impregnated SBA-15 sorbent formed is denoted as SBA-15/P-y where P indicates the PEI amine and y represents the wt% of PEI in the dried adsorbent.

3.3 Characterization

N₂ adsorption/desorption, Scanning electron microscopy (SEM), High resolution transmission electron microscopy (HRTEM), Thermo-gravimetric analysis (TGA), Elemental analysis and Fourier transform infrared spectroscopy (FTIR) methods were used for the characterization of calcined SBA-15 and amine grafted SBA-15 adsorbents.

3.3.1 N₂ adsorption/desorption

The N₂ adsorption/desorption isotherms of the sorbents were measured using Autosorb iQ (Quantachrome, USA) in the relative pressure (P/P_0) range of 0–0.997 at -196 °C. Different degassing conditions were used for calcined SBA-15 and amine grafted SBA-15 samples. The calcined SBA-15 sample was degassed at 250 °C for 120 min under high vacuum before starting analysis whereas amine functionalized SBA-15 sorbent samples were degassed at 80 °C for only 60 min under high vacuum in order to avoid amine loss. Volume of liquid N₂ adsorbed by the sorbent at the relative pressure (P/P_0) of 0.997 was taken as the total pore volume. T-plot method was used for measuring micropore volume. The multi-point Brunauer Emmett Teller (BET) method at the relative pressure (P/P_0) range of 0.05–0.30 was used for the calculation of the surface area. Pore size distribution of calcined SBA-15 and amine grafted samples was computed using the Barrett-Joyner-Halenda (BJH) method.

3.3.2 SEM and HRTEM

Electron microscopy is very important tool to determine the size, shape and structure of an adsorbent. SEM (Hitachi S-2700) analysis of the calcined SBA-15 was done to study the morphology of the sample. The sample was gold coated for the SEM analysis. High resolution TEM (JEOL 2010) was performed in order to examine the structure with higher precision. Copper grids with formvar coating were used for sample deposition in HRTEM. The HRTEM machine was equipped with a LaB₆ electron gun.

3.3.3 Amine loading using TGA and Elemental analysis

Amine loading of the functionalized sample was measured using TGA (TGA/DSC 1 STARe System, Mettler Toledo). The sample was kept under nitrogen atmosphere till 900 °C inside thermo-gravimetric analyzer. The amine loading results were calculated on the dry basis mass of amine functionalized adsorbent samples after water vaporization at 100 °C in TGA. Elemental analysis was also performed on amine grafted sorbents for carbon, nitrogen, hydrogen and sulfur percentage using Elementar analyzer (Model: Vario Micro, USA). From the elemental analysis results, the nitrogen (N) wt% and amine loading of the grafted and raw SBA-15 samples were calculated.

3.3.4 Fourier Transform Infrared Spectroscopy (FTIR)

FTIR spectra of the raw SBA-15 sample and DAEPTS amine grafted sorbent samples were measured using MB 3000 FTIR spectrometer (ABB, Canada). The

machine has built-in MIRacle three-reflection diamond ATR instrument (Pike Technologies, USA). The results were analyzed using Horizon MB FTIR software. 100 scans were performed for FTIR spectrum of every sorbent sample in the frequency range of 550-4000 cm^{-1} . The resolution of 2 cm^{-1} was used.

3.4 CO₂ adsorption and desorption using TGA

CO₂ adsorption/desorption measurements of amine functionalized SBA-15 adsorbents were performed using a thermo-gravimetric analyzer (TGA/DSC 1 STARe System, Mettler Toledo). The TGA experimental set-up used for the tests is presented in Figure 3.2. The grafted adsorbents were powdered in the size range of 150-250 microns. For every adsorption experiment, around 10-20 mg of powdered sorbent material in platinum pan was used for the TGA measurements. The grafted adsorbent sample was activated before CO₂ adsorption at 150 °C under 150 cm^3/min of N₂ gas for around 1 h. All the CO₂ adsorption capacities measured in this work are for 120 min of adsorption time at the specified adsorption temperature under CO₂/N₂ gas mixture at 1 atm. During all the TGA runs, 20 cm^3/min of N₂ was always flowing as protective gas and the gas composition for adsorption was calculated keeping 20 cm^3/min of N₂ as protective gas into consideration. So, 150 cm^3/min of 100% CO₂ is denoted as 88.2% CO₂/11.8% N₂ after taking into consideration 20 cm^3/min of N₂ as protective gas. Similarly, 150 cm^3/min of 10% CO₂/90% N₂ is denoted as 8.8% CO₂/91.2% N₂ gas mixture after taking into account 20 cm^3/min of N₂ as protective gas. To study multi-cycle performance of the grafted SBA-15 sorbent, 100 consecutive cycles of

adsorption/desorption were conducted thermogravimetrically using 88.2% CO₂/11.8% N₂ gas mixture. Each cycle comprised of 10 min of CO₂ adsorption at 75 °C and followed by 10 min of desorption at 150 °C. The regeneration of the adsorbent was done using TSA method under pure N₂ gas purge. The moisture effect was studied by exposing the sorbent to a humid stream of CO₂/N₂ gas mixture. Dry CO₂/N₂ gas mixture was passed via a water saturator maintained at 25 °C using a water bath to obtain humid CO₂/N₂ gas stream. Relative humidity (RH) of the humid gas was measured using a hygrometer (Control Company, USA). Relative humidity of around 95% at 25 °C (equivalent to about 2.98 vol% moisture in the gas mixture) was maintained for the humid CO₂/N₂ gas mixture for the adsorption tests. The grafted sample was also tested for adsorption due to moisture alone using humid N₂ gas at RH of about 95% at 25 °C.

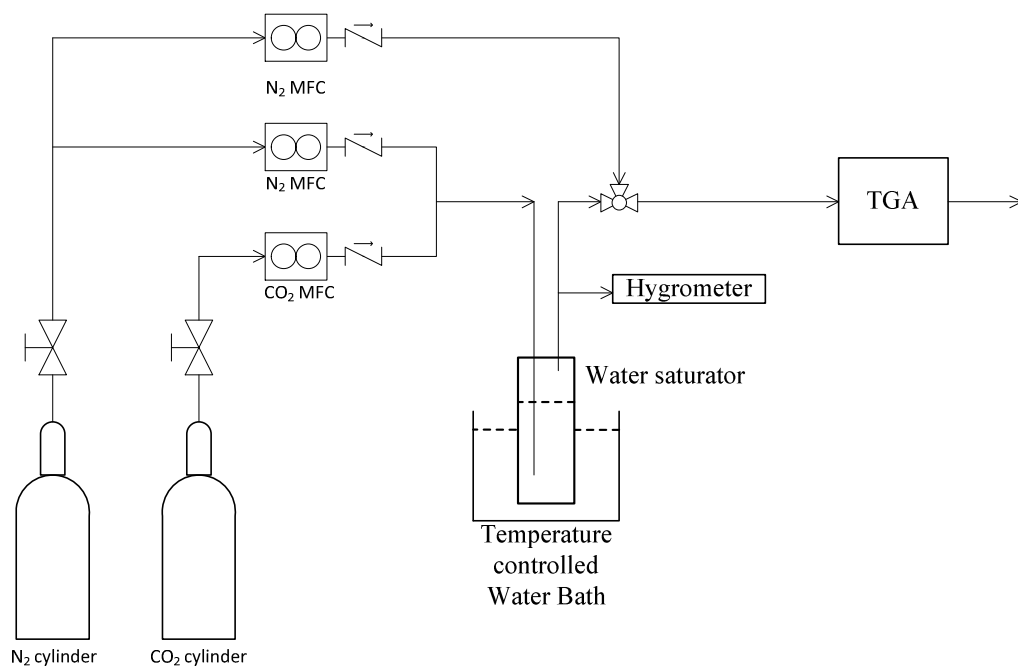


Figure 3.2. TGA experimental set-up for performance evaluation of amine functionalized SBA-15 adsorbent.

3.5 CO₂ adsorption/desorption using different bed configurations

3.5.1 Packed bed

CO₂ adsorption and desorption performance was evaluated using packed bed to analyze the advantages and disadvantages of using packed bed for CO₂ capture. The packed bed performance was compared with structured bed results. The schematic representation of the packed bed used for the CO₂ adsorption/desorption tests is shown in Figure 3.3. The packed bed used in this study has simple quartz U-tube geometry with the dimensions given in Figure 3.3. The transparent nature of the quartz U-tube bed allowed easy and reliable monitoring of the adsorbent inside the bed. Packed bed was filled with sorbent

material upto 5 cm length for all the tests in this study to maintain uniformity of the results. Small cotton pieces were placed above and below the adsorbent bed to contain the adsorbent material. Experimental set-up of the packed bed adsorption/desorption system is presented in Figure 3.4. All the mass flow controllers (MFCs, Brooks Instrument 4800 series) used for CO₂ and N₂ had flow accuracy in the range of $\pm 3\%$.

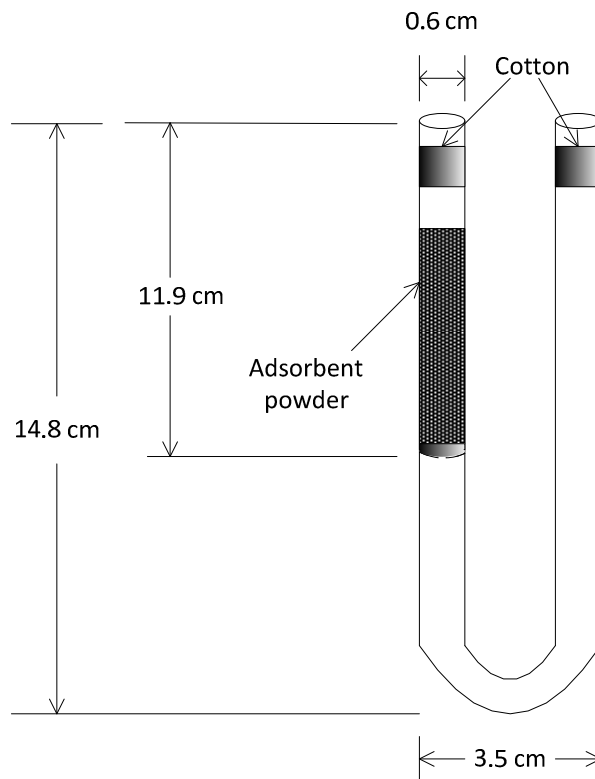


Figure 3.3. Diagram of U-tube used as packed bed for CO₂ adsorption/desorption tests.

Preheating section comprised of coiled copper tube of large length was provided before the packed bed in order to raise the gas temperature to the desired operating temperature of the packed bed. The temperature of the preheating

section and packed bed was maintained using refrigerated/heating oil circulator (F25-HE, Julabo). The gas concentrations of CO₂ and N₂ at the outlet of the packed bed were measured using gas mass spectrometer (OmniStar, Pfeiffer Vacuum).

Adsorption performance with packed bed was evaluated using 50 wt% PEI impregnated SBA-15 adsorbent sample and the bed was filled with around 130 mg of adsorbent sample in each run. The adsorbent powder was sieved in the range of 150-250 microns before filling up the packed bed. Before the experiment with SBA-15/P-50 sample adsorbent, same test was run with CO₂ inert alpha-alumina powder to take into account the delay time of the system. Adsorption was performed with 10% CO₂/90% N₂ gas mixture and desorption with pure N₂. Before any adsorption experiment, the sorbent sample was held at 105 °C for 60 min under pure N₂ to remove the adsorbed CO₂ and moisture from the sorbent. For experiments with humid gas, 95% RH at 25 °C was maintained and measured using a hygrometer (Control Company, USA). To study multi-cycle performance of the impregnated SBA-15 adsorbent in packed bed, 20 consecutive cycles of adsorption/desorption were conducted using 10% CO₂/90% N₂ dry and humid gas mixtures. Each cycle involved adsorption in 10% CO₂/90% N₂ gas mixture at 75 °C and desorption in pure N₂ at 90 °C.

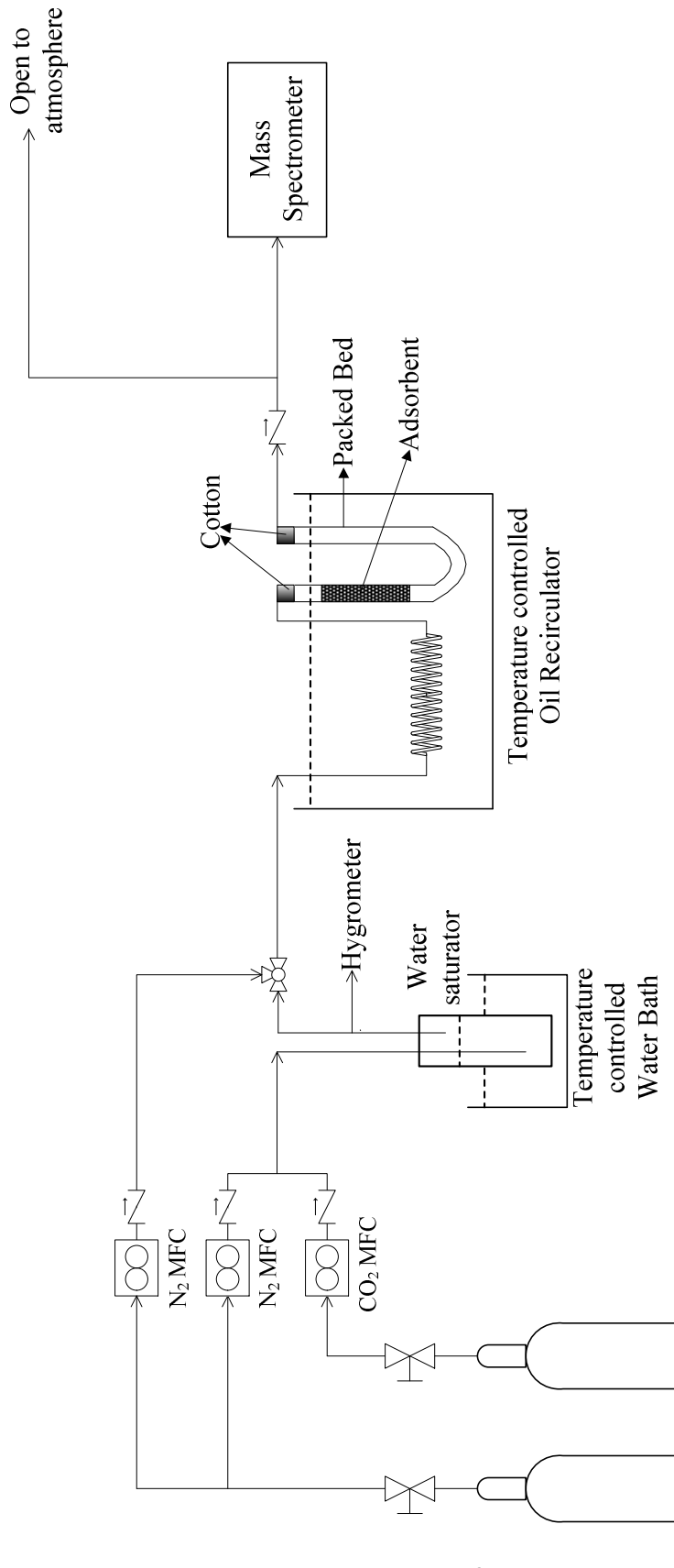


Figure 3.4. Packed bed experimental set-up used for CO₂ adsorption/desorption tests.

3.5.2 Structured bed

In this work, a structured bed system was considered to study the mass transfer due to adsorption/desorption inside the porous bed structure. The lateral and cross-sectional views of a single-tube structured bed are presented in Figure 3.5. In this bed configuration, amine impregnated solid sorbent is contained by macro-porous barrier layers inside a concentric porous tube and CO₂ laden bulk gas flows through the annular region. CO₂ diffuses across the barrier layer and gets preferentially adsorbed on the amine functionalized solid sorbent.

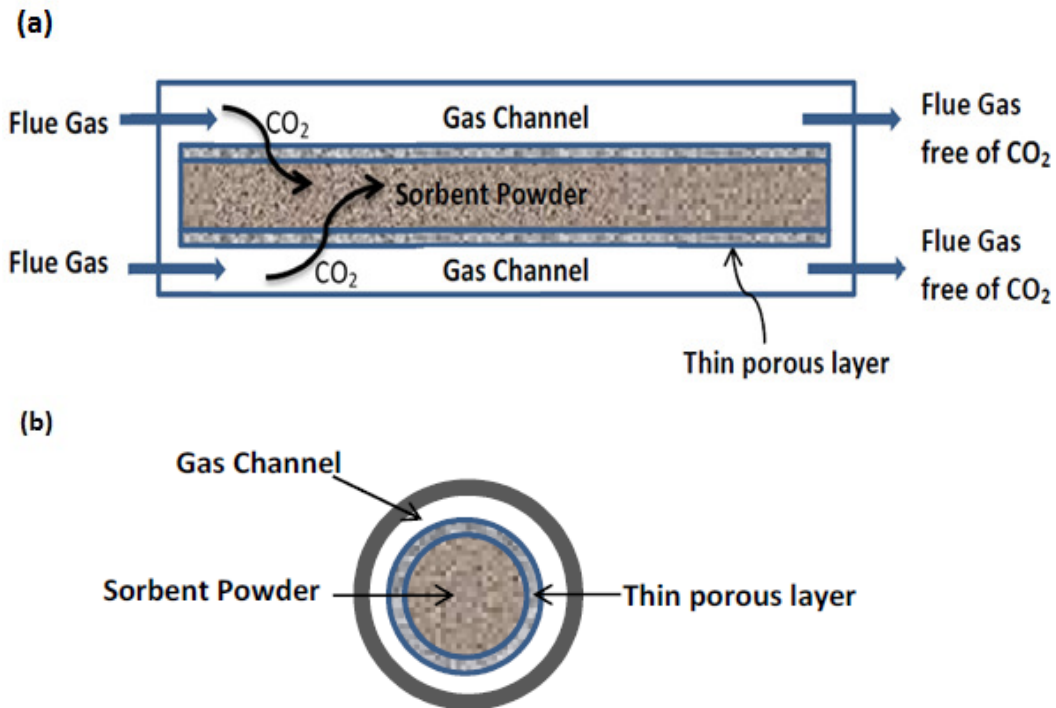


Figure 3.5. Proposed structured bed adsorption/desorption system with single tube, (a) lateral view, (b) cross-sectional view.

In the practical industrial scale, structured bed will be used with multiple membrane tubes rather than single tube. Single-tube structured bed was used for

initial CO₂ adsorption/desorption performance evaluation in this work. After the initial analysis with single tube, the bed was upgraded to 3 tubes. In future work, number of tubes in structured bed will be increased even further stage-wise after satisfactory performance evaluation at each stage. The lateral and cross-sectional views of three-tube structured bed configuration is presented in Figure 3.6.

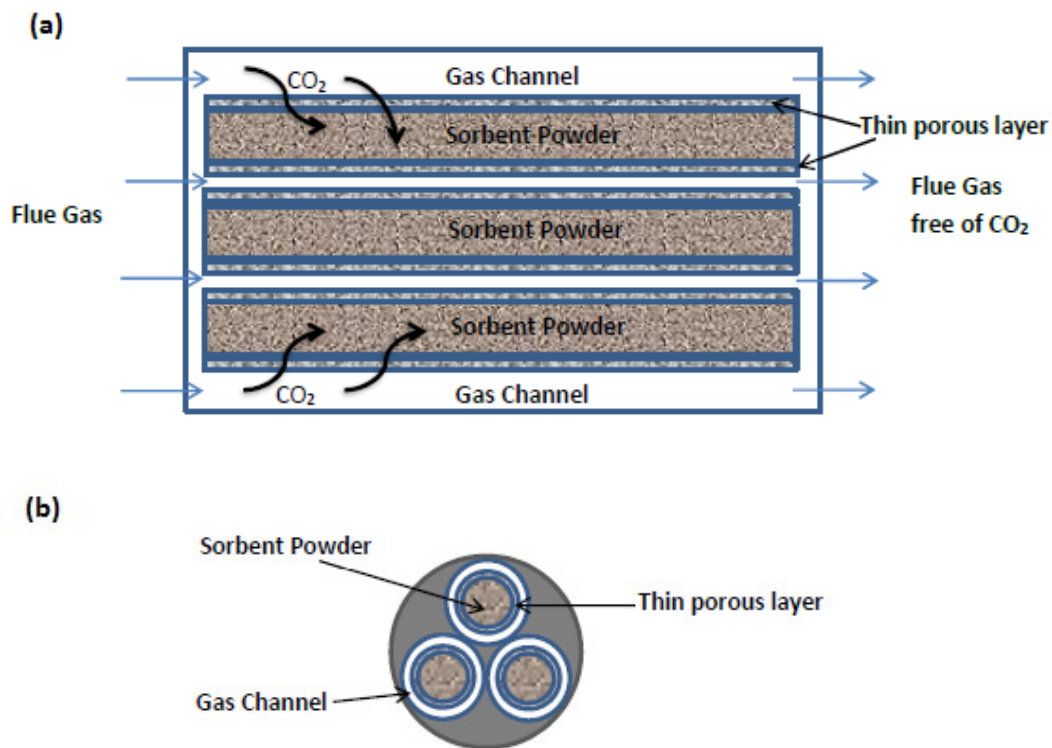


Figure 3.6. Proposed structured bed adsorption/desorption system with three tubes, (a) lateral view, (b) cross-sectional view.

The structured sorbent bed set-up (membrane tube material: alumina, membrane tube length: 20 cm and reactor channel spacing: 250 μm) was tested for CO₂ adsorption/desorption performance with 50 wt% PEI impregnated SBA-15 adsorbent. Reactor with single and three membrane tubes were used for the

experiments. Each alumina membrane tube was filled with approximately 200 mg of SBA-15/P-50 solid sorbent during every run. Before the experiment with SBA-15/P-50 sample adsorbent, same test was run with CO₂ inert alpha-alumina powder to take into account the delay time of the system.

The structured bed experimental set-up is shown in Figure 3.7. The experimental set-up was equipped with a real-time gas analyzer and flexible reactor chamber. The experimental set-up was divided into 4 zones: gas injection/mixing, gas pre-heating, reactor and gas sampling. Each zone is discussed below in brief:

Zone 1 (gas injection/mixing): Standard compressed gas cylinders of CO₂ and N₂ were used as gas sources. The outlet of the gas cylinders were connected to release valves with set point of 20 psi in order to protect instrument upstream of flow controllers. A series of mass flow controllers (MFCs) delivered and blended the required amount and composition of gases. Check valves were provided upstream and downstream of MFCs to avoid back flow of gases. The MFCs were controlled by a virtual instrument (VI) program using Labview software (National Instruments).

Zone 2 (gas pre-heating): In this section, approximately 20 cm long stainless steel (SS) tubing of 1.27 cm outer diameter (OD) was provided to preheat the gas before feeding it to the reactor. The heating source was provided by wrapping heating tape around the SS tubing. Heating tape target temperature was controlled with a temperature controller (Omega).

Zone 3 (reactor): The membrane holder (reactor) is made of stainless steel with around 20 cm length. The reactor is heated by wrapping heating tape around it.

Zone 4 (gas analysis): Gas mixture from the outlet of reactor was passed through a gas mass spectrometer (OmniStar, Pfeiffer Vacuum).

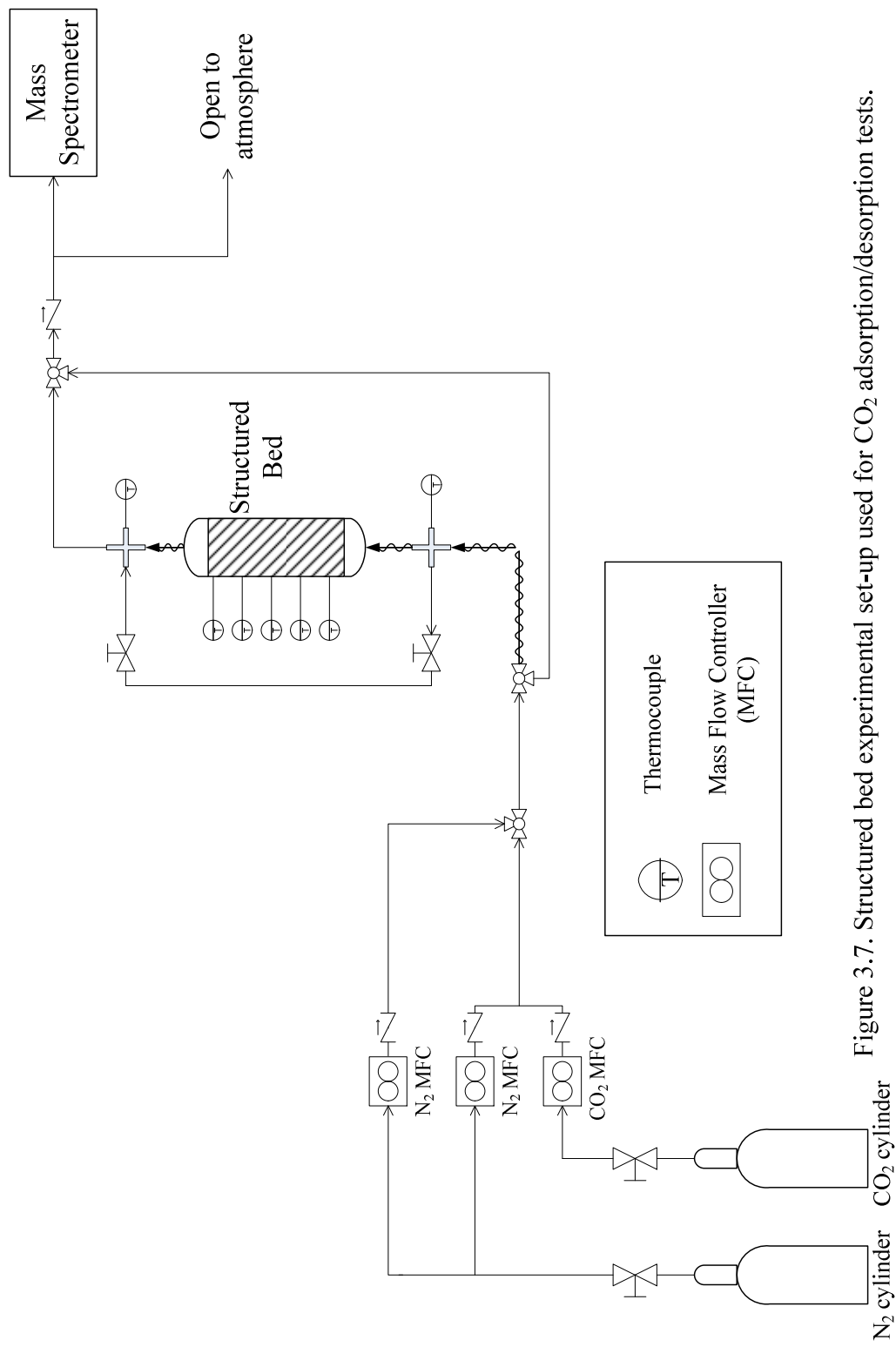


Figure 3.7. Structured bed experimental set-up used for CO₂ adsorption/desorption tests.

3.5.3 Capacity calculation

This section describes the procedure for the calculation of adsorption capacity from the mass spectrometer (MS) data for packed and structured bed configurations. The breakthrough time in this work is defined as the time when CO₂ concentration reaches 0.1% at the outlet of the bed. It is measured from the MS data for adsorption performance evaluation. The CO₂ sorption capacity is calculated from the breakthrough curves obtained with the amine functionalized adsorbent sample and inert alumina powder. The equivalent time of CO₂ adsorption is calculated using Equation (1). Using the equivalent adsorption time, the adsorption capacity is calculated using Equation (2), as follows:^{4,5}

$$t_{ad} = \int_0^T \left(\frac{C_b}{C_0} - \frac{C_a}{C_0} \right) dt \quad (1)$$

$$q = \frac{t_{ad} C_0 F}{m} \quad (2)$$

where

t_{ad}	Equivalent adsorption time
T	Total adsorption time
C_a	CO ₂ concentration at any time t using the adsorbent sample
C_b	CO ₂ concentration at any time t using the inert alumina powder
C_0	CO ₂ concentration in the feed
F	Feed gas flowrate
m	Weight of adsorbent used during the run
q	Adsorption capacity

References

1. Zhao, D.; Feng, J.; Huo, Q.; Melosh, N.; Fredrickson, G. H.; Chmelka, B. F.; Stucky, G. D. Triblock copolymer syntheses of mesoporous silica with periodic 50 to 300 angstrom pores. *Science* **1998**, 279, 548-552.
2. Harlick, P. J. E.; Sayari, A. Applications of pore-expanded mesoporous silica. 5. Triamine grafted material with exceptional CO₂ dynamic and equilibrium adsorption performance. *Ind. Eng. Chem. Res.* **2007**, 46, 446–458.
3. Xu, X.; Song, C.; Andresen, J. M.; Miller, B. G.; Scaroni, A. W. Preparation and characterization of novel CO₂ “molecular basket” adsorbents based on polymer-modified mesoporous molecular sieve MCM-41. *Microporous Mesoporous Mater.* **2003**, 62, 29–45.
4. Chang, H.; Wu, Z.-X. Experimental study on adsorption of carbon dioxide by 5A molecular sieve for helium purification of high-temperature gas-cooled reactor. *Ind. Eng. Chem. Res.* **2009**, 48, 4466–4473.
5. Liu, J.; Tian, J.; Thallapally, P. K.; McGrail, B. P. Selective CO₂ capture from flue gas using metal–organic frameworks—A fixed bed study. *J. Phys. Chem. C* **2012**, 116, 9575–9581.

Chapter 4

Results and Discussion

This chapter is divided into two parts:

Part 1: Synthesis of amine functionalized adsorbents using grafting technique.

Part 2: Performance evaluation of structured bed configuration with straight gas flow channels using amine impregnated adsorbent.

Part 1

The content of part 1 of this chapter is arranged as:

- This chapter discusses the characterization and CO₂ adsorption/desorption performance results of DAEAPTS amine grafted SBA-15 adsorbents.
- The characterization results of amine grafted SBA-15 samples is obtained using N₂ adsorption/desorption, SEM, HRTEM, TGA, elemental analysis and FTIR analysis. N₂ adsorption/desorption method examines the textural properties of calcined and amine grafted SBA-15 samples. The SEM and TEM section gives information on the structural properties of calcined SBA-15. FTIR analysis of calcined and amine grafted SBA-15 samples is done to show the different types of bonds present. Amine loading of the grafted SBA-15 samples is measured using TGA and elemental analysis methods.

- The CO₂ adsorption/desorption performance of amine grafted SBA-15 samples is investigated in this chapter. CO₂ adsorption capacity and amine adsorption efficiency is evaluated for grafted SBA-15 samples with variable amine loading in order to find the optimum amine loading. The effect of adsorption temperature and CO₂ partial pressure on the CO₂ adsorption capacity of grafted sample is discussed. Also, heat of adsorption values are measured for amine grafted sample at different adsorption temperatures and CO₂ concentrations. Effect of amine loading on the adsorption kinetics of amine grafted samples is examined in kinetics section. The adsorption and desorption kinetics of optimal amine loaded sample is evaluated in both dry and humid CO₂/N₂ gas streams. The adsorption capacities and kinetics are presented for grafted sample in dry CO₂/N₂, humid CO₂/N₂, moisture and dry N₂ streams to show the effect of moisture. The last section of this chapter discusses the multi-cycle stability of grafted sample after 100 cyclic runs in dry and humid CO₂/N₂. FTIR results are analysed to understand the effect of cyclic runs on the amine grafting of samples.

4.1 Characterization

The DAEAPTS grafted SBA-15 adsorbent samples were characterized using N₂ adsorption/desorption, SEM, HRTEM, FTIR, TGA and Elemental analysis methods. The characterization results of DAEAPTS amine grafted samples are discussed in this section.

4.1.1 N₂ adsorption/desorption

The textural properties like pore size, pore volume, surface area of calcined SBA-15, and amine grafted sorbents are tabulated in Table 4.1. The N₂ adsorption/desorption isotherms of calcined SBA-15 displays typical type IV isotherm indicative of defined mesoporosity in the framework (Figure 4.1). The uniform distribution of pore size in calcined SBA-15 is shown in the inset of Figure 4.1, the curve has a sharp peak at about 6.8 nm. For calcined SBA-15, the total pore volume is about 1.184 cm³/g and BET surface area around 676 m²/g. In comparison to calcined SBA-15, DAEAPTS amine grafted sorbent SBA-15/D-4 has lower total pore volume and BET surface area of 0.122 cm³/g and 15.9 m²/g, respectively. The reason for the reduction in pore volume and surface area is possibly because of the presence of DAEAPTS amine in the SBA-15 support channels leading to pore blocking/distorting. This confirms that some DAEAPTS was not removed during toluene and hexane washing process and remained inside the pores of the SBA-15 support blocking the connecting pore channels between the mesopores.

Table 4.1. Textural properties of raw and amine grafted SBA-15 samples.

Sample	Pore Diameter [nm]	Total Pore Volume [cm ³ /g]	Micropore Volume ^a [cm ³ /g]	Surface Area [m ² /g]
Calcined SBA-15	6.8	1.184	0.065	676
SBA-15/D-4	3.3	0.122	~0	15.9

a: Using t-plot method

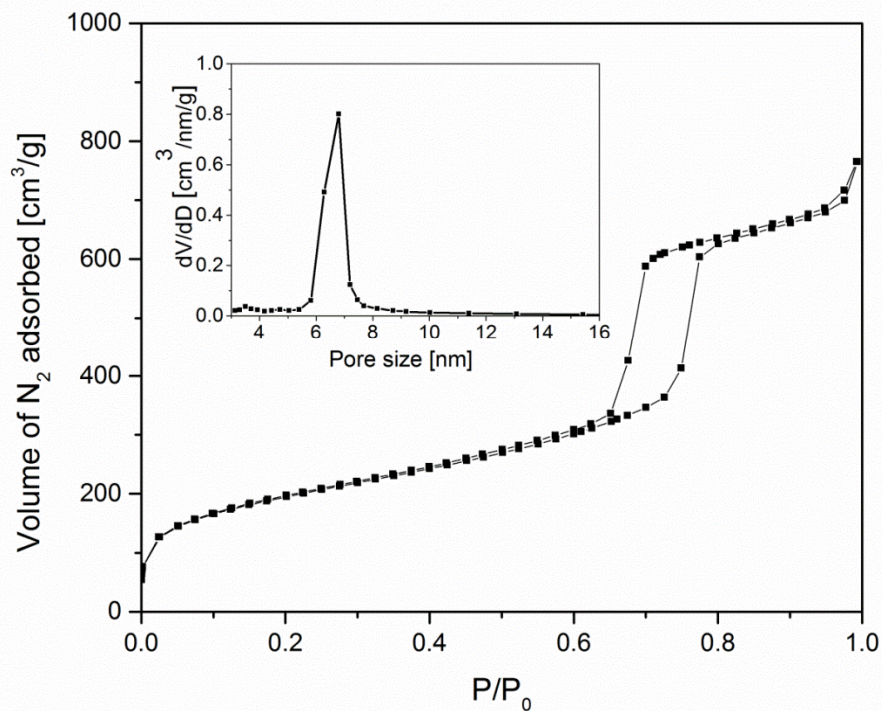


Figure 4.1. N₂ adsorption/desorption isotherm and pore size distribution of calcined SBA-15.

4.1.2 SEM and HRTEM

The SEM image of calcined SBA-15 presented in Figure 4.2(a) shows the rope like structure of SBA-15 sample. The high resolution TEM images of calcined SBA-15 are given in Figure 4.2(b) and 4.2(c).¹ Figure 4.2(b) displays that SBA-15 pore channels are highly ordered and cylindrical in shape. The mean wall thickness calculated from this Figure is around 4.7 nm. Figure 4.2(c) shows the 2-D hexagonal arrangement of the calcined SBA-15 pore channels.¹ Mesoporous silica support structure MCM-41 has mean wall thickness normally around 1.5 nm, which is lower than that of SBA-15 material.^{2,3} The larger wall thickness of

SBA-15 support structure gives it better hydrothermal stability as compared to MCM-41.^{4,5}

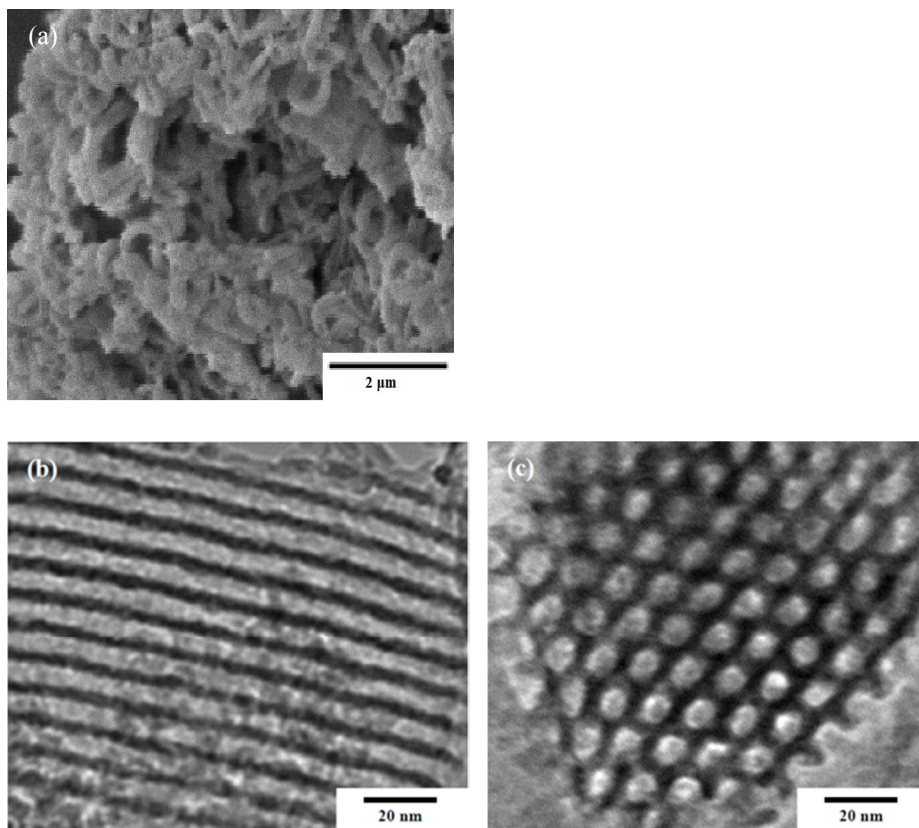


Figure 4.2. Raw calcined SBA-15 sample: (a) SEM image, (b) and (c) High resolution TEM images.¹ (Reprinted (adapted) with permission from Zhao et al.¹ Copyright 2013 American Chemical Society.)

4.1.3 FTIR analysis

FTIR analysis was performed to find out the kind of functional groups and chemical bonds present in calcined SBA-15 and amine grafted SBA-15 samples.

The spectrum for calcined SBA-15 in Figure 4.3 shows peak at 1040 cm^{-1} and a thick shoulder at 1200 cm^{-1} , which is typical of $(\text{SiO})_n$ siloxane stretching.⁶ The spectrum for calcined SBA-15 also has a peak at 807 cm^{-1} which is indicative of

Si–O–Si vibration, and represents the calcined SBA-15 silica framework.⁷ In amine grafted SBA-15 spectrum, the N–H bond in the amine groups is verified by peaks at 3288, 1648 and 1570 cm^{-1} , whereas, alkane C–H bond is testified by peaks at 2935, 2874, 2820, 1470 and 1298 cm^{-1} , and $\text{CH}_2\text{-N}$ bond is supported by peak at 1407 cm^{-1} , which shows the grafting of DAEPTS amine over SBA-15 support.⁶⁻⁹

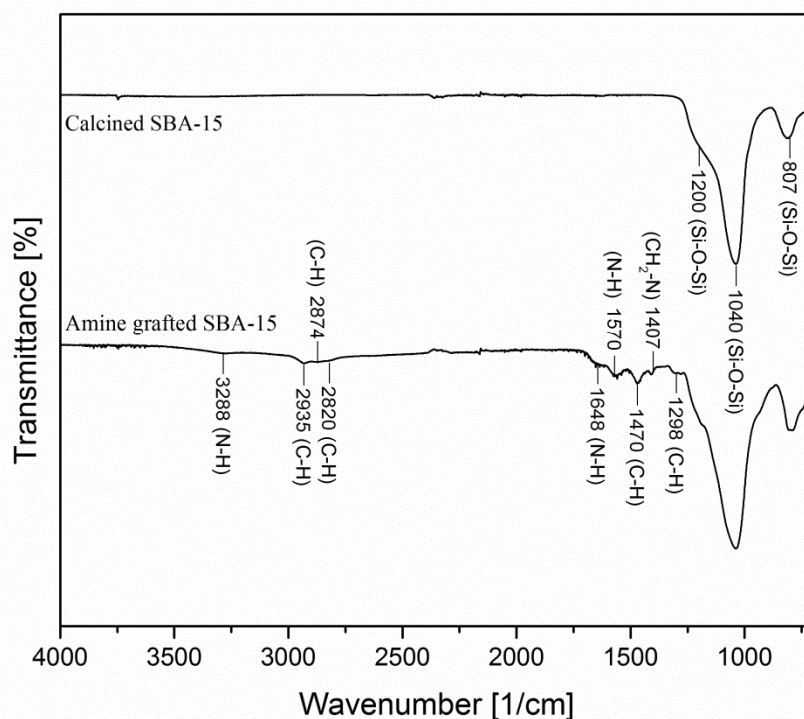


Figure 4.3. FTIR analysis of calcined SBA-15 and amine grafted SBA-15 adsorbent sample.

4.1.4 Amine loading using TGA and Elemental analysis

Amine content of a grafted adsorbent indicates the measure of CO_2 capture and it can be determined from the thermal analysis of the adsorbent. Figure 4.4 presents the thermal behaviour of amine grafted adsorbents SBA-15/D-x with different

amine loadings. The thermal behaviour curve of all amine grafted sorbents has sharp peak near 100 °C denoting water and adsorbed CO₂ removal till this point. It can be observed that there is very negligible drop in weight with increase in temperature till 200 °C for all the amine grafted sorbents, indicating that the amine grafted adsorbents are stable till 200 °C.

Figure 4.5 depicts the typical thermal behavior of amine grafted SBA-15/D-4 adsorbent as measured by TGA under dry N₂ environment. Here, temperature was first maintained at 105 °C for about 60 min and then held at 200 °C and 650 °C for 30 min each. After reaching about 900 °C, the sample was exposed to air for another 30 min. It is noticed that there is a weight loss of about 6.3% upto 105 °C (marked as (a) in Figure 4.5). The weight loss upto 105 °C is due to the removal of water and adsorbed CO₂ from atmosphere. It is also found that there is no significant drop in weight (only about 2.4 wt%) for the amine grafted sorbent with increase in temperature till 200 °C which is marked as (b) in Figure 4.5. This is mainly attributed to the loss of methoxy ligands.¹⁰ The weight loss marked as (c) in Figure 4.5 from 200 °C to 900 °C is attributed to the loss of amino groups from the adsorbent. It confirms that there is very negligible amine leaching till 200 °C.

Table 4.2 presents the amine loading of amine grafted SBA-15 samples with different amounts of amine used during synthesis as obtained using TGA and elemental analysis. Amine loading of each grafted sorbent was calculated using TGA as the weight drop from 100 °C to 900 °C and then converting it into dry

basis mass at 100 °C. Amine loading results were also obtained from elemental analysis. There is a good agreement between the amine loading values obtained from TGA as well as elemental analysis with a maximum error of 12.57%.

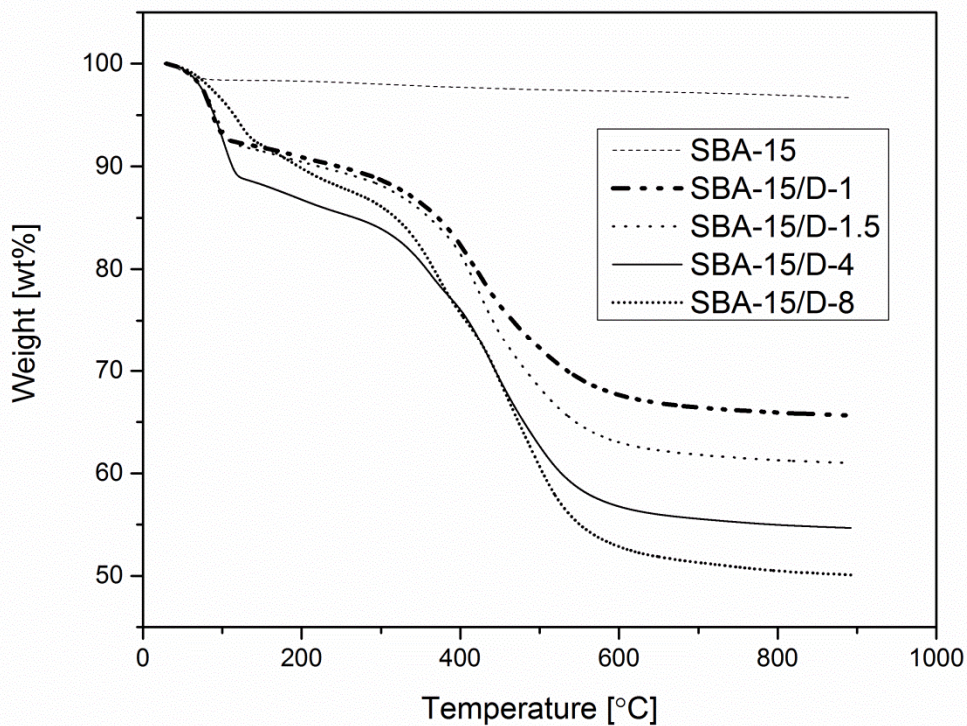


Figure 4.4. Thermal behavior of calcined SBA-15 and amine grafted adsorbents SBA-15/D-x with different amine loadings using TGA.

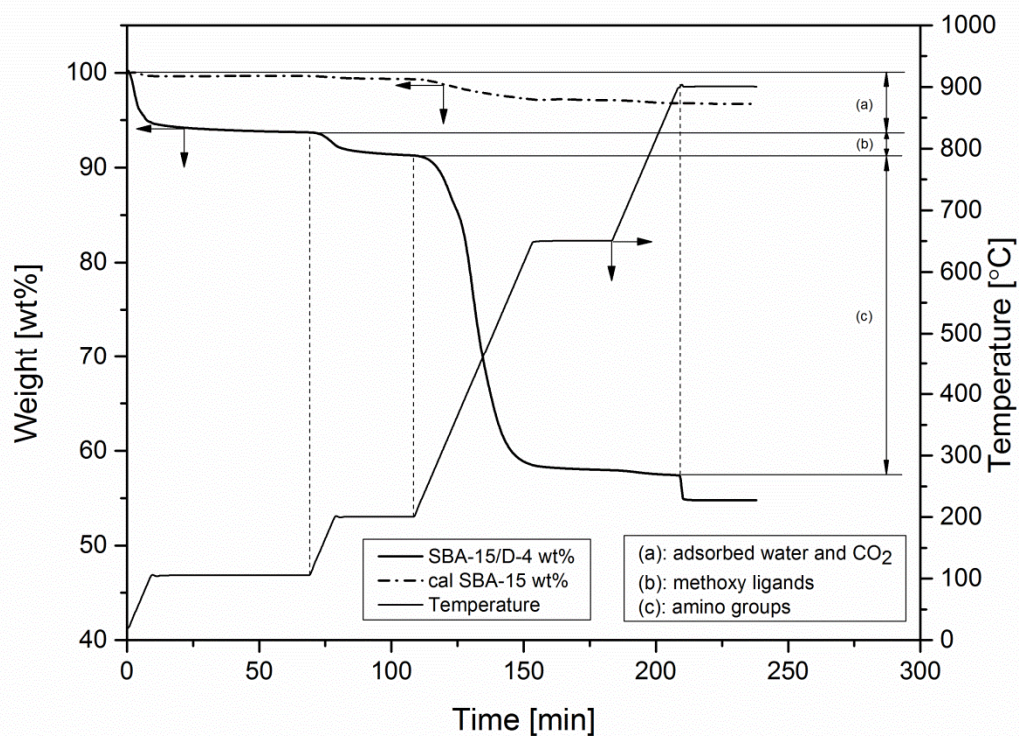


Figure 4.5. A typical thermal behavior curve of calcined SBA-15 and DAEAPTS grafted adsorbent SBA-15/D-4 using TGA.

Table 4.2. Amine content of DAEAPTS grafted SBA-15/D-x sorbents prepared with different initial amine loadings using TGA and elemental analysis.

Sample	Amine loading from TGA [wt%]	Amine loading from elemental analysis [wt%]	Relative error [%]
SBA-15	0.00	0.00	0.00
SBA-15/D-1	28.21	32.27	12.57
SBA-15/D-1.5	33.49	37.54	10.77
SBA-15/D-4	39.64	42.44	6.59
SBA-15/D-8	46.22	51.01	9.38

4.2 Adsorption performance

4.2.1 Effect of amine loading on CO₂ adsorption performance

DAEAPTS grafted SBA-15 adsorbents with varying amine content were prepared to examine the effect of amine loading on CO₂ uptake performance. Figure 4.6 presents the variation of CO₂ adsorption capacity with amine loading at two different CO₂ compositions of 8.8% CO₂/N₂ and 88.2% CO₂/N₂. For both the CO₂ compositions in this Figure, the CO₂ adsorption capacity attained highest value for SBA-15/D-4 sample. It was found that CO₂ sorption capacity kept on increasing as the amine loading was raised from 28.21 wt% to 39.64 wt%. Whereas beyond 39.64 wt%, CO₂ adsorption capacity decreased sharply indicating that SBA-15/D-4 sample has the optimum amine loading of 39.64 wt% with CO₂ sorption capacity of 2.36 mmol/g in 88.2% CO₂/11.8% N₂ gas mixture at 75 °C. Possible explanation of capacity reduction over 40 wt% amine loading may be due to bulk deposition of amine over the amine monolayer on the SBA-15 surface, which leads to diffusional resistance and hence reduced capacity.

Table 4.3 compares the CO₂ sorption capacity and amine adsorption efficiency of amine grafted SBA-15 samples with variable amine loadings in 8.8% CO₂/91.2% N₂ gas mixture at 75 °C. As per Table 4.3, the highest amine efficiency is shown by SBA-15/D-4 sample (0.23 mmol CO₂/mmol N) whereas the amine efficiency for SBA-15/D-8 is 0.10, which supports the hypothesis that amine loading after 40 wt% is due to bulk deposition and not because of monolayer formation.

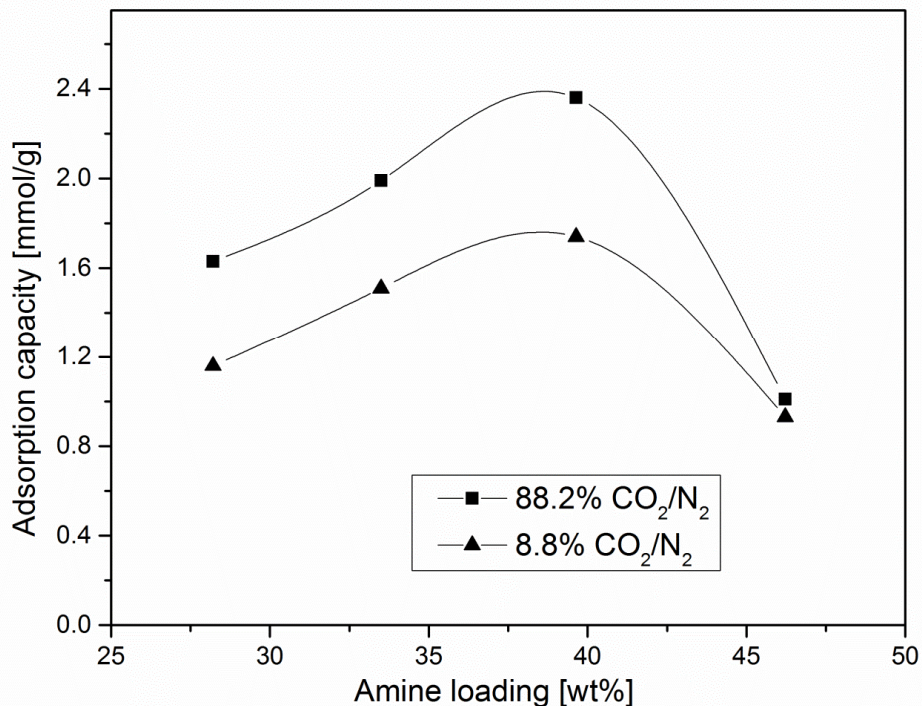


Figure 4.6. CO₂ adsorption capacity variation with amine loading for different SBA-15/D-x adsorbent samples in 88.2% CO₂/11.8% N₂ and 8.8% CO₂/91.2% N₂ gas mixtures at 75 °C and 1 atm.

Table 4.3. Amine loading, nitrogen content, CO₂ adsorption capacity and amine adsorption efficiency of amine grafted sorbents with variable amine loadings. Adsorption capacity and amine adsorption efficiency measured in 8.8% CO₂/91.2% N₂ gas mixture at 75 °C and 1 atm.

Sample	Amine loading [wt%]	Adsorption capacity [mmol/g]	N content [mmol N/g]	Amine adsorption efficiency [mmol CO ₂ /mmol N]
SBA-15	0.00	0.04	0.00	0.00
SBA-15/D-1	28.21	1.16	5.82	0.20
SBA-15/D-1.5	33.49	1.51	6.77	0.22
SBA-15/D-4	39.64	1.74	7.65	0.23
SBA-15/D-8	46.22	0.93	9.20	0.10

4.2.2 Effect of adsorption temperature and CO₂ partial pressure

Figure 4.7 presents the CO₂ adsorption performance of SBA-15/D-4 sample at different adsorption temperatures under 88.2% CO₂/11.8% N₂ and 8.8% CO₂/91.2% N₂ gas mixtures. In 88.2% CO₂/11.8% N₂ gas mixture, the adsorption capacity for this sample increased from 1.20 mmol/g at 25 °C to 2.36 mmol/g at 75 °C and then decreased to 1.94 mmol/g at 105 °C. Similarly for 8.8% CO₂/91.2% N₂ gas mixture, the adsorption capacity achieved maximum value of 1.74 mmol/g at 75 °C. Therefore CO₂ sorption capacity increases with an increase in adsorption temperature till 75 °C and then starts decreasing beyond this temperature. The CO₂ adsorption capacity of DAEAPTS grafted sample in the lower temperature range (about 25 °C) is quite low in both 88.2% CO₂/N₂ and 8.8% CO₂/N₂ gas mixtures. The possible reason for this behavior is the slow diffusion of CO₂ to the active amino sites inside amine grafted SBA-15 pores due to pore blocking by amine molecules, and relatively slow reaction of CO₂ and amine. These lead to kinetic limitations, even though the lower temperatures are thermodynamically more suitable for CO₂ capture.¹¹ The kinetic limitation and diffusional resistance diminishes as the temperature increases. But beyond 75 °C, the CO₂ adsorption capacity decreased in both gas mixtures. This indicates that the thermodynamic equilibrium between CO₂ and DAEAPTS grafted SBA-15 sorbent controlled CO₂ adsorption at higher temperatures beyond 75 °C.¹² Hence, thermodynamic limitations leads to reduction in CO₂ adsorption capacity at temperatures higher than 75 °C. Thus, the optimum balance between

thermodynamic and kinetic limitations occurs at 75 °C and results in highest adsorption capacity at this temperature.

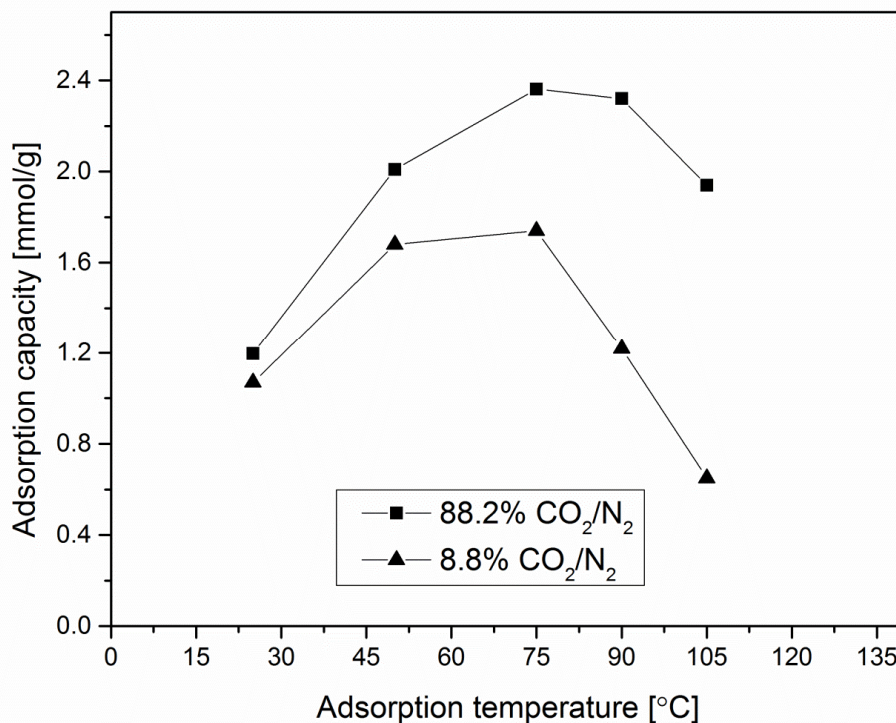


Figure 4.7. Amine grafted sorbent SBA-15/D-4 variation of CO₂ adsorption capacity with adsorption temperature for 88.2% CO₂ and 8.8% CO₂ in N₂ at 1 atm.

Figure 4.8 presents the effect of partial pressure of CO₂ on the sorption capacity of SBA-15/D-4 sample measured using thermogravimetric method under different CO₂ partial pressures and at 75 °C which is optimum temperature for this sorbent. The adsorption capacity increases sharply with CO₂ partial pressure initially at lower partial pressures, while further increasing in CO₂ partial pressure results in a plateau of CO₂ adsorption capacity near a value about 2.3 mmol/g. It is worth mentioning here that the adsorption capacities reported in this work are working

adsorption capacities, not equilibrium adsorption capacities. This is because of incomplete degassing to remove CO₂ and moisture via TGA method and incomplete adsorption even after long exposure time. It was observed in this work that even after exposing the adsorbent under CO₂ for much longer time up to 20 h, adsorption was still occurring but extremely slowly.

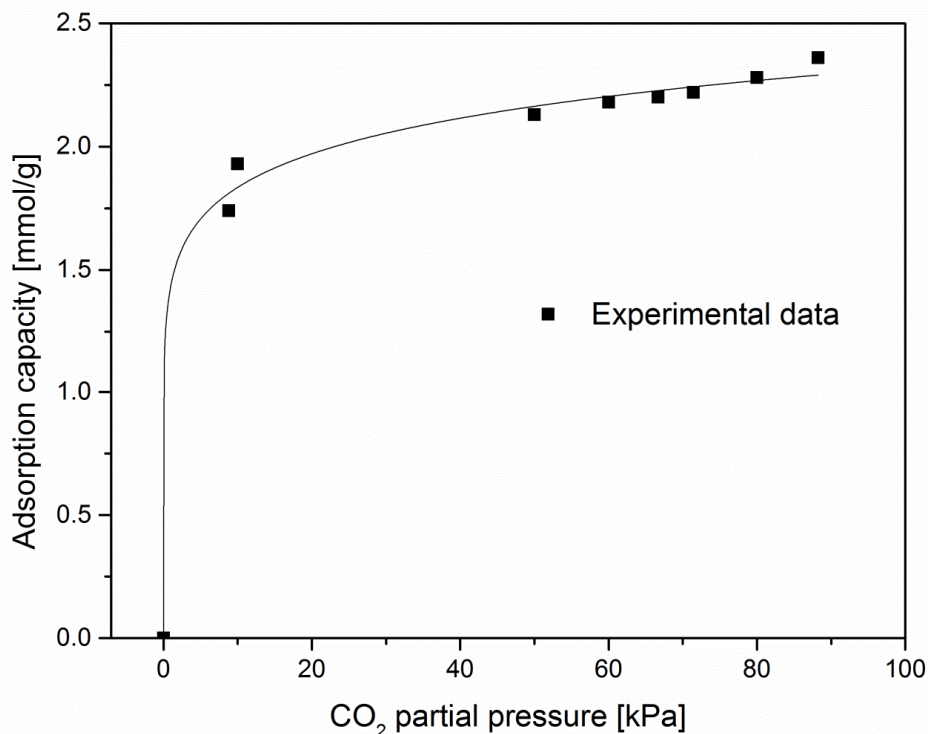


Figure 4.8. Amine grafted sorbent SBA-15/D-4 variation of CO₂ adsorption capacity with CO₂ partial pressure at 75 °C and 1 atm.

4.2.3 Heat of adsorption

Determination of heat of adsorption is very crucial for heat integration of the CO₂ capture system. Figure 4.9 provides the heat of adsorption values of SBA-15/D-4 sample at different adsorption temperatures in 8.8% CO₂/91.2% N₂ and 88.2% CO₂/11.8% N₂ gas mixtures. The heat of adsorption values were measured using

differential scanning calorimetry analysis (TGA/DSC 1 STARe System, Mettler Toledo). All the heat of adsorption values presented here are higher than 60 kJ/mol CO₂ (1.36 kJ/mg CO₂) which shows that the adsorbent captured CO₂ using amine via chemisorption (along with physisorption) throughout the entire adsorption temperature range in both gas compositions.¹³ The heat of adsorption in both gas compositions increases slightly with temperature. Heat of adsorption increases from 1.66 kJ/mg CO₂ at 25 °C to 1.78 kJ/mg CO₂ at 90 °C in 8.8% CO₂/91.2% N₂. Similarly in 88.2% CO₂/11.8% N₂ gas mixture, the heat of adsorption increases from 1.71 kJ/mg CO₂ at 25 °C to 1.93 kJ/mg CO₂ at 90 °C. It was observed that the heat of adsorption values in 88.2% CO₂/N₂ is marginally higher than that in 8.8% CO₂/N₂ at all the adsorption temperatures. The possible explanation for this behavior is that higher concentration of CO₂ leads to more CO₂ capture via chemisorption which gives higher heat of adsorption.

The effect of moisture on the heat of adsorption of amine grafted sorbent was also investigated. Figure 4.10 presents the heat of adsorption values for SBA-15/D-4 sample at different adsorption temperatures in dry and humid 8.8% CO₂/91.2% N₂. Heat of adsorption values increases gradually with temperature in both dry and humid gas mixtures. It was observed that the sorbent adsorbs both CO₂ and moisture during adsorption with humid gas mixture, so the heat of adsorption values presented here are measured in kJ per mg of (CO₂ + H₂O) adsorbed. Hence, the heat of adsorption in humid gas is due to adsorption of both CO₂ as well as moisture. It was found that heat of adsorption due to moisture alone is

very low in comparison to heat of adsorption due to CO₂. This explains that heat of adsorption in humid gas is lower than in dry gas at all temperatures because humid gas values has heat of adsorption components from both CO₂ and H₂O. This is particularly evident at 25 °C because of the large amount of moisture adsorbed by grafted adsorbent at this temperature. Table 4.4 presents the heat of adsorption values of SBA-15/D-4 sample in dry 8.8% CO₂/N₂, humid 8.8% CO₂/N₂ and humid N₂ at different adsorption temperatures.

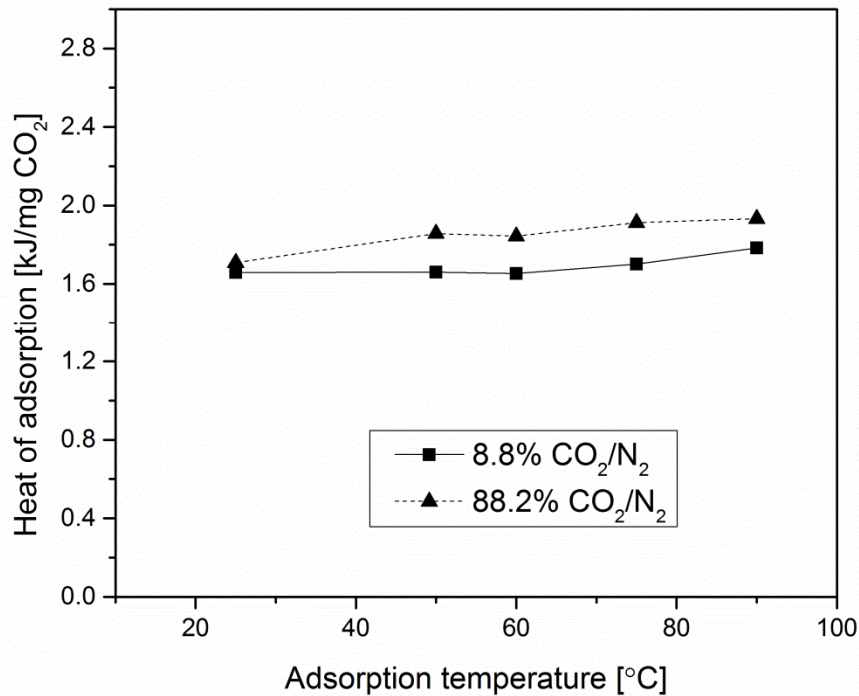


Figure 4.9. Heat of adsorption variation with adsorption temperature for SBA-15/D-4 sample in 8.8% CO₂/91.2% N₂ and 88.2% CO₂/11.8% N₂ gas mixtures.

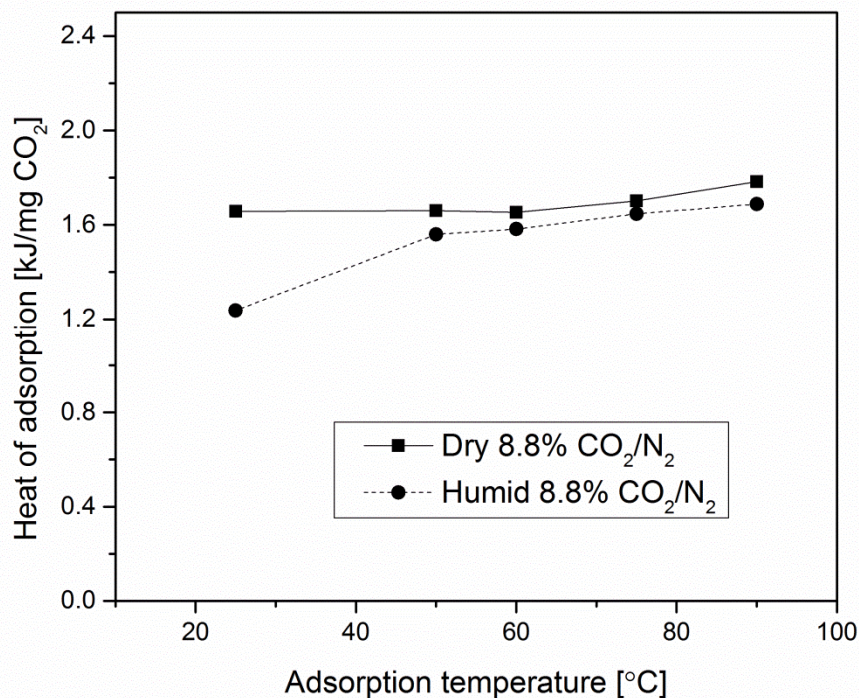


Figure 4.10. Heat of adsorption variation with adsorption temperature for SBA-15/D-4 sample in dry and humid 8.8% CO₂/91.2% N₂ gas mixtures.

Table 4.4. Heat of adsorption values of SBA-15/D-4 sample using dry CO₂, humid CO₂ and moisture streams in N₂ at different adsorption temperatures.

Adsorption temperature [°C]	$\Delta H_{\text{dry}}^{\text{a}}$ [kJ/mg CO ₂]	$\Delta H_{\text{humid}}^{\text{b}}$ [kJ/mg (CO ₂ +H ₂ O)]	$\Delta H_{\text{moisture}}^{\text{c}}$ [kJ/mg H ₂ O]
25	1.66	1.24	0.14
50	1.66	1.56	0.74
60	1.65	1.58	1.17
75	1.70	1.65	1.33
90	1.78	1.69	1.23

a: Heat of adsorption in dry 8.8% CO₂/91.2% N₂

b: Heat of adsorption in humid 8.8% CO₂/91.2% N₂

c: Heat of adsorption in the presence of only moisture

4.2.4 Kinetics

The kinetics play a vital role in determining the performance of a sorbent. In order for the sorbent to have any meaningful use, its kinetics needs to be sufficiently fast. Figure 4.11 presents the CO₂ adsorption capacity as a function of time for amine grafted adsorbents with different amine loading at 75 °C in 88.2% CO₂/N₂ for 120 min. The inset of Figure 4.11 shows the sorption capacity variation with time for only 100 s to observe the kinetics at the start of adsorption. For SBA-15/D-1, SBA-15/D-1.5 and SBA-15/D-4 samples, there is sharp increase in CO₂ adsorption capacity in the first few minutes of adsorption time indicating fast kinetics whereas for SBA-15/D-8 sample, the kinetics is slow. The slow kinetics of SBA-15/D-8 can be attributed to the SBA-15 support pore blocking/distorting due to bulk amine deposition over the SBA-15 support. Figure 4.12 presents the first derivative of adsorption capacity with time for different amine loaded samples under the same conditions. The peak height of the derivative adsorption capacity curves is found in the order: SBA-15/D-4 > SBA-15/D-1.5 > SBA-15/D-1 > SBA-15/D-8 > SBA-15. The peak values also support that adsorption kinetics are fast for SBA-15/D-1, SBA-15/D-1.5 and SBA-15/D-4 whereas SBA-15/D-8 show slow adsorption kinetics.

Adsorption and desorption kinetics of amine grafted adsorbent SBA-15/D-4 sample is presented in Figure 4.13 in dry and humid 88.2% CO₂/11.8% N₂ gas mixtures. In this test, CO₂ was adsorbed on the sample for 10 min at 75 °C and then desorbed at 150 °C in pure N₂ for 10 min. In dry gas, the sample reached

80% of the maximum CO₂ sorption capacity of 2.36 mmol/g in only 5 min of adsorption time whereas in humid gas, it reached 80% capacity in only 2.5 min of adsorption time. Although the adsorption kinetics is fast in both dry and humid gas but humid gas adsorption kinetics is relatively better. For both dry and humid gas, more than 95 % of the total desorption happened in less than 5 min of desorption time.

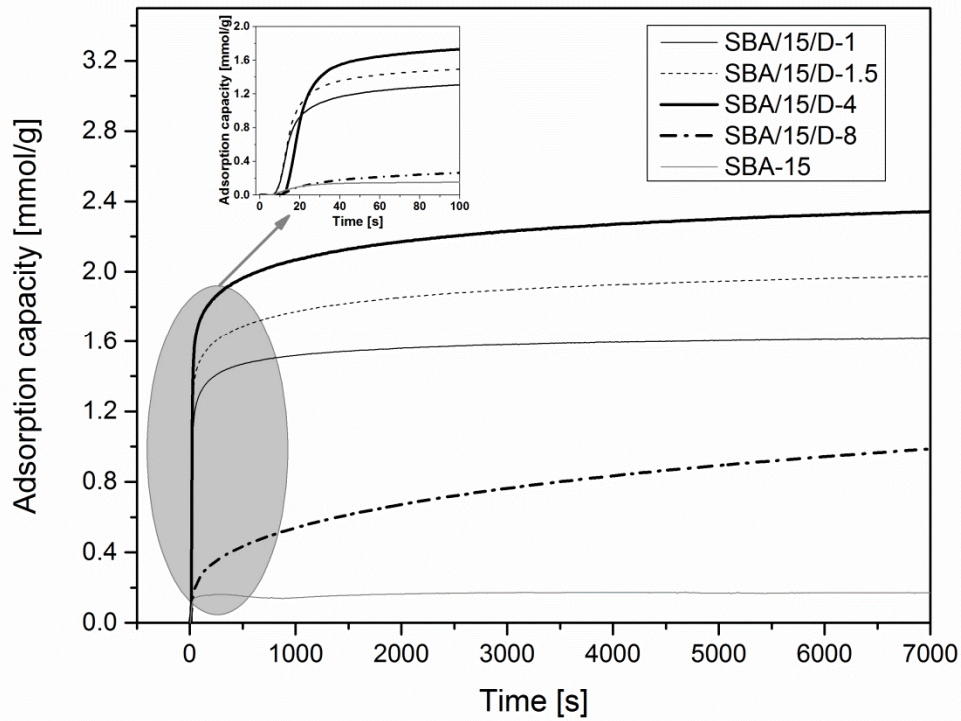


Figure 4.11. CO₂ adsorption capacities of different SBA-15/D-x adsorbents as a function of time in 88.2% CO₂/11.8% N₂ gas mixture at 75 °C and 1 atm.

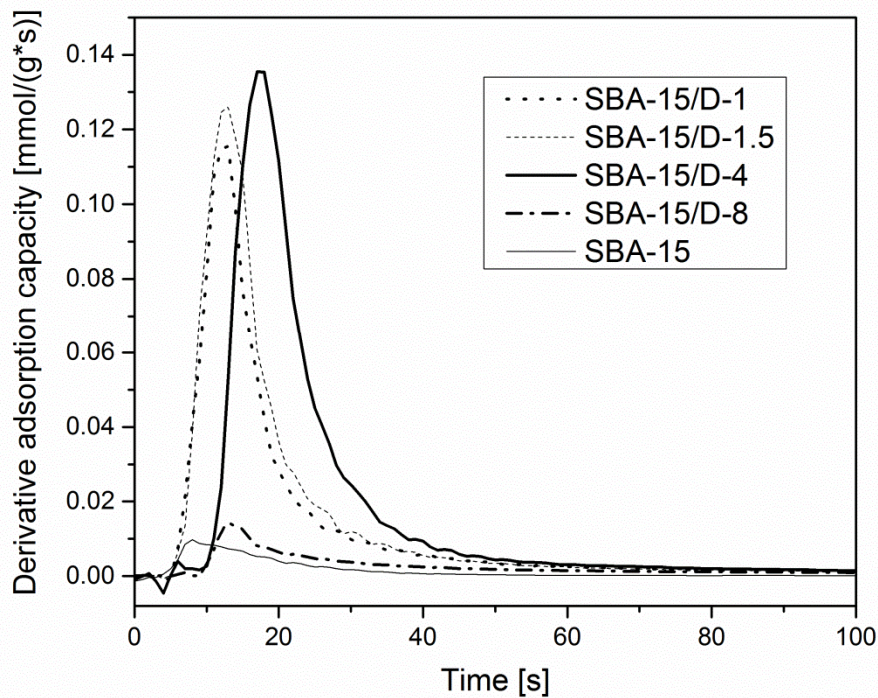


Figure 4.12. Derivative adsorption capacity variation with time in 88.2% CO₂/11.8% N₂ gas mixture at 75 °C for different SBA-15/D-x adsorbents.

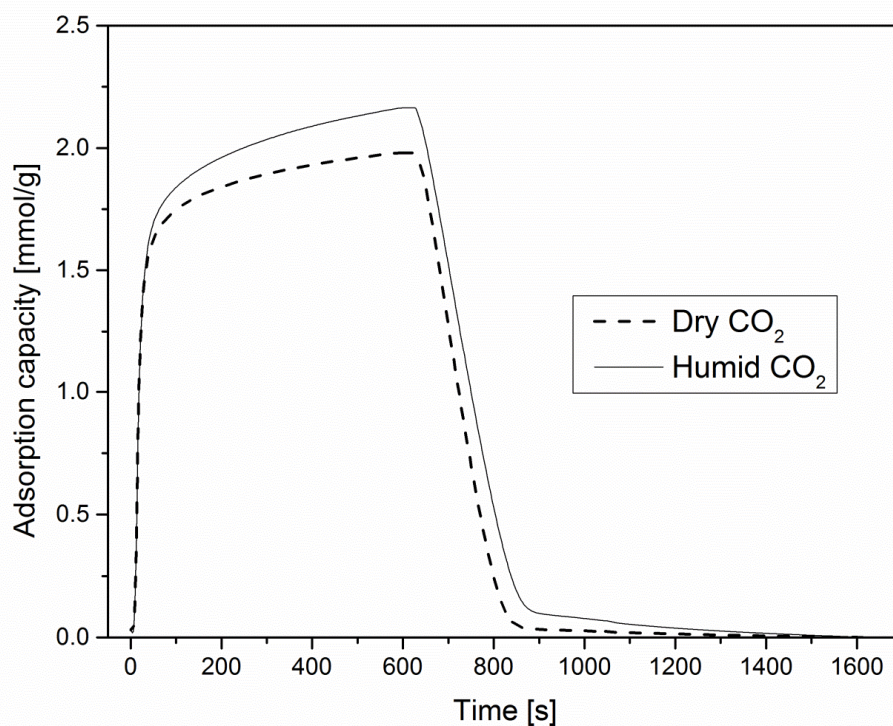


Figure 4.13. Comparison of adsorption-desorption kinetics of SBA-15/D-4 sample in dry and humid 88.2% CO₂/11.8% N₂ gas mixtures at 75 °C and 1 atm.

4.2.5 Effect of moisture

Amine grafted sample SBA-15/D-4 was tested for CO₂ adsorption using humid CO₂/N₂ gas mixture to determine the effect of moisture in CO₂ adsorption performance. Figure 4.14 compares the CO₂ adsorption capacity of amine grafted SBA-15/D-4 sample in humid and dry 8.8% CO₂/91.2% N₂ gas mixture at different adsorption temperatures. Amine grafted sample SBA-15/D-4 was also tested for only moisture adsorption in humid N₂ steam in order to find out whether the sample absorbs any moisture or not. It was observed that the increase in adsorption capacity in humid CO₂/N₂ gas mixture at different adsorption temperatures is mainly due to moisture adsorption only rather than CO₂

adsorption. But there is no negative effect of moisture on the CO₂ sorption capacity as the CO₂ capacities were maintained in the presence of moisture in humid CO₂ stream.

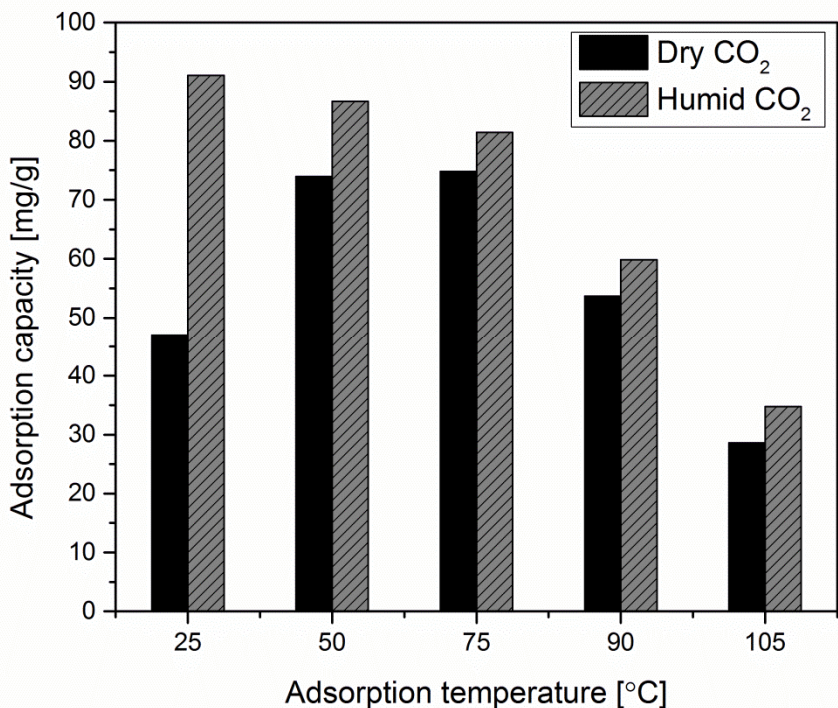


Figure 4.14. Comparison of CO₂ adsorption capacity of SBA-15/D-4 sample in dry and humid CO₂ streams at different adsorption temperatures. 8.8% CO₂/91.2% N₂ gas mixture was used.

Figure 4.15 presents the adsorption capacities of dry CO₂, moisture and N₂ at different adsorption temperatures. N₂ adsorption is negligible for this adsorbent, which means the adsorbent is highly selective towards CO₂. Adsorption capacity due to moisture alone is very low as compared to CO₂ adsorption capacity except at 25 °C where adsorption capacity due to moisture is particularly high.

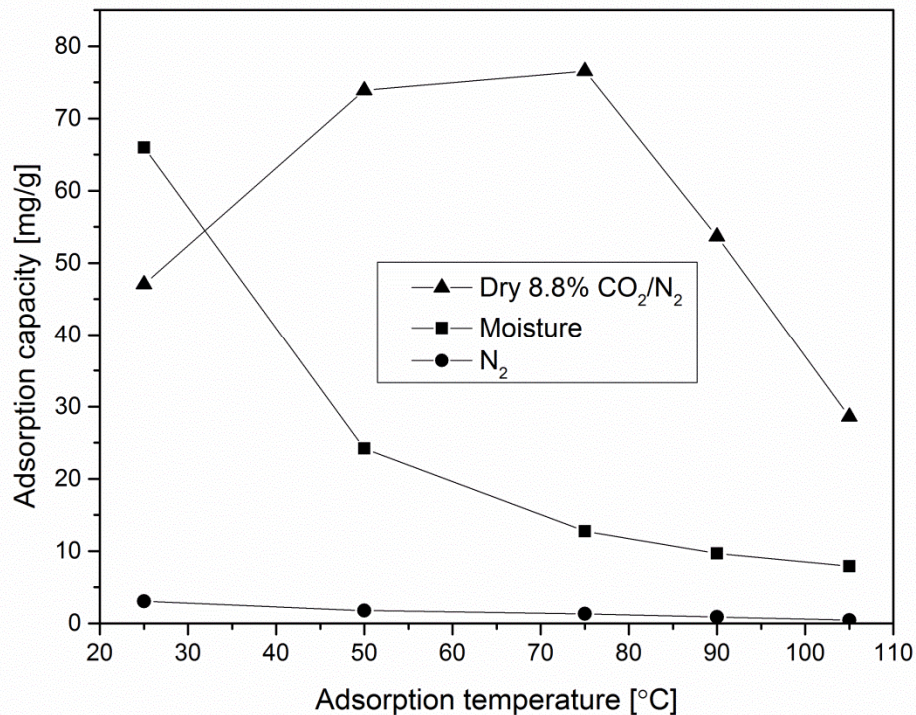


Figure 4.15. Comparison of dry CO₂, moisture and N₂ adsorption capacities at different adsorption temperatures for SBA-15/D-4 sample.

Figure 4.16 compares the CO₂ adsorption capacity of SBA-15/D-4 sample with time in dry and humid 88.2% CO₂/N₂ at 75 °C. CO₂ sorption capacity in humid gas is slightly higher than in dry gas mainly due to water adsorption. Both dry and humid CO₂/N₂ gas streams showed fast kinetics for this sample. The kinetics of moisture and dry N₂ adsorption are also presented in this Figure. N₂ adsorption capacity as shown in this Figure is almost negligible. Moisture adsorption capacity is very small in comparison to CO₂ adsorption capacity and the kinetics is also slow for moisture adsorption.

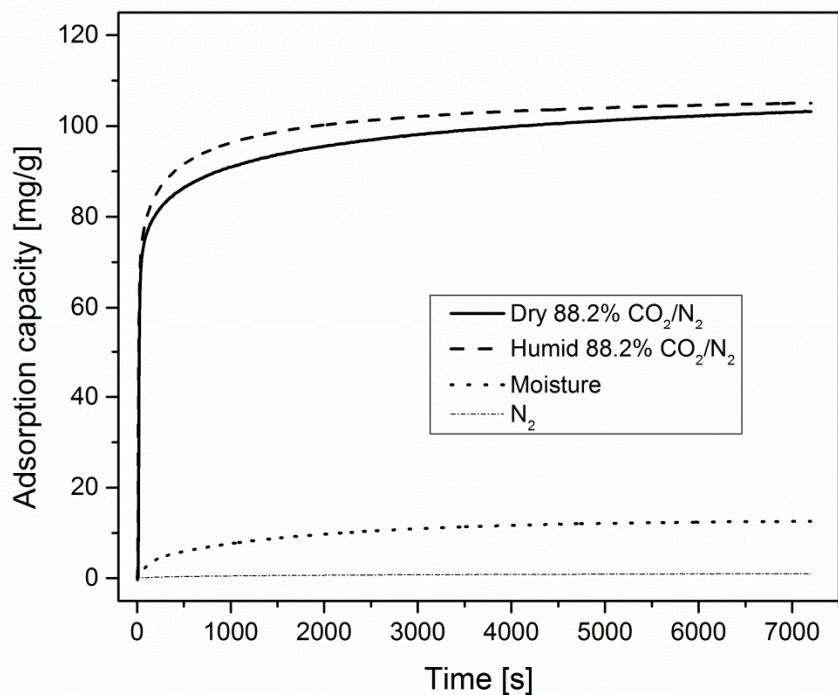


Figure 4.16. Comparison of dry 88.2% CO₂/N₂, humid 88.2% CO₂/N₂, moisture and N₂ adsorption capacities as a function of time for SBA-15/D-4 sample at 75 °C.

4.2.6 Multi-cycle stability

One of the most important criteria in evaluating adsorbent for post-combustion CO₂ capture applications is multi-cycle stability of the adsorbent. Figure 4.17 presents 100 short adsorption/desorption cycles in dry and humid 88.2% CO₂ in N₂ at 1 atm. For this test, each cycle comprised of 10 min of adsorption at 75 °C in CO₂/N₂ gas mixture and 10 min of desorption at 150 °C in pure N₂ gas. The capacity observed after 1st and 100th cycle under dry gas is 2.05 mmol/g and 1.90 mmol/g respectively. For humid gas, 1st and 100th cycle capacity is 2.17 mmol and 2.02 mmol/g respectively. The drop in capacity after 100 cycles in humid gas is

6.94% and in dry gas is 7.11%. Amine leaching, measured from the drop in weight of the sample (from TGA data), after 100 cycles in humid gas is 3.99 wt% and in dry gas is 4.24 wt%. So, with short cycles, both dry gas and humid gas have almost same stability. Hence, the presence of moisture does not lead to degradation of the grafted adsorbent over multiple cycles. Overall, the sorbent exhibits decent stability over 100 adsorption/desorption cycles in both dry and humid gas mixtures.

Figure 4.18 shows the FTIR analysis of amine grafted SBA-15 samples: fresh, after 100 cycles with dry CO₂ and humid CO₂. As discussed above in the FTIR characterization section, the peaks at 3288, 2935, 2820, 1570, 1470, 1407 and 1298 cm⁻¹ are typical of amine grafting as shown in spectrum for fresh amine grafted SBA-15 sample. All these peaks are also retained by the grafted adsorbent sample after 100 cycles in dry and humid CO₂, which imply that the amine grafting is preserved even after 100 adsorption/desorption cycles. Although 100 cycles in dry and humid gas has led to some amine leaching and capacity reduction as mentioned above. The peak at 1662 cm⁻¹ in the spectrums of amine grafted samples after 100 cycles in dry and humid CO₂ gas is due to the presence of C=N bond generated upon amine oxidation after 100 cycles in dry and humid CO₂.¹⁴ Overall, the amine grafted samples after 100 cycles in dry and humid CO₂ has maintained amine grafting but some of the grafted amine is degraded and resulted in capacity reduction.

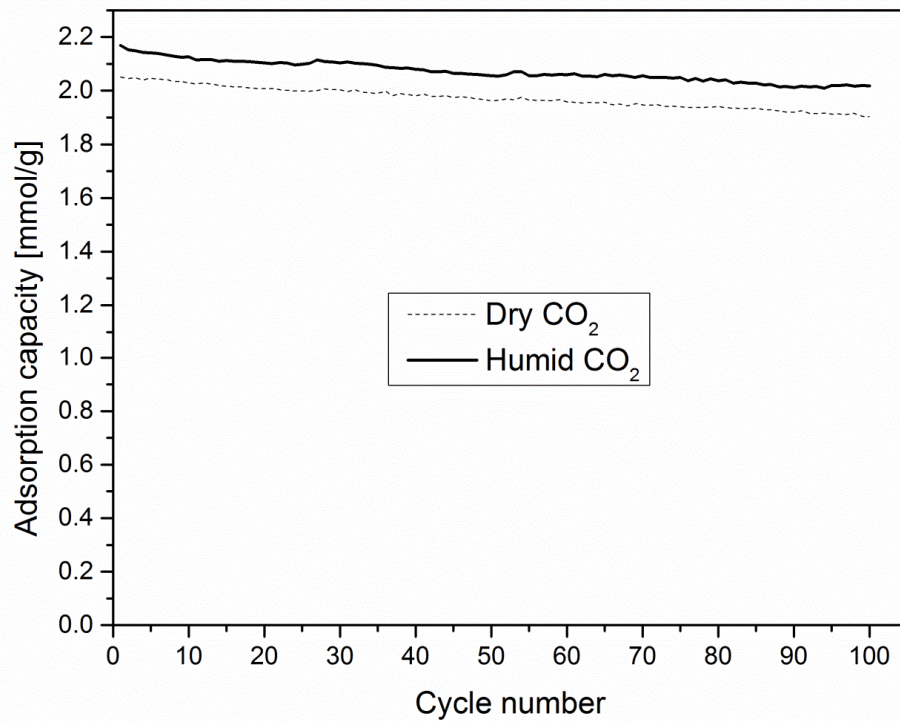


Figure 4.17. Multi-cycle stability of SBA-15/D-4 sample in dry and humid 88.2% CO₂/11.8% N₂ gas mixture at 1 atm.

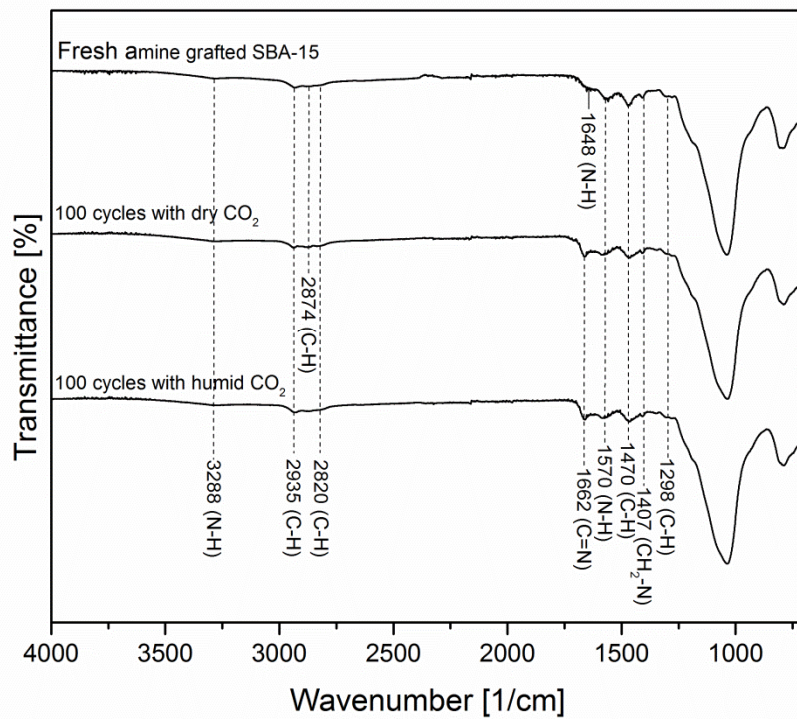


Figure 4.18. FTIR analysis of fresh amine grafted SBA-15 sample and amine grafted samples after 100 cycles with dry and humid CO₂/N₂ gas mixtures.

Part 2

The content of part 2 of this chapter is arranged as:

- This chapter evaluates the CO₂ adsorption performance of PEI impregnated SBA-15 adsorbent with structured bed and packed bed configurations.
- Structured bed performance is investigated with single tube and three tubes. Single-tube structured bed is examined for adsorption performance at various adsorption temperatures and CO₂ concentrations. Three-tube structured bed performance is evaluated at different adsorption temperatures. Adsorption/desorption kinetics and multi-cycle stability for 6 cyclic runs is also discussed for three-tube structured bed.
- The adsorption performance of PEI impregnated SBA-15 sample in packed bed is observed for different adsorption temperatures and gas flowrates. Multi-cycle stability for 20 cyclic runs and adsorption/desorption kinetics of impregnated sample in packed bed is presented in dry and humid CO₂/N₂ gas streams.
- In the end, the adsorption capacity obtained using three-tube structured bed and packed bed is compared at different adsorption temperatures.

4.3 Bed performance

CO₂ capture performance was investigated in novel structured bed configuration and packed bed configuration in this work. Bed performance in this work was evaluated using PEI impregnated SBA-15 sorbent. The PEI impregnated SBA-15

adsorbent was selected because of its ease of preparation, high CO₂ adsorption capacity and fast kinetics at post-combustion flue gas conditions. The structured bed performance was studied in two phases. In the first phase of work, structured bed with single tube was studied for preliminary analysis of the CO₂ adsorption/desorption performance. After satisfactory performance evaluation in the first phase, structured bed with three membrane tubes was tested for CO₂ adsorption/desorption performance in the second phase of the work.

4.3.1 Single-tube structured bed

4.3.1.1 Effect of adsorption temperature

PEI impregnated adsorbent SBA-15/P-50 was tested at different adsorption temperatures in single-tube structured sorbent bed for CO₂ adsorption with pure CO₂ and corresponding adsorption capacities are shown in Figure 4.19. The maximum CO₂ adsorption capacity achieved was 2.63 mmol/g at 75 °C and minimum adsorption capacity was found at 90 °C.

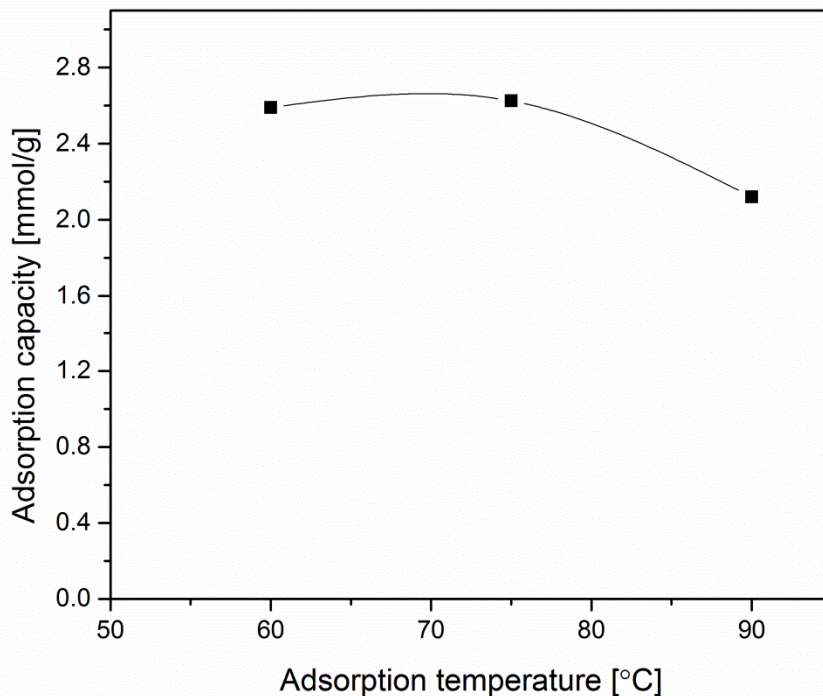


Figure 4.19. Variation of adsorption capacity with adsorption temperature in pure CO₂. SBA-15/P-50 sample used inside single-tube structured bed.

4.3.1.2 Effect of CO₂ concentration

Figure 4.20 presents the structured bed breakthrough profile of PEI impregnated sample SBA-15/P-50 in 10% CO₂/90% N₂ gas mixture at 75 °C. 50 cm³/min gas flowrate was used for this test. Before adsorption, sample sorbent was heated to 105 °C for 60 min to remove all the moisture from the sample. CO₂ adsorption capacity obtained for this test using structured sorbent bed is around 1.88 mmol/g whereas CO₂ adsorption capacity measured in TGA for this adsorbent at 75 °C in 10% CO₂/90% N₂ gas mixture is around 2.62 mmol/g. Under these experimental conditions, the structured bed adsorption capacity comes around 72% of the capacity measured using TGA. The reason for lower adsorption capacity in single

tube structured bed as compared to TGA is because of improper heating control in single tube structured bed due to the exothermic nature of the CO₂ adsorption. The heat released during CO₂ adsorption in single tube structured bed raised the temperature of the sorbent bed and led to the reduction in adsorption capacity.

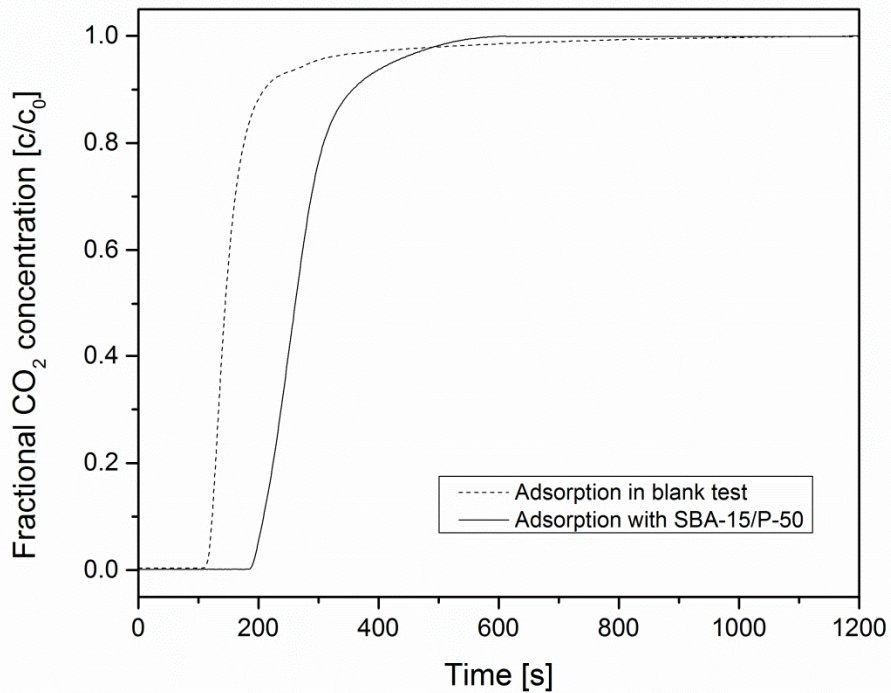


Figure 4.20. Breakthrough curve for SBA-15/P-50 sample inside single-tube structured bed in 10% CO₂/90% N₂ at 75 °C.

The breakthrough curve for SBA-15/P-50 sample in single-tube structured bed with pure CO₂ gas at 75 °C is shown in Figure 4.21. Breakthrough time in pure CO₂ for SBA-15/P-50 sample was found to be 110 s whereas breakthrough time for blank test was around 94 s. The gap between adsorbent curve and blank curve in pure CO₂ (as shown in Figure 4.21) is much smaller as compared to the gap in

10% CO₂/90% N₂ (as shown in Figure 4.20) due to much higher concentration of gas in pure CO₂.

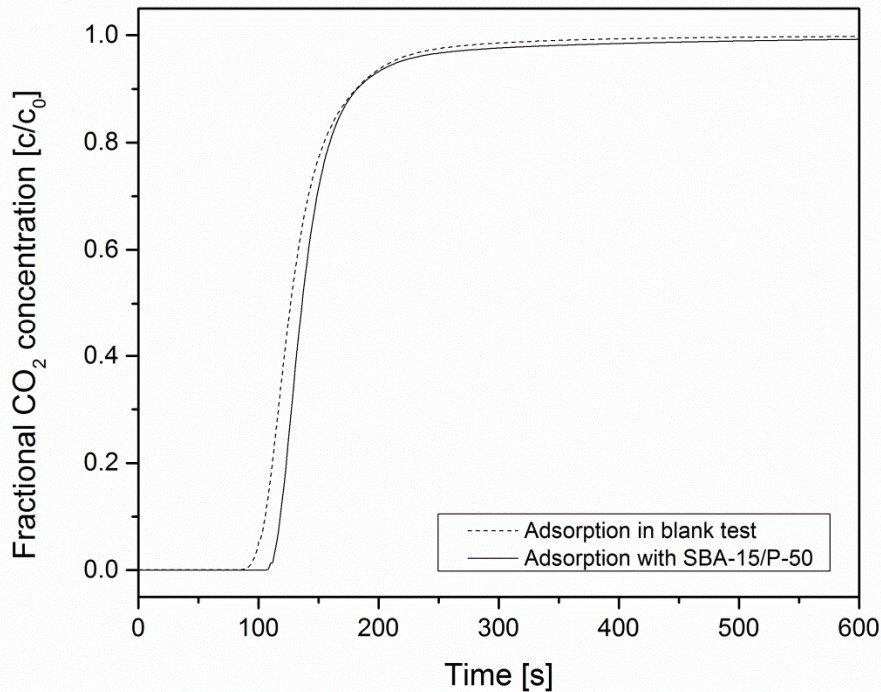


Figure 4.21. Breakthrough curve for SBA-15/P-50 sample inside single-tube structured bed in pure CO₂ at 75 °C.

4.3.2 Three-tube structured bed

4.3.2.1 Effect of adsorption temperature

Breakthrough profiles of amine impregnated sample SBA-15/P-50 inside three-tube structured bed using 10% CO₂/90% N₂ gas mixture at different adsorption temperatures is shown in Figure 4.22. The breakthrough time for this sample at 75 °C was 242 s and breakthrough time for blank test was around 64 s. Minimum value of breakthrough time was found at 25 °C (184 s).

Variation of adsorption capacity with adsorption temperature in three-tube structured bed is shown in Figure 4.23. 10% CO₂/90% N₂ gas mixture with flowrate of 100 cm³/min was used for the tests. The highest value of adsorption capacity was obtained at 75 °C. The adsorption capacity increased from 1.28 to 3.05 mmol/g as the adsorption temperature varied from 25 to 75 °C. But sorption capacity stopped increasing further and dropped to 3.00 mmol/g as the adsorption temperature varied from 75 to 90 °C. This adsorption capacity trend indicates that kinetic limitations and diffusion resistances inhibit CO₂ adsorption at lower temperatures and thermodynamic equilibrium control CO₂ adsorption at higher temperatures.

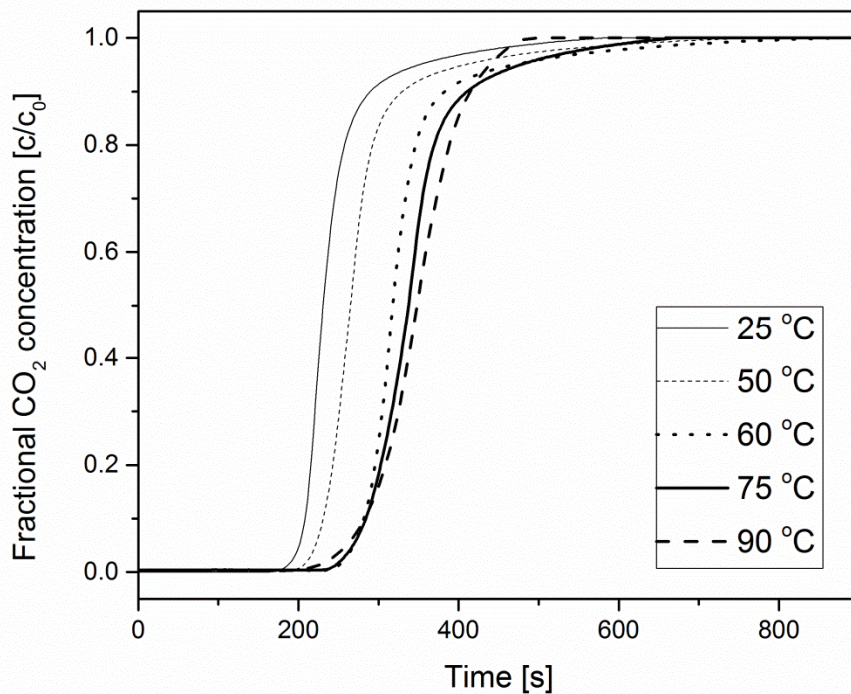


Figure 4.22. Comparison of structured bed breakthrough profiles of SBA-15/P-50 sorbent in 10% CO₂/90% N₂ at different adsorption temperatures.

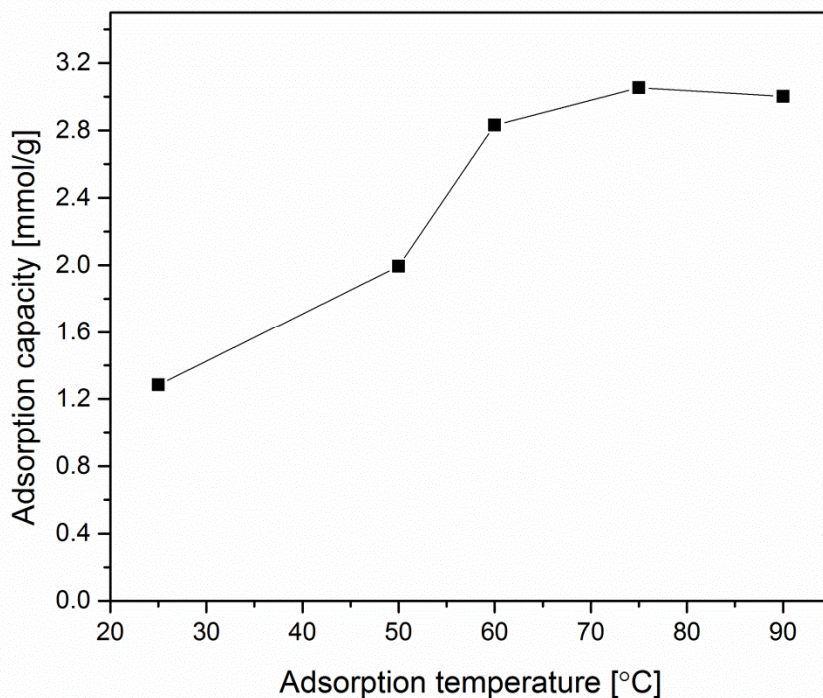


Figure 4.23. Variation of adsorption capacity with adsorption temperature for SBA-15/P-50 sample in three-tube structured bed. 10% CO₂/90% N₂ gas mixture used.

4.3.2.2 Kinetics

Adsorption and desorption kinetics of SBA-15/P-50 sample in three-tube structured bed is shown in Figure 4.24. Adsorption was done in 10% CO₂/90% N₂ gas mixture at 75 °C and desorption in pure N₂ at 90 °C. The sharp rise in fractional CO₂ concentration during adsorption segment and sharp decrease in fractional CO₂ concentration during desorption segment of breakthrough curve shows that both adsorption and desorption kinetics are fast. Small peak in the desorption segment of breakthrough curve indicates the release of CO₂ adsorbed by the impregnated sorbent. This small peak in the desorption segment

corresponds to the time when desired regeneration temperature (90 °C) is reached inside the sorbent bed.

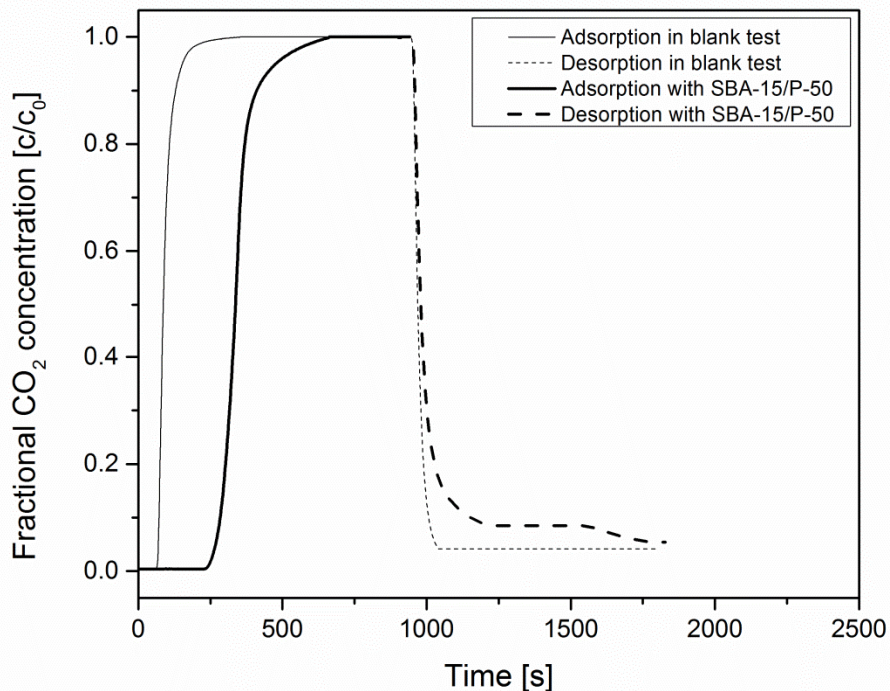


Figure 4.24. Adsorption/desorption kinetics of SBA-15/P-50 sample in three-tube structured bed.

4.3.2.3 Multi-cycle stability

The multi-cycle stability of the amine impregnated sample SBA-15/P-50 was tested in three-tube structured bed and shown in Figure 4.25. 10% CO₂/90% N₂ gas mixture was used at 75 °C for adsorption and pure N₂ was used at 90 °C for desorption. The drop in capacity from 1st cycle to 2nd cycle was big (3.05 to 2.56 mmol/g) but from 2nd cycle onwards the drop in capacity was negligible. The possible reason for large drop in capacity from 1st cycle to 2nd cycle may be because of the permanent deactivation of some of the impregnated PEI amine

after reaction with CO₂ in the first cycle. It can also be due to the leaching of some loosely bound impregnated amine from the sorbent after 1st cycle with CO₂.

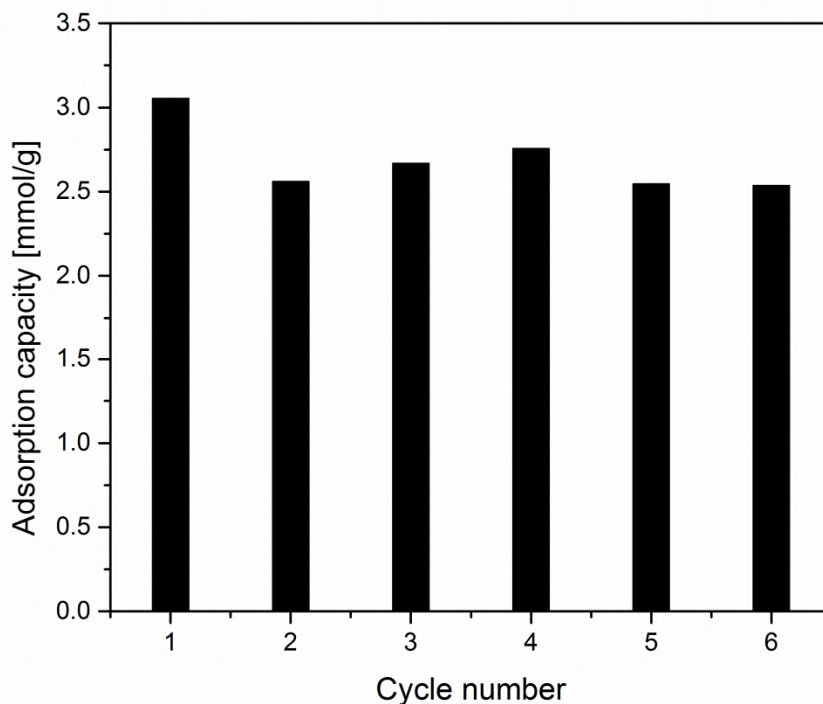


Figure 4.25. Multi-cycle stability of SBA-15/P-50 sample in three-tube structured bed.

4.3.3 Packed bed performance

4.3.3.1 Effect of adsorption temperature

CO₂ adsorption performance of PEI impregnated sample SBA-15/P-50 was tested in packed bed. Figure 4.26 presents the variation of CO₂ adsorption capacity with adsorption temperature in 10% CO₂/ 90% N₂ gas mixture. Flowrate of the gas mixture for all the adsorption temperatures was kept at 20 cm³/min. It was observed that adsorption capacity increased with temperature till 75 °C and then started decreasing beyond 75 °C, making 75 °C as the optimum temperature for

adsorption of CO₂. As discussed above, this CO₂ adsorption behaviour can be attributed to kinetic limitations and diffusional resistances at lower temperatures (<75 °C) and thermodynamic limitations at higher temperatures (>75 °C).

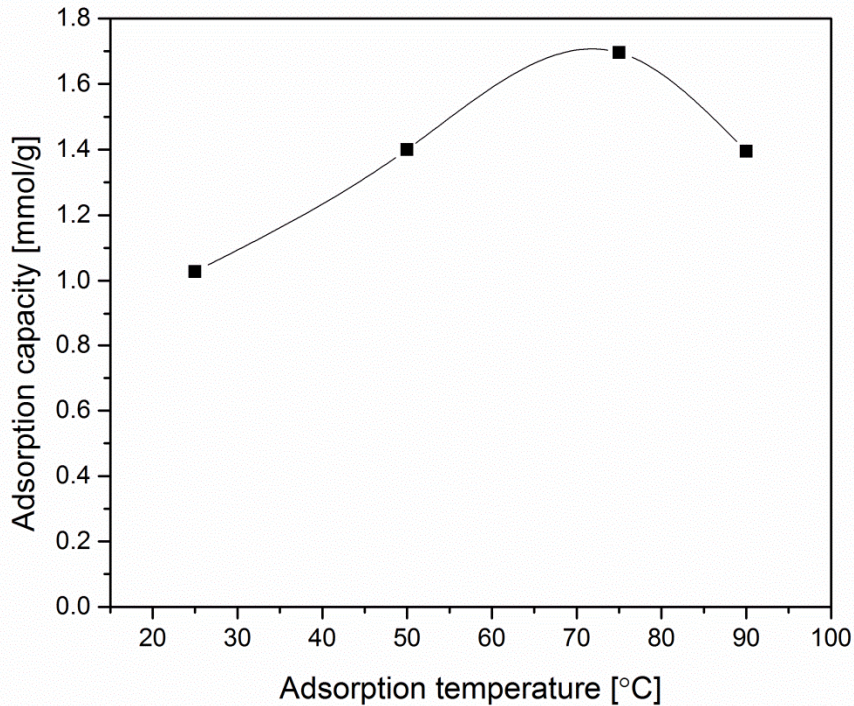


Figure 4.26. Variation of CO₂ adsorption capacity with adsorption temperature for SBA-15/P-50 sample in packed bed using 10% CO₂/90% N₂ gas mixture.

Figure 4.27 shows the breakthrough profiles at the outlet of packed bed filled with SBA-15/P-50 sample at different adsorption temperatures in 10% CO₂/90% N₂ gas mixture with total flowrate of 20 cm³/min. The breakthrough time, defined by the time when CO₂ concentration reaches 0.1% at the outlet of the bed, is highest for 75 °C. The order of breakthrough time at different adsorption temperatures is as shown below:

75 °C (162 s) > 90 °C (154 s) > 50 °C (147 s) > 25 °C (113 s)

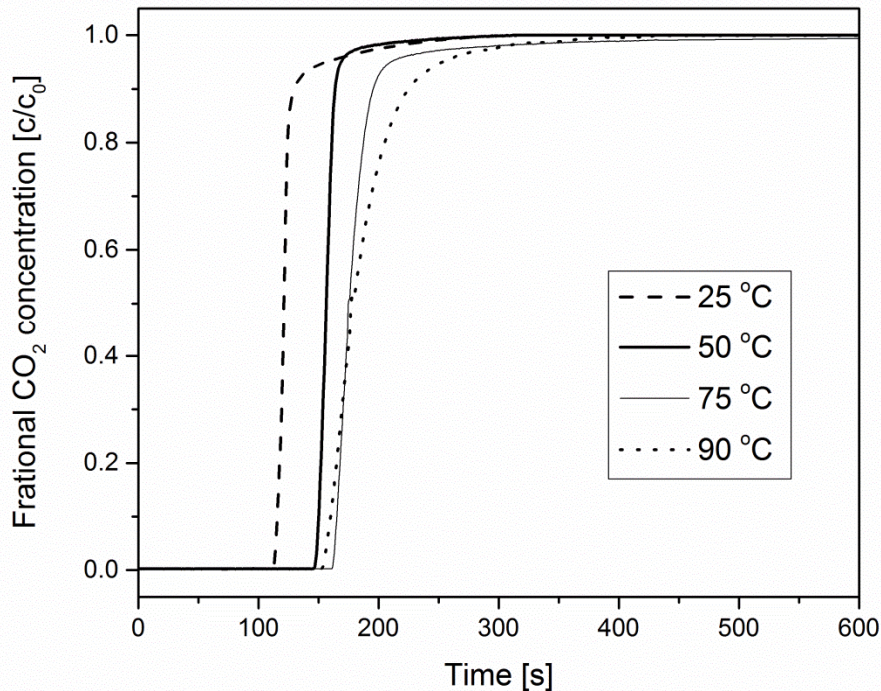


Figure 4.27. Comparison of packed bed breakthrough curves at different adsorption temperatures in 10% CO₂/90% N₂ gas mixture.

4.3.3.2 Effect of gas flowrate

The effect of gas flowrate on the adsorption performance of SBA-15/P-50 sample in packed bed was studied. Figure 4.28 shows the variation of adsorption capacity with gas flowrate comprising 10% CO₂/90% N₂ at 75 °C adsorption temperature. As per this Figure, the adsorption capacity keeps on increasing as the gas flowrate increases from 10 to 50 cm³/min. The reason for this behaviour can be as higher flowrate contains more CO₂ which is able to saturate the adsorbent in packed bed better as compared to lower flowrates which are not able to saturate the adsorbent completely due to longer breakthrough times required at lower flowrates. Another possible explanation is since adsorption is exothermic process, so it can create

localized temperature increase and sorbent overheating during the CO₂ adsorption which can lead to desorption of CO₂. Lower gas flowrates may not be able to remove the heat from the sorbent during adsorption and hence adsorb less CO₂.

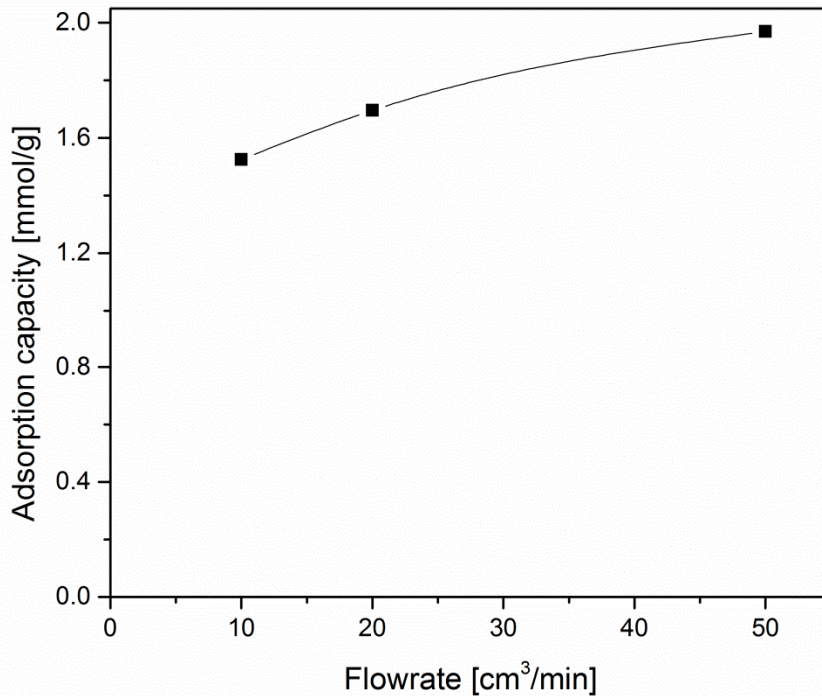


Figure 4.28. Variation of CO₂ adsorption capacity with gas flowrate for SBA-15/P-50 sample inside packed bed at 75 °C.

Figure 4.29 presents the breakthrough curves at different gas flowrates containing 10% CO₂/ 90% N₂ gas mixture at 75 °C adsorption temperature. The order of breakthrough time for different gas flowrates is as follows:

$$10 \text{ cm}^3/\text{min} (255 \text{ s}) > 20 \text{ cm}^3/\text{min} (126 \text{ s}) > 50 \text{ cm}^3/\text{min} (58 \text{ s})$$

As expected the breakthrough time decreases with increase in gas flowrate which can be the reason for better saturation of the adsorbent at higher gas flowrate. The

gas flowrate decreases 5 times from 50 cm³/min to 10 cm³/min but breakthrough time increased by only 4.4 times from 50 cm³/min to 10 cm³/min.

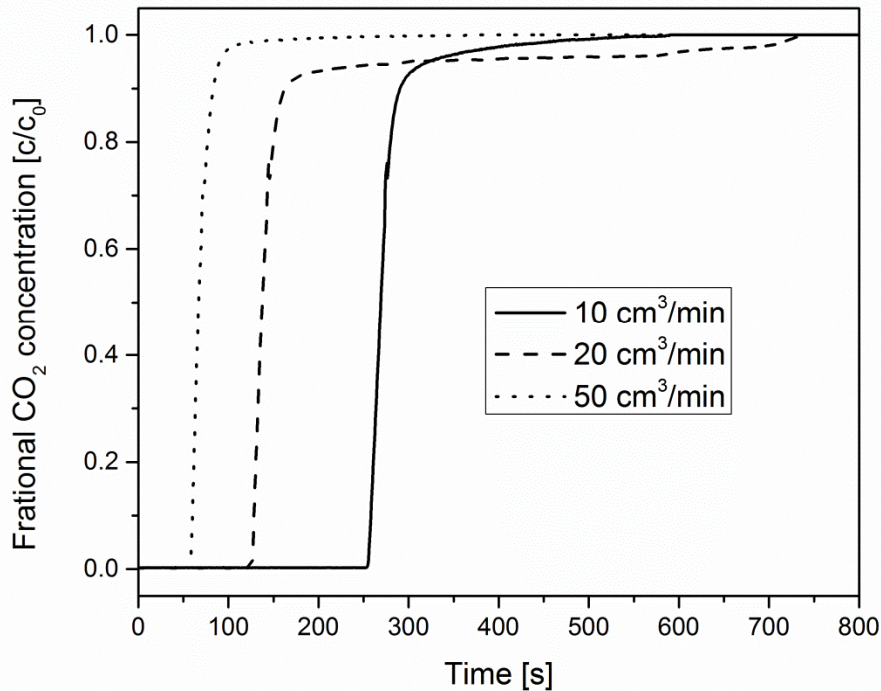


Figure 4.29. Comparison of packed bed breakthrough curves at different gas flowrates comprising 10% CO₂/90% N₂ gas mixture at 75 °C.

4.3.3.3 Multi-cycle stability

One of the most important criteria in adsorbent selection for real industrial application is long-term stability. Multi-cycle stability of amine impregnated sample SBA-15/P-50 was tested in packed bed. The multi-cycle stability was investigated in both dry and humid 10% CO₂/90% N₂ to also check the effect of moisture on the packed bed performance of this sample. Before the experiment for multi-cycle study, the adsorbent was dried at 105 °C under N₂ for 1 h. For all the cycles, adsorption was done at 75 °C in 20 cm³/min of 10% CO₂/90% N₂ gas

mixture and desorption at 90 °C in 50 cm³/min of pure N₂. The cyclic study with humid gas was performed by maintaining about 95% RH (equivalent to around 2.98% moisture) at 25 °C. The results for 20 adsorption/desorption cycles in dry and humid CO₂/N₂ gas is shown in Figure 4.30. It was observed that the CO₂ adsorption capacity in humid gas is higher than that in dry gas for all the cyclic runs. The drop in adsorption capacity after 20 cycles in dry 10% CO₂/N₂ was around 5.75% whereas in humid 10% CO₂/N₂, the drop was around 1.31%. So, it can be said that the sample inside packed bed showed good stability for 20 adsorption/desorption cycles in both dry and humid 10% CO₂/N₂. Moisture enhanced the multi-cycle stability of this sample 4.4 times and has an overall positive impact on the stability of the impregnated sample in packed bed. The increased multi-cycle stability in the presence of moisture is suggested to be because of the hydrophilic nature of PEI amine. The hydrophilic nature of PEI amine allows it to adsorb the moisture and hence does not permit degradation of the sorbent structure by moisture.¹⁵

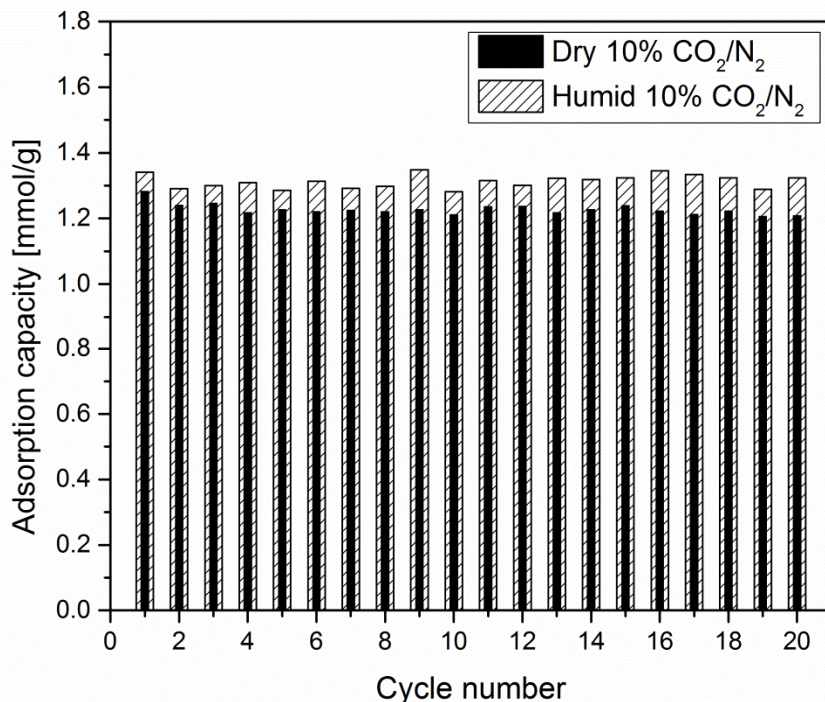


Figure 4.30. Multi-cycle stability of SBA-15/P-50 sample inside packed bed in dry and humid 10% CO₂/N₂ gas streams at 75 °C.

4.3.3.4 Kinetics

Kinetics of an adsorbent needs to be sufficiently fast in order to capture CO₂ efficiently. Figure 4.31 presents the adsorption and desorption kinetics of SBA-15/P-50 sample inside packed bed in dry 10% CO₂/N₂ gas mixture. A blank curve is also shown in this Figure for better comparison. Adsorption was done in 10% CO₂/90% N₂ at 75 °C and desorption in pure N₂ at 90 °C. The rectangular nature in the adsorption segment of a breakthrough curve denotes that adsorption kinetics is fast. The adsorption kinetics of the sample is observed to be fast as indicated by the sharp increase in fractional CO₂ concentration from 0 to 1. The small peak in the desorption segment of the breakthrough curve denotes the release of CO₂

adsorbed by the adsorbent. This small peak indicates that desorption temperature (90 °C) is reached inside the sorbent bed. Both adsorption and desorption kinetics is in the order of minutes. Breakthrough time observed for SBA-15/P-50 sample (146 s) is much higher than that for inert alumina powder in blank test (28 s).

Figure 4.32 presents the adsorption and desorption kinetics of the sample SBA-15/P-50 in humid 10% CO₂/N₂. Similar to the results in dry CO₂/N₂ stream, both adsorption and desorption kinetics are fast in humid CO₂/N₂ as well and is in the order of minutes. Again, the small peak in desorption segment indicates the release of adsorbed CO₂.

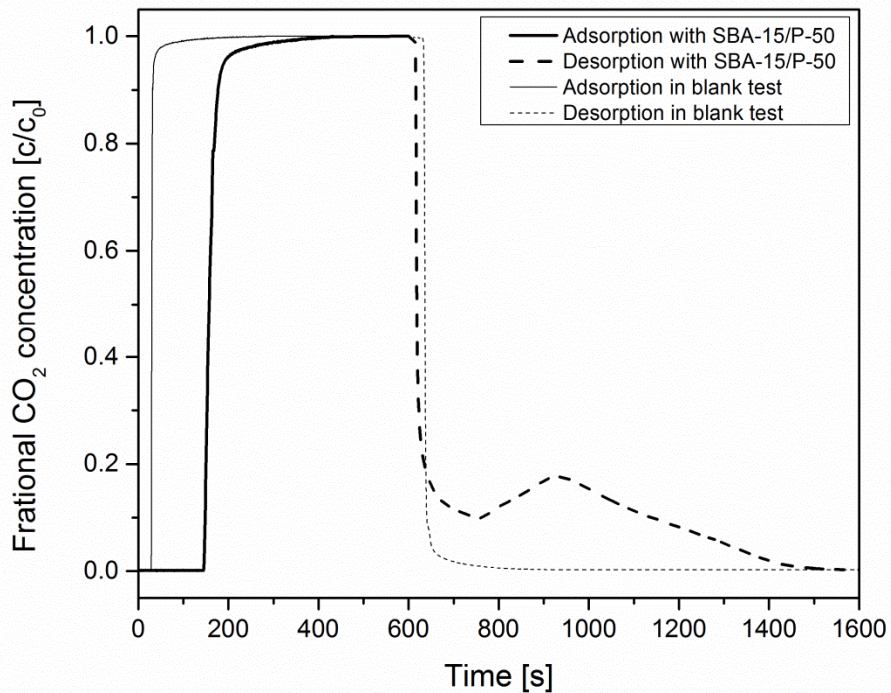


Figure 4.31. Adsorption/ desorption kinetics of SBA-15/P-50 sample inside packed bed in dry 10% CO₂/N₂ gas mixture.

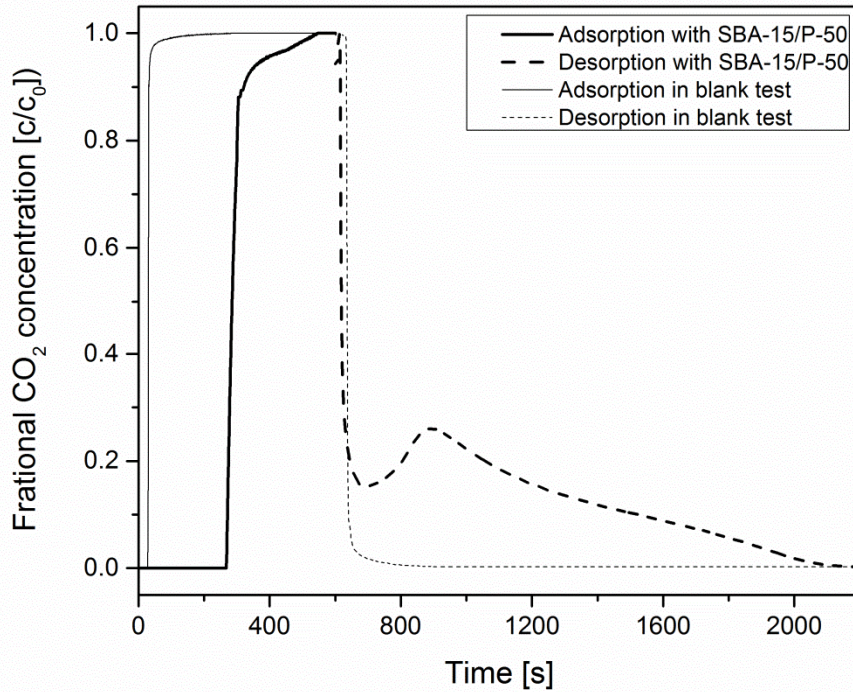


Figure 4.32. Adsorption/ desorption kinetics of SBA-15/P-50 sample inside packed bed in humid 10% CO₂/N₂ gas mixture.

4.3.4 Packed and structured bed comparison

CO₂ adsorption performance using packed bed and structured bed was compared. The effect of adsorption temperature on the CO₂ adsorption capacity of SBA-15/P-50 sample in packed bed and three-tube structured bed is shown in Figure 4.33. In both the set-ups, 10% CO₂/90% N₂ gas mixture was used. The impregnated sorbent in both packed bed and structured bed showed the same nature of curve with adsorption capacity increasing from 25 °C to 75 °C and then decreasing from 75 °C to 90 °C. The maximum value of adsorption capacity was obtained at 75 °C in both of the set-ups. The adsorption capacity values obtained in structured bed are much higher than that found in packed bed at all

temperatures. The adsorption capacity in structured bed at 75 °C is 1.8 times higher than in packed bed. The reason for this behaviour is attributed to the distribution of adsorbent powder over a large surface area in the structured bed as compared to packed bed which allows the adsorbent in structured bed to have more contact with CO₂ and it leads to more CO₂ adsorption in structured bed. Sorbent distribution in a smaller volume in packed bed as compared to structured bed could also have created problems like localized heating of adsorbent during the adsorption and hence led to reduced adsorption capacity in packed bed.

Overall, structured bed arrangement offers higher CO₂ adsorption capacity and lower pressure drop than conventional packed bed, so it can be said that there is good potential of structured bed for application in CO₂ capture. However, the heat management of structured bed configuration was not evaluated in this work and needs proper investigation to further examine the effectiveness of structured bed for post-combustion CO₂ capture.

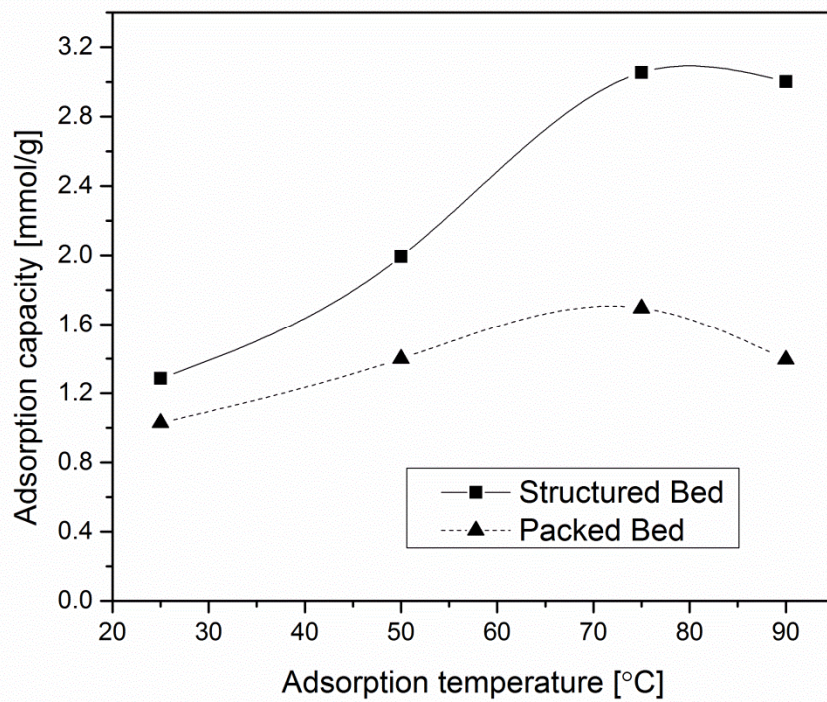


Figure 4.33. Comparison of adsorption capacity of SBA-15/P-50 sample using structured bed and packed bed at different adsorption temperatures.

Notes

A version of this chapter has been submitted for publication in Energy and Fuels Journal.

References

1. Zhao, A.; Samanta, A.; Sarkar, P.; Gupta, R. Carbon dioxide adsorption on amine impregnated mesoporous SBA-15 sorbents: experimental and kinetics study. *Ind. Eng. Chem. Res.* **2013**, 52 (19), 6480–6491.
2. Zhao, D.; Huo, Q.; Feng, J.; Chmelka, B. F.; Stucky, G. D. Nonionic triblock and star diblock copolymer and oligomeric surfactant syntheses of highly ordered, hydrothermally stable, mesoporous silica structures. *J. Am. Chem. Soc.* **1998**, 120 (24), 6024-6036.
3. Kruk, M.; Jaroniec, M.; Sakamoto, Y.; Terasaki, O.; Ryoo, R.; Ko, C. H. Determination of pore size and pore wall structure of MCM-41 by using nitrogen adsorption, transmission electron microscopy, and X-ray diffraction. *J. Phys. Chem. B* **2000**, 104 (2), 292-301.
4. Zhang, F.; Yan, Y.; Yang, H.; Meng, Y.; Yu, C.; Tu, B.; Zhao, D. Understanding effect of wall structure on the hydrothermal stability of mesostructured silica SBA-15. *J. Phys. Chem. B* **2005**, 109 (18), 8723-8732.
5. Fulvio, P. F.; Pikus, S.; Jaroniec, M. Tailoring properties of SBA-15 materials by controlling conditions of hydrothermal synthesis. *J. Mater. Chem.* **2005**, 15 (47), 5049-5053.
6. Knöfel, C.; Martin, C.; Hornebecq, V.; Llewellyn, P. L. Study of carbon dioxide adsorption on mesoporous aminopropylsilane-functionalized silica and titania combining microcalorimetry and in situ infrared spectroscopy. *J. Phys. Chem. C* **2009**, 113 (52), 21726-21734.

7. Yang, Y.-H.; Li, F.-F.; Yang, C.; Zhang, W.-Y.; Wu, J.-H. Grafting morphologies of TEPA on SBA-15(P) and its effect on CO₂ adsorption performance. *Acta Phys. Chim. Sin.* **2012**, 28 (1), 195-200.
8. Danon, A.; Stair, P. C.; Weitz, E. FTIR study of CO₂ adsorption on amine-grafted SBA-15: Elucidation of adsorbed species. *J. Phys. Chem. C* **2011**, 115 (23), 11540-11549.
9. Khatri, R. A.; Chuang, S. S. C.; Soong, Y.; Gray, M. Thermal and chemical stability of regenerable solid amine sorbent for CO₂ capture. *Energy Fuels* **2006**, 20, 1514–1520.
10. Harlick, P. J. E.; Sayari, A. Applications of pore-expanded mesoporous silicas. 3. Triamine silane grafting for enhanced CO₂ adsorption. *Ind. Eng. Chem. Res.* **2006**, 45, 3248–3255.
11. Xu, X.; Song, C.; Andresen, J. M.; Miller, B. G.; Scaroni, A. W. Novel polyethylenimine-modified mesoporous molecular sieve of MCM-41 type as high-capacity adsorbent for CO₂ capture. *Energy Fuels* **2002**, 16, 1463–1469.
12. Heydari-Gorji, A.; Yang, Y.; Sayari, A. Effect of the pore length on CO₂ adsorption over amine-modified mesoporous silicas. *Energy Fuels* **2011**, 25, 4206-4210.
13. Samanta, A.; Zhao, A.; Shimizu, G. K. H.; Sarkar, P.; Gupta, R. Post-combustion CO₂ capture using solid sorbents: A review. *Ind. Eng. Chem. Res.* **2012**, 51, 1438-1463.
14. Calleja, G.; Sanz, R.; Arencibia, A.; Sanz-Pérez, E. S. Influence of drying conditions on amine-functionalized SBA-15 as adsorbent of CO₂. *Top. Catal.* **2011**, 54 (1-4), 135-145.
15. Xu, X.; Song, C.; Miller, B. G.; Scaroni, A. W. Influence of moisture on CO₂ separation from gas mixture by a nanoporous adsorbent based on polyethylenimine-modified molecular sieve MCM-41. *Ind. Eng. Chem. Res.* **2005**, 44, 8113–8119.

Chapter 5

Conclusions and Future Work

5.1 Conclusions

In this work, post-combustion CO₂ capture performance of DAEAPTS grafted SBA-15 adsorbent was studied. Variable amine loaded DAEAPTS grafted SBA-15 adsorbents were prepared and characterized. The optimum amine loading of grafted SBA-15 adsorbent was determined. The effect of adsorption temperature (25-105 °C) and CO₂ partial pressure (8-101.3 kPa) on the CO₂ adsorption capacity of SBA-15-DAEAPTS adsorbents was investigated in order to determine the optimum adsorption conditions. The effect of moisture on CO₂ adsorption/desorption performance of amine grafted adsorbent was studied. Main findings of this work are as follows:

- It was found that SBA-15/D-4 sample has the optimal amine loading of 40 wt% based on CO₂ adsorption capacity, amine adsorption efficiency and adsorption kinetics. The SBA-15 adsorbent synthesized with 40 wt% DAEAPTS amine loading displayed maximum capture capacity of 2.3 mmol/g under simulated gas conditions (88.2% CO₂/N₂) at 75 °C and 1 atm.
- It was observed that the adsorption capacity increases sharply with CO₂ partial pressure till 10 kPa CO₂ partial pressure while further increase in CO₂ partial pressure results in saturation of CO₂ adsorption capacity near about 2.3

mmol/g. So, the grafted adsorbent has good potential in post-combustion capture conditions where CO₂ is available at around 10 kPa partial pressure.

- The CO₂ adsorption capacity in humid CO₂ stream appeared to have increased as compared to sorption capacity in dry CO₂ stream but thorough analysis of the results concluded that the increase in adsorption capacity was due to the adsorption of moisture rather than CO₂. It was observed that there is no negative effect in the adsorption performance of grafted adsorbent due to the presence of moisture in the humid CO₂ stream.
- The grafted sample showed good stability for 100 short adsorption-desorption cycles in both dry and humid CO₂/N₂ streams. The drop in capacity after 100 cycles in dry and humid CO₂/N₂ streams was around 7.11% and 6.94% respectively. The cycle time was kept short to allow fast cyclic study.
- The grafted sorbent showed considerably fast adsorption and desorption kinetics in both dry and humid CO₂ streams. The adsorbent reached 80% of the total adsorption capacity in 5 min in dry 88.2% CO₂/N₂ and in only 2.5 min in humid 88.2% CO₂/N₂. The adsorbent achieved 95% of the total regeneration in less than 5 min of desorption time using N₂ as regeneration gas.

Packed bed configuration and novel tubular structured bed configuration with straight gas flow channels was tested for post-combustion CO₂ capture in this work. Packed bed and structured bed were investigated for CO₂ capture with PEI impregnated SBA adsorbent. The structured bed set-up was designed and built to

host single and multi-tube reactors with minimum modification. Structured bed with one tube and three tubes were examined for CO₂ capture performance. The structured bed and packed bed were studied for adsorption temperature effect, adsorption/desorption kinetics and multi-cycle stability. Main findings of the work are as follows:

- Single-tube structured bed showed adsorption capacity upto 2.6 mmol/g on variation of adsorption temperature.
- The impregnated adsorbent in three-tube structured bed displayed adsorption capacity in the range of 1.28-3.05 mmol/g as the adsorption temperature varied from 25 to 90 °C with maximum capacity at 75 °C.
- The cyclic run of adsorbent in three-tube structured bed showed that there is big drop in capacity from 1st to 2nd cycle (3.05 to 2.56 mmol/g) but negligible drop from 2nd cycle onwards. Overall, the adsorbent in structured bed exhibited good stability for 6 cyclic runs.
- 75 °C was observed as the optimum adsorption temperature for CO₂ adsorption performance in packed bed. From the adsorption temperature and gas flowrate variation, the highest adsorption capacity of 1.97 mmol/g was found at 75 °C and 50 cm³/min gas flowrate for impregnated adsorbent in packed bed.
- The adsorbent in packed bed displayed good multi-cycle stability and drop in capacity after 20 cycles in dry CO₂/N₂ stream was around 5.75%. Presence of moisture improved the multi-cycle stability of impregnated adsorbent in

packed bed and drop in capacity after 20 cycles in humid CO₂/N₂ stream was only 1.31%.

- The comparison of CO₂ adsorption capacities of PEI impregnated SBA-15 adsorbent in packed bed and three-tube structured bed showed that adsorption capacity in structured bed is higher than capacity in packed bed throughout the entire temperature range.

5.2 Future work

Based on the research done in this work, some points, related to amine functionalized adsorbents and structured bed configuration use in post-combustion CO₂ capture, are suggested for future studies as follows:

- Study of the regeneration conditions of amine functionalized adsorbents is required to further improve their performance. Alternative to N₂ like steam, CO₂, etc. as desorption gases has to be studied for practical applications. Also, alternate desorption processes like VSA, PSA etc. may provide improved long-term stability for amine functionalized adsorbents.
- Investigate the effect of impurities like SO_x, NO_x in flue gas mixture on the adsorption performance of amine functionalized adsorbents to determine their actual potential for CO₂ capture.
- Heat management of structured bed was not studied in this work and needs investigation in future work for more accurate assessment of structured bed performance for post-combustion CO₂ capture.